The fate of geogenic uranium in the environment:
An example from the Swiss Plateau

Inauguraldissertation
der Philosophisch-naturwissenschaftlichen Fakultät
der Universität Bern

vorgelegt von

Anja Pregler

aus Deutschland

Leiter der Arbeit

Prof. Dr. Andreas Türler

Departement für Chemie und Biochemie (Universität Bern)
Abteilung Strahlenschutz und Sicherheit (Paul Scherrer Institut)

The fate of geogenic uranium in the environment: An example from the Swiss Plateau

Inauguraldissertation
der Philosophisch-naturwissenschaftlichen Fakultät
der Universität Bern

vorgelegt von

Anja Pregler

aus Deutschland

Leiter der Arbeit

Prof. Dr. Andreas Türler

Departement für Chemie und Biochemie (Universität Bern)
Abteilung Strahlenschutz und Sicherheit (Paul Scherrer Institut)

Von der Philosophsich-naturwissenschaftlichen Fakultät angenommen.

Bern, 21.08.2020

Der Dekan
Prof. Dr. Zoltan Balogh

This work is dedicated to

JOST EIKENBERG

* 27.06.1956 † 19.07.2017

Summary

Increased U concentrations in ground and drinking water have been found in the western part of Switzerland. The focus of the study was set to Mont Vully, 20 km northwest of Berne. The origin of U was investigated and has been verified to derive from an interface between the Upper Marine Molasse and the Lower Freshwater Molasse, two stratigraphic units in the Molasse Basin. During the genesis of this interface, fossils have been deposited and U was adsorbed onto them due to the reducing environment that has been present. The last glaciation formed the typically hilly area of the Swiss Plateau leading to the outcropping of the interface with the U-rich fossils. Oxygen-rich rainwater that infiltrated the water permeable Upper Marine Molasse was dammed at the Lower Freshwater Molasse which acts as an aquitard resulting in a steady leaching process of the fossils at the interface. This U-rich groundwater (350 mBq/L ^{238}U) fed wetlands that were formed at least 8 kyrs ago on an impermeable clay layer in the adjacent land north of Mont Vully. The reducing conditions that were present in the wetland resulted in an accumulation of U that was adsorbed onto organic matter. Lasting for thousands of years, the infiltration of U-rich groundwater generated a peat horizon with up to 500 Bq/kg ^{238}U. In the beginning of the 19th century, plenty of wetlands were drained in order to create arable land leading to a change in redox conditions underground. O-rich rainwater was then able to circulate through the peat horizon and oxidized the adsorbed U. The enabling of the leaching processes resulted in increased U concentrations in the drainage pipes with more than 600 mBq/L ^{238}U. The investigation with airborne gamma ray spectrometry that was performed with a helicopter equipped with 4 NaI detectors revealed that further U accumulations in the area around Mont Vully could be possible.

The second study site at the agricultural area around the Lyssbach was chosen for the analysis of the leaching behaviour of U. Sampling once a month the drainage pipe that drains a peat horizon with a ^{238}U concentration of 2000 Bq/kg revealed that the leaching process depended on diverse factors such as the amount of water available and the carbonate content. By combining parameters such as the annual precipitation and the ^{238}U concentration and flow rate of the drainage pipe revealed an overall leaching rate of 0.3% per year of the total U inventory (600 kBq/m^2). This implies that leaching has to take place in the same intensity for the next several hundreds of years until the peat horizon near the Lyssbach is almost U-free. Additional laboratory experiments including a sequential extraction and leaching experiments with varying pH, time and carbonate content verified this calculation and displayed other scenarios if the leaching conditions change.

The investigation of U uptake by plants was accomplished in four different study sites at the Swiss Plateau. Analyzing the soil and flooding water revealed some increased U concentrations. The following measurements of rice plants, divided into stems, leaves and panicles, as well as rice crops yielded minor transfer factors leading to the assumption that the uptake of U is too small to have an influence on increasing health risks due to the uptake of U by food.

Keywords

Uranium

Environment

Swiss Molasse

Swiss Plateau

Leaching

Sequential Extraction

Peat

Airborne Gamma Ray Spectrometry

Rice

Transfer Factors

Environmental Radioactivity

Contents

List of Figures

List of Tables

Abbreviations

DHC	Diammonium hydrogen citrate
H_2O_2	hydrogen peroxide
HCl	hydrochloric acid
HNO_3	nitric acid
$KMnO_4$	potassium permanganate
LSC	Liquid Scintillation Counting
MnO_2	manganese oxide
Na_2SO_4	sodium sulphate
$NaHSO_4$	sodium bisulphate
Pb	Lead
Po	Polonium
Ra	Radium
Rn	Radon
Th	Thorium
U	Uranium
U/TEVA	Uranium and tetravalent actinides

Chapter 1 Introduction

Alarming incidents in nuclear power plants like the shutdown of a reactor due to precariousness of the reactor building or simply the location of old power plants in a natural hazardous area severely alienate the broad public and sensibilise people to radioactivity. Not at the latest, the Chernobyl accident in 1986 or the explosion of the nuclear reactor Fukushima-Daiichi in 2011 court the public's resentment towards radioactivity. But what is often neglected is the fact that radioactivity, in principle, is a natural phenomenon with the three natural decay series of ^{238}U, ^{235}U and ^{232}Th. As a result, not only artificial radionuclides but also naturally occurring radioactivity move into focus of the population, sometimes without differentiation. Especially Uranium (U) is most often associated with nuclear power plants since their fuel rod consists of enriched U. But it should always be kept in mind that ^{238}U is a primordial nuclide, i.e. it was already present on Earth while its formation. ^{238}U and its daughters are present all over the world in different forms and concentrations. The following sections describe the characteristics, applications and occurrences of U on Earth.

1.1 Uranium: Properties and Applications

The chemical element uranium is a silvery heavy metal with the atomic number 92. It is a primordial radionuclide with an abundance of 1.8 ppm in the Earth's crust (Mason & Moore, 1982) and with three naturally occurring radioisotopes: ^{238}U, ^{235}U and ^{234}U in the isotopic ratios of 99.27%, 0.72% and 0.0054%, respectively (Chabaux et al. 2008). Due to the long half-life of ^{238}U ($T_{1/2}$ = 4.45*10^{9} years) and its heavy atomic mass of 238.05 g/mol, the specific activity of ^{238}U is rather low with 12 kBq/g (L'Annunziata, 2012). The half-lives of ^{234}U and ^{235}U are shorter with 2.455*10^{5} years and 7.038*10^{8} years, respectively (Magill et al., 2006). Since the discovery of the element U in pitchblende by Martin Heinrich Klaproth in 1789 who named it after the planet Uranus (Hübner, 1989), many studies have been performed until Henri Becquerel discovered the radioactive properties of U in 1896 (DiGregorio, 2020). The applications of U are manifold: it started with the use of oxides in glass giving it a slightly yellow to greenish color, then adding U to a ceramic glaze resulting in orange U tiles (Fig. 1) and finally to the point of the most dangerous application of U as the utilization for the production of Plutonium used in atomic weapons. Most popular, of course, is the use of U as fuel rod for nuclear power plants (Fig 1). For this purpose, natural U has to be enriched in ^{235}U by centrifugation. The enrichment is typically around 3% to 5% of ^{235}U in ^{238}U. The depleted U in turn was used as high-density penetrators in ammunition. Nuclear power plants utilize the heat that is released by the fission of U in order to roll turbines which in turn generate electricity (Tsoulfanidis, 2018). Although the production of nuclear power releases neither air pollutants nor greenhouse gases, the lifetime of nuclear power plants is socially limited in many parts of the world. The reason therefore are on the one hand severe accidents such as the accident at Chernobyl in 1986 and Fukushima-Daiichi in 2011, which released radioactivity into the environment in a way that even today mankind is exposed to it. And on the other hand, used fuel rods and other radioactive contaminated materials from a power plant have to be kept in intermediate storages until a radioactive waste disposal is found. This search for deep geological repositories is still ongoing in all over the world since diffusion experiments and geological studies have firstly to be performed and evaluated. In Switzerland, the Swiss Federal Nuclear Safety Inspectorate (ENSI) and the National Cooperative for the Disposal of Radioactive Waste (NAGRA) are in charge for this overwhelming project (www.ensi.ch and www.nagra.ch).

Fig. 1: Different applications of U. Left side: U glass; Middle: U tile; Right side: Nuclear Power Plant Mühleberg, Switzerland.

1.2 Uranium in the environment: Rocks, soils and water

Beside these civil applications, U occurs in many different environments within various amounts in rocks, soils and in water. The most common U-bearing mineral in rocks is uraninite, formerly called pitchblende. It consists largely of UO_2 with some varying amounts of U_3O_8 and some rare earth elements (Ivanovich & Harmon, 1992). Due to the radioactive decay series of ^{238}U, uraninite also contains decay products such as Pb-isotopes or Ra. Uraninite is the economically most important U ore and mined until today especially in Kazakhstan, Canada, Australia, Niger, Namibia and Russia (Tsoulfanidis, 2018). Exploration of U ores results in mine tailings and thus inevitably in a pollution of the environment by releasing radionuclides from the contaminated area into water sources. Another origin of U can be found in sedimentary environments such as phosphate rock (Chabaux et al., 2008). Phosphate rock (or phosphorite) is predominantly mined for the production of phosphate used, amongst others, for fertilizers. The main deposits can be found in Morocco, China and the USA (Fantel et al., 1985). By the application of fertilizers onto agricultural fields, small amounts of U can simultaneously be deposited onto the fields (Barisic et al., 1992, Liesch et al., 2015, Takeda et al., 2006). Beside this occurrence generated by fertilizers, there is another origin for the appearance of U in soil: U-bearing minerals. Every soil contains to a certain extend micro- to nanoscale minerals. These minerals in turn can have U fixed in their crystal lattice with the most common example zircon (Ivanovich & Harmon, 1992). The mean concentration of U in soil ranges from 300 µg/kg up to 12 mg/kg (UNSCEAR, 1993). However, solid occurrences are not the only form in which U can be found in the environment, it can also be dissolved in water under certain circumstances. For example, the concentration of U in seawater is estimated to reach 3 ppb what makes U recovery from seawater profitable (Maaz et al., 2020).

The occurrence of U is often not a steady state but a continuous movement within the particular environments. There is not one situation that is applicable to all over the world. For this reason, this study illustrates the example of the fate U in the environment for the Swiss Plateau.

1.3 Health risks from Uranium

It is important to evaluate the behaviour of U in the environment since the health risks for living beings from U can be severe. The health risk from U derives not only from the radiotoxicity but also, or even especially from its chemical toxicity (ATSDR, 2013). The uptake of U may occur by inhalation or contaminated wounds, but the ingestion of U via food and drinking water primarily accounts for the U exposure of the general public (WHO, 2001). Following health effects include nephrotoxicity, genotoxicity and developmental defects (Brugge, 2014). The most concerned organs in human bodies are the kidneys. Consequently, the World Health Organization (WHO) recommends a limit of 30 µg/L in drinking water (WHO, 2001) and the Swiss Federal Department of Home Affairs followed in 2017 (EDI, 2017). However, there is no legal limit of U concentrations and other natural radioactive elements in food anymore. For this reason, it is important to survey at least drinking water for its content of radioactive isotopes.

1.4 Aims of the thesis

The overall aim of this doctoral thesis was to illustrate the manifold occurrences and behaviour – and thus the fate – of U in different natural environments. The impulse for this investigation was the discovery of increased U concentrations in ground and drinking water in the western part of Switzerland with unknown origin (Stalder et al., 2012). For this reason, the Swiss Plateau was chosen as field of study for the thesis. During the elaboration of the thesis, three superior questions have to be answered.

The first point of interest was the origin of the increased U concentrations in the Swiss Plateau. The study of Stalder et al., 2012 comprised the analyses of more than 5500 water samples from all over Switzerland for its U concentration. The origin of U in the drinking water, however, was not covered in the study. This question of the provenance of U is important to understand the paths of U in nature. Conclusions of the host rock can be drawn if U was found in groundwater. The frequency and intensity of increased U concentrations in the Swiss Plateau may be determined during this study. Also important in relation with the origin of U was the behaviour of U in the groundwater and its further destinations. The goal was to illustrate the whole flow path of U in ground water from bedrock through potential barriers until it reaches surface water. Consequently, the overall aim of the first part was to identify the sources and sinks for U.

The second goal of this doctoral thesis was to evaluate the behaviour of U if it was stuck somewhere during its way. By accomplishing several leaching experiments, the leaching properties of U that was adsorbed onto organic matter in a peat horizon may be determined. By combining results from observations in nature with experiments conducted in the laboratory, a prediction of the lifetime for U in the special natural environment in the Swiss Plateau may be calculated.

The third and last question for the fate of U in nature covers the transfer of U into food. Rice plantations were chosen as example for the study of U uptake of plants from soil and water. It was investigated whether rice plants incorporate U from an area with increased U in the soil or in the flooding water. In this scenario, humans could be exposed to an increased amount of U. Since U is a toxic heavy metal, it is important to identify the transfer factors from soil to plant in order accomplish a risk evaluation for the consumption of such food.

Finally, the overall goal of answering all these questions was to contribute to the understanding of the fate of geogenic U in nature with the focus on the special environment of the Swiss Plateau.

Chapter 2 Materials and methods

The different U and Th series isotopes that were of importance for the study were separated and measured by a broad variety of methods. Some of the methods were already briefly explained in the material sections of Chapter 3, 5 and 6. In this chapter, the collection of samples is specified and the methods used for separation are explained more in detail.

2.1 Material

2.1.1 Water samples

Water samples from the different study areas were always collected in polyethylene bottles and subsequently acidified with a few drops of concentrated HNO_3 in order to prevent the radionuclides to adsorb onto the bottle walls. The amount of the sampled water depended upon the desired isotopes of interest and the following separation procedure. The volume ranged from 20 mL for the Rn analysis to 2 L if a whole ^{238}U-series isotopes determination was intended. The exact procedures are explained in detail in section 2.2.

2.1.2 Soil samples

Soil samples were either collected via drilling procedures into 1 m depth by the Cora drilling unit (Fig. 2) or the soil samples were picked manually from the study area. Each sample was subsequently dried in the oven at 105°C for 5 hours and ground to a homogeneous powder with the help of a porcelain mortar. The final powder was stored in closed bags or boxes until an aliquot was used for further preparation. If not stated otherwise, about 1 g was used for wet ashing that was accomplished by boiling the powder in 20 ml concentrated HNO_3 under reflux together with a defined amount of ^{232}U as a radiotracer (Fig. 2). As soon as no nitrous gases were visible anymore, the solution was evaporated to complete dryness. The residual soil components were placed into the oven for 15 hours at 500°C for dry ashing. The residue from this step was dissolved in 8 M HNO_3 together with 30% H_2O_2 and boiled under reflux and continuous stirring for 2 hours. After cooling down, the suspension was filtrated in order to separate the liquid from the insoluble compounds. The resulting solution was used for the further radiochemical separation method explained in section 2.2.

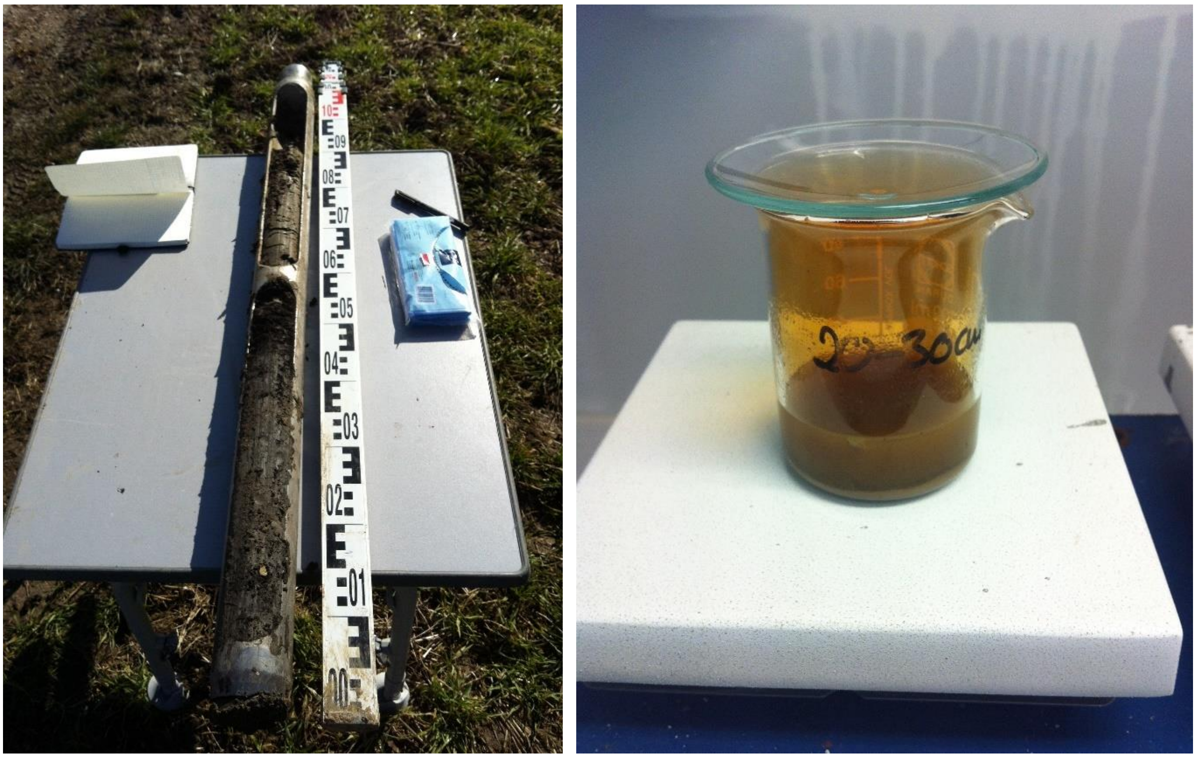

Fig. 2: Soil samples. Left side: Soil after drilling into 1 m depth; Right side: Boiling an aliquot in concentrated HNO_3.

2.2 Radiochemical separation methods

The decay chain of the three naturally occurring radioisotopes ^{238}U, ^{235}U and ^{232}Th are illustrated in Fig. 3 indicating the half-life, the decay mode and the decay energy. The isotopes that were analyzed in the water samples of this study with radiochemical methods were ^{238}U, ^{234}U, ^{226}Ra, ^{222}Rn, ^{210}Pb and ^{210}Po from the ^{238}U decay series, ^{235}U from the corresponding ^{235}U series and ^{228}Ra and ^{224}Ra from the ^{232}Th series. ^{223}Ra from the ^{235}U series was also analyzed since it was used as a radiotracer. It is of importance to separate the elements of interest from each other since decay energies are overlapping which makes it impossible to measure them simultaneously by alphaspectrometry. The detailed procedures to accomplish these separations are explicitly described in the following sections for each element.

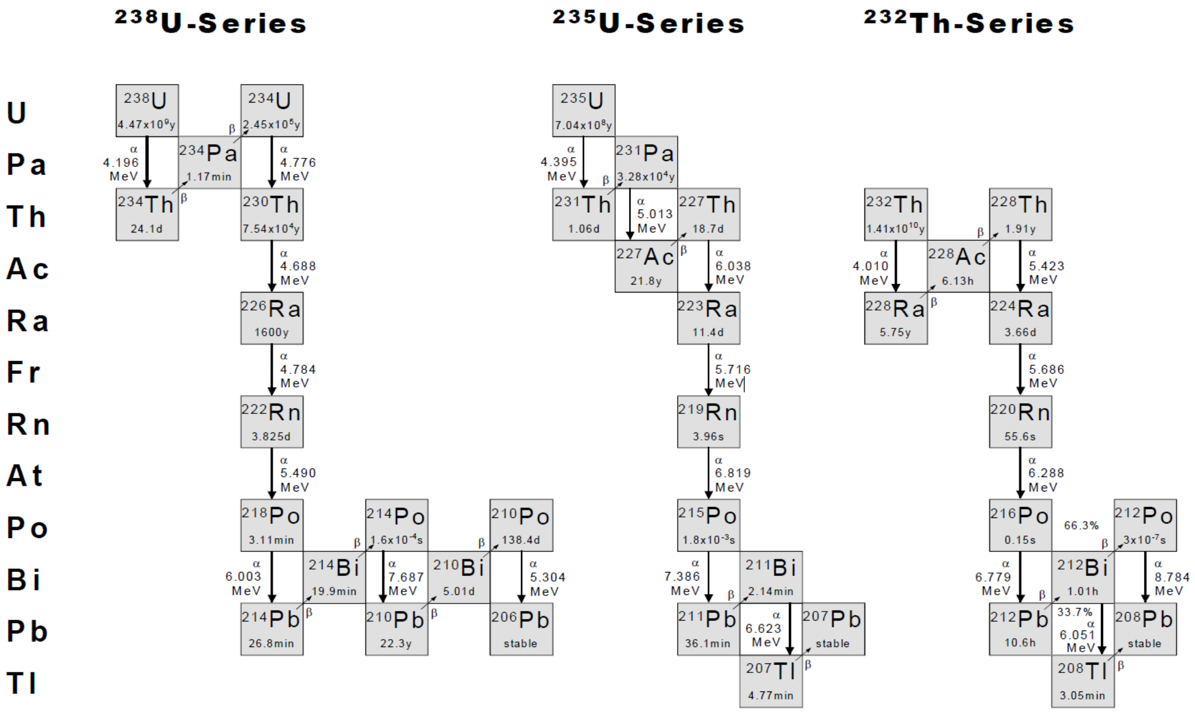

Fig. 3: ^{238}U, ^{235}U and ^{232}Th decay series indicating the half-life, the decay type and decay energy (Eikenberg 2002).

2.2.1 Uranium

For the analysis of the three naturally occurring Uranium isotopes ^{238}U, ^{234}U and ^{235}U in water samples approximately 250 mL are needed. A ^{232}U-tracer is added to the sample in order to check the chemical yield of the following chromatographic extraction. In case of the soil samples, the tracer was already added before the ashing process (explained in section 2.1.2) and the solution that was obtained after wet and dry ashing and the following filtration step was used for the chromatographic extraction. The first step of this procedure was to evaporate the sample or solution to complete dryness: in case of water samples the sample water itself and in case of the soil samples the solution that was obtained after filtration. The residue in both cases is re-dissolved in 3 M HNO_3. This solution was passed then through an Eichrom **U/TEVA U**ranium and **TE**tra**V**alent **A**ctinides column, that retains U and other tetravalent actinides and are thus separated from their matrix. U itself was then separated from Ra, Po and Th by several washing steps with 3 M HNO_3, 8 M HNO_3 and 5 M HCl, respectively. Finally, U was eluted from the resin with 0.02 M HCl. The whole procedure was adapted from Horwitz et al. (1992) regarding the volumes and concentrations of the eluate fractions according to an PSI internal standard operating procedure. The eluted solution together with 0.6 mL H_2SO_4 and 0.6 mL 1 M $NaHSO_4$ was evaporated to complete dryness and calcinated for 10 minutes. The residue is dissolved with 4.8 mL 0.125 M $NaHSO_4$ and 5.2 mL 1 M

Na_2SO_4 and transferred into a plastic vial, which acts as electrodeposition cell. The detailed procedure of the electrodeposition onto a stainless steel disk is described in Bajo and Eikenberg (1999).

2.2.2 Radium

The following separation methods for Ra were only applied to water samples and not to soil samples.

Alphaspectrometry of ^{226}Ra and ^{224}Ra via adsorption onto MnO_2 discs

One method to analyze Ra isotopes is by spontaneous adsorption onto a MnO_2-coated disk (Surbeck, 2000). These discs were produced in house by placing a cleaned nylon disc with 28 mm in diameter into a 2% $KMnO_4$ solution at 70°C and let the MnO_2 precipitate onto the plate for two hours under continuous stirring. After this step, the MnO_2 discs were carefully washed and dried with a paper towel to remove slightly bound particles. One of these discs was then mounted in a teflon holder in that way that only one side was in contact with the solution. The pH of 200 mL of the water sample was set to 7-8 with 1 M NaOH and the disc in the teflon holder was placed into the sample solution under continuous stirring. After one day exposure time, about 60% of the Ra is adsorbed onto the MnO_2 layer and the two α -particle emitting isotopes ^{226}Ra and ^{224}Ra can be measured via α-spectrometry. For the surveillance of the chemical yield, a special ^{223}Ra generator was designed which was used as radiotracer. As basis for this generator, an already existing ^{227}Ac tracer was used. Due to the half-life of 21.8 years and 18.7 days of ^{227}Ac and ^{227}Th, respectively, the two isotopes are in secular equilibrium with each other after 10 half-lives of the daughter isotope, i.e. after 187 days. Since the reference date of the ^{227}Ac tracer is in 1993, the secular equilibrium is approved. A defined amount of the ^{227}Ac tracer was passed through an U/TEVA column, which retains Ac, Th and Ra. In order to obtain a pure ^{223}Ra tracer, Ra was then eluted using 10 mL 3 M HNO_3 whereas Ac and Th remain on the column. The activity of the generated ^{223}Ra tracer should equal the activity of the ^{227}Ac tracer that was loaded onto the column and decrease with the ^{223}Ra half-life of 11.4 days. This calculation was checked by measuring the real activity in the tracer by γ-spectrometry (Fig. 4). Due to the ^{227}Ac and ^{227}Th that remains on the U/TEVA column, ^{223}Ra with its relatively short half-life in comparison to their progenitors grows onto the column and reaches secular equilibrium after approximately 114 days (Fig. 5). After a sufficient ingrowth time, ^{223}Ra can be eluted again and further used as tracer. This procedure was accomplished several times in order to perform an adsorption experiment of Ra onto the MnO_2 discs. For this experiment, a defined amount of ^{223}Ra tracer was exposed to the MnO_2 discs for different time periods, ranging from 1 hour to 50 hours (Fig. 6). The experiment reveals that 24 hours is a sufficient time for Ra to adsorb about 60% onto the MnO_2 discs. However, the effective adsorption varies with each water sample. For this reason, the ^{223}Ra tracer was added to each real water sample that was analyzed for its Ra isotopes.

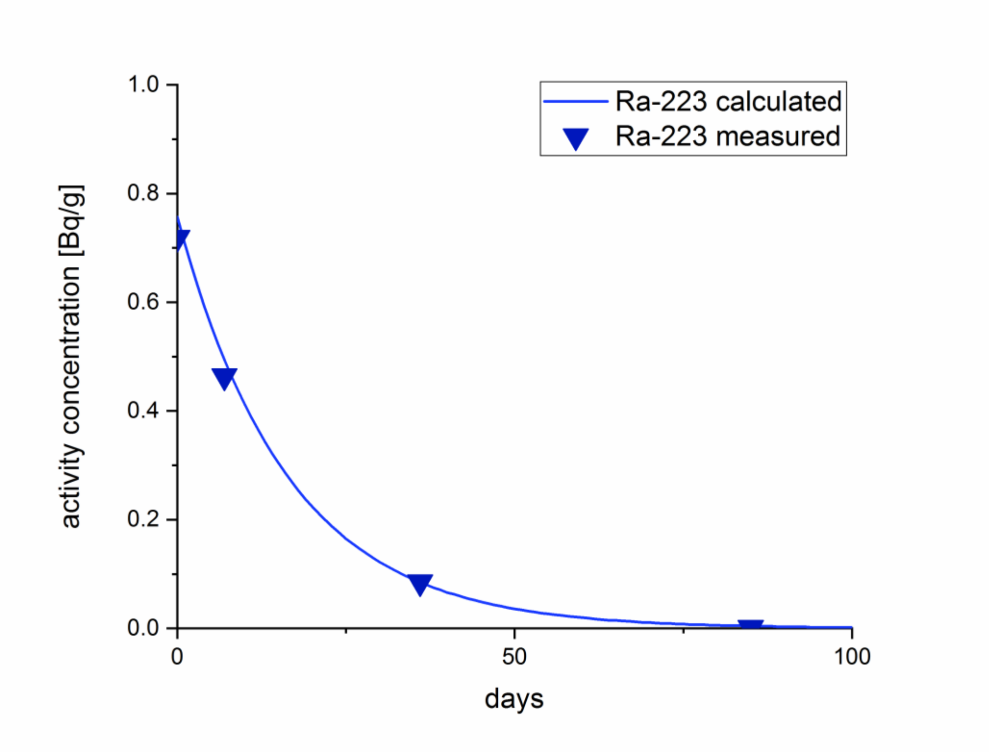

Fig. 4: Decay of ^{223}Ra tracer (calculated and measured).

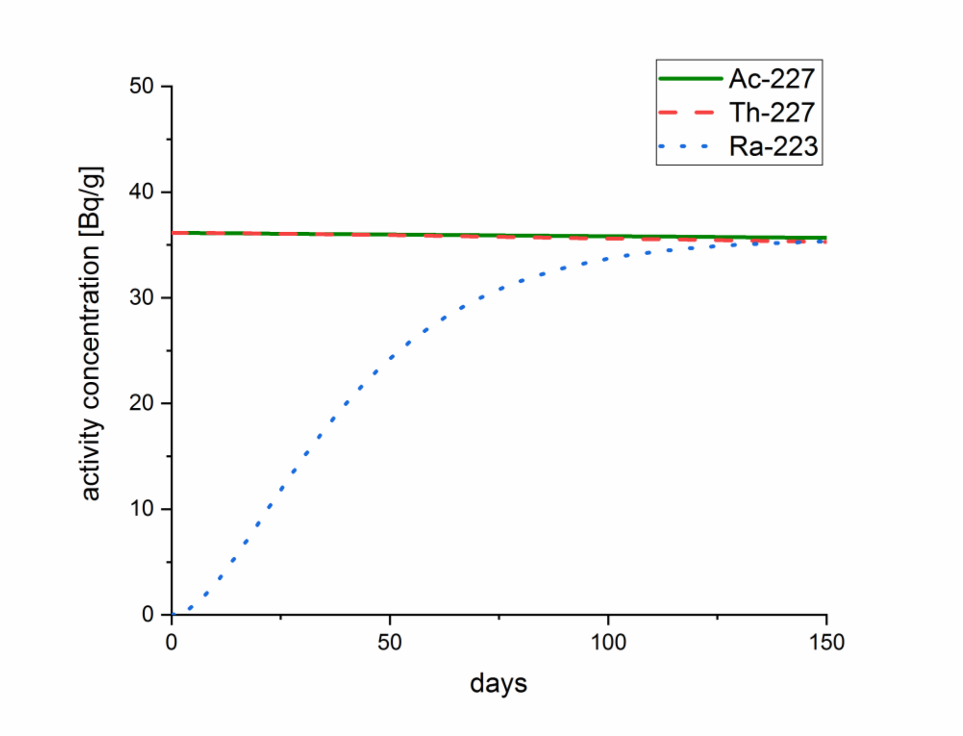

Fig. 5: Ingrowth of ^{223}Ra onto the U/TEVA column after separation from ^{227}Ac and ^{227}Th.

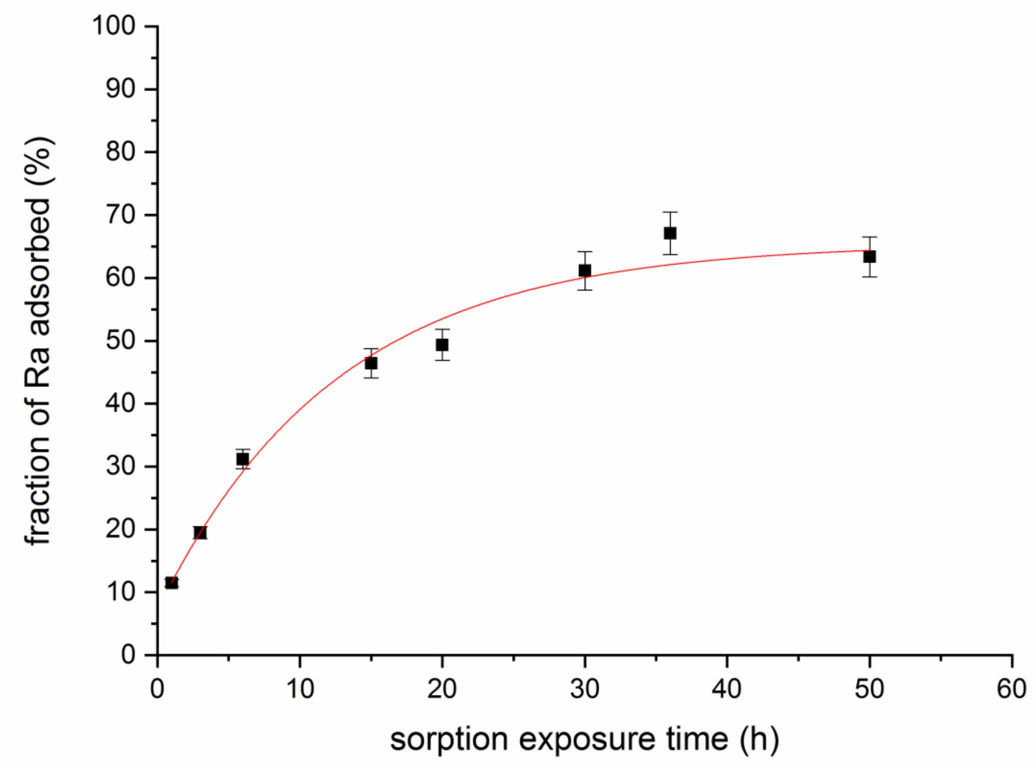

Fig. 6: Adsorption experiments of ^{223}Ra onto MnO$_2$ discs.

^{228}Ra via ingrow of ^{228}Th

The detection of the beta-emitter ^{228}Ra can be accomplished with the same MnO$_2$ discs described above but with a certain delay time after the Ra adsorption. ^{228}Ra with its half-life of 5.8 years decays to the beta-emitter ^{228}Ac with 6 hours half-life, which in turn decays to the α -emitter ^{228}Th with a half-life of 1.9 years. ^{228}Ra can thus be measured by α-spectrometry via the ingrowth of ^{228}Th onto the MnO$_2$ discs. This method was tested for all water samples that were analyzed with the help of MnO$_2$ discs. However, even after an ingrowth period of approximately three years and an α-spectrometry measurement time of 7 days, all ^{228}Th values were below the detection limit of 2 mBq/L. This means, that ^{228}Ra was not or only in very small amounts present in the water samples. The activity concentration of ^{226}Ra did not change significantly after the three years waiting time due to its half-life of 1600 years.

LSC-measurements of ^{226}Ra, ^{224}Ra and ^{228}Ra following RadDisc filtration

Another method to determine the Ra isotopes is via filtration of the water samples through a 3M Empore RadDisc filter (Fig. 7). The detailed procedure of this method is published in Wallner et al., 2008). Since activity concentrations of Ra isotopes were expected to be rather low, about 1.5 L of sample volume was needed. The 1.5 L were acidified with 189 mL concentrated HNO_3 and passed through the filter by a vacuum pump with a flow rate of < 50 mL/min. Ra was eluted each with 5 mL EDTA and mixed with 15 ml Goldstar scintillation cocktail from Triskem. The measurement of the vial containing potentially the α-emitters ^{226}Ra and ^{224}Ra as well as the β-emitter ^{228}Ra was executed with an HIDEX 300 SL scintillation counter with simultaneous α/β-counting and pulse shape analysis. A detailed explanation of this counting method is given in Eikenberg et al. (2014).

2.2.3 Radon

No special separation method is necessary for the Rn analysis in water. The critical point for a correct measurement value is the storage of the water sample until analysis. Therefore, the water was directly sampled in 20 mL glass vials with a gas tight septum in the cap. For the analysis, a 20 mL plastic vial was prepared with 10 mL of the water immiscible scintillation cocktail MaxiLight from HIDEX. 10 mL of the water sample was injected into the cocktail with the help of a syringe. The vial had to be shaken vigorously followed by 3 hours waiting time until ^{222}Rn and its short-lived daughters were equilibrated. The measurement was accomplished with the HIDEX 300 SL scintillation counter with simultaneous α/β-separation in order to differentiate between the α-decays of ^{222}Rn, ^{218}Po and ^{214}Po and the β-decays of ^{214}Pb and ^{214}Bi in the decay chain.

2.2.4 Lead

^{210}Pb in water samples can simultaneously be analyzed with the RadDisc filtration method used for the Ra isotopes. The preparation was the same, the only difference was the elution step for Pb with 5 mL diammonium hydrogen citrate (DHC) prior to the Ra elution. The eluate was mixed with 15 ml Optiphase Hisafe 3 scintillation cocktail from Eichrom and measured with the HIDEX 300 SL scintillation counter.

2.2.5 Polonium

The activity concentration of ^{210}Po in water samples was determined by spontaneous adsorption of Po onto a silver disc (Fig. 7; Lee et al., 2014). Therefore, a defined amount of a ^{209}Po tracer together with 50 mL of concentrated HCl was added to 150 mL water sample. About 1 g of ascorbic acid was added to reduce potential Fe(III) in the sample water to Fe(II). The silver disc with 28 mm in diameter was carefully cleaned with acetone to remove grease residues and mounted into a teflon holder in that way, that only one side of the silver disc was in contact with the sample solution. The holder was completely placed into the solution and rests there for about 24 hours under continuous stirring. After adsorption, the silver disc was washed with deionized water, dried with compressed air and can be directly measured by α -spectrometry for about one week.

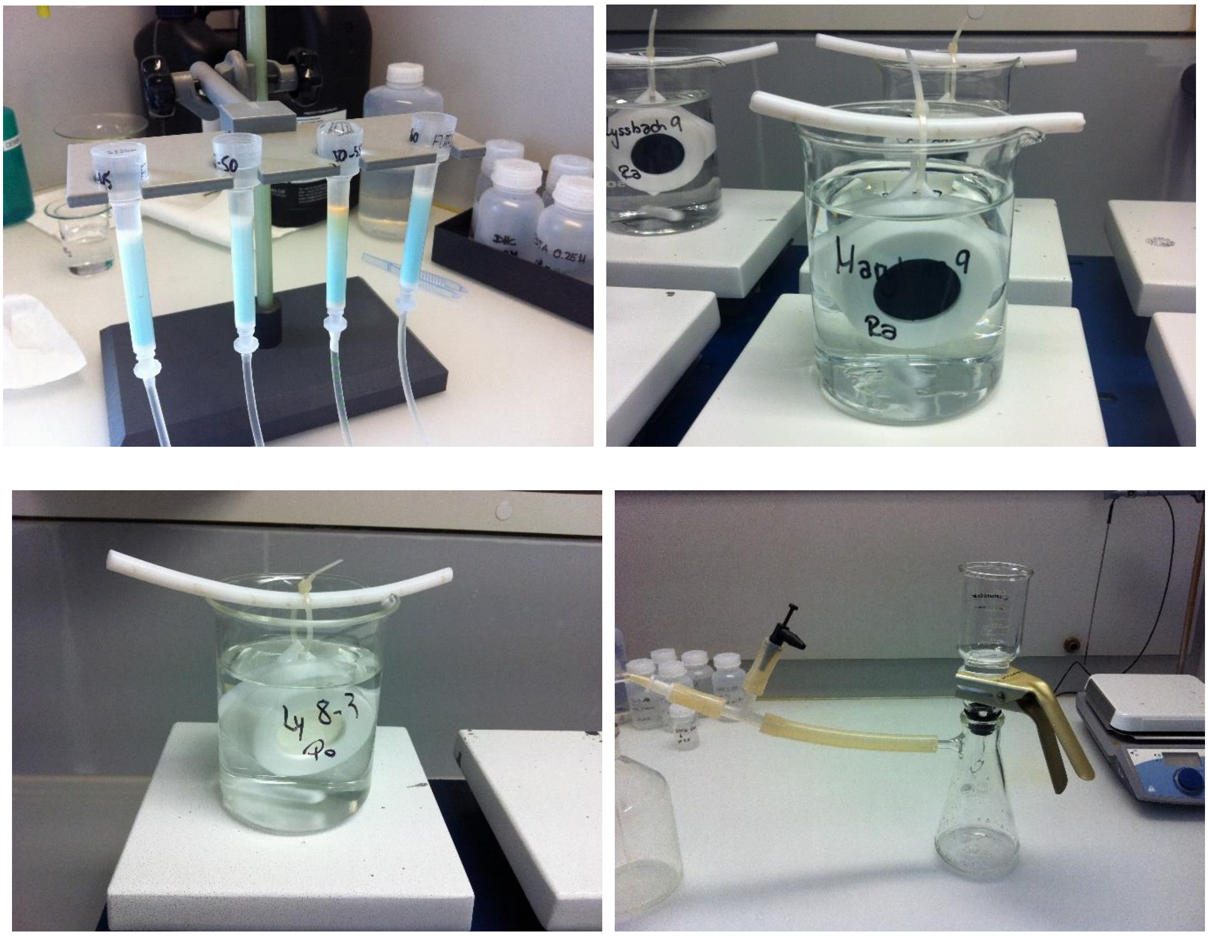

Fig. 7: Different radiochemical separation methods. Top left: UTEVA columns to separate U; Top right: Adsorption of Ra onto an MnO_2 disc; Down left: Adsorption of Po onto a Ag-planchet; Down right: Filtration of water samples in order to separate Ra form other radionuclides.

2.3 Radioactivity measurements

2.3.1 α-spectrometry

The principle of α-spectrometry is based on a specific energy quantum released by each isotope that disintegrates through α -decay (L'Annunziata, 2012). The energy range of α -emitters is 1 - 10.5 MeV which can be precisely measured using a PIPS (Passivated Implanted Planar Silicon) detector in a vacuum chamber. It is of importance to separate the elements of interest from their matrix to prevent overlapping emission energies of different α -decays. For the samples of the present thesis, this was achieved either by chromatographic separation and subsequent electrodeposition, or by spontaneous adsorption onto an element-specific material as explained already in detail in section 2.2. It is also necessary to add a radiotracer that behaves chemically the same in order to verify the chemical yield of the separation or adsorption process. The α -detector used for all measurements in this thesis was the Octête PC from ORTEC in combination with the Interwinner 7.1 program for computation. The half-life as well as the decay energies of all isotopes that have been measured by α-spectrometry together with the corresponding radiotracer are listed in Tab. 1.

Tab. 1: α-decay energies with the highest transition probabilities of the analyzed isotopes in water samples and corresponding radiotracers. All values from Magill et al., (2006). Counts from energies with lower transition probabilities were added to the higher ones.

Isotope	*Half-life*	*Decay energy [MeV]*
^{232}U	68.9 years	5.320
^{238}U	$4.468 \cdot 10^{9}$ years	4.198
^{235}U	$7.038 \cdot 10^{8}$ years	4.398
^{234}U	$2.455 \cdot 10^{5}$ years	4.775
^{223}Ra	11.43 days	5.716
^{226}Ra	1600 years	4.784
^{224}Ra	3.66 days	5.685
^{210}Po	138.38 days	5.304
^{209}Po	102 years	4.881
^{230}Th	$7.54 \cdot 10^{4}$ years	4.687
^{228}Th	1.913 years	5.423

2.3.2 Liquid scintillation counting

The principle of liquid scintillation counting (LSC) is based on the emission of photons that are detected by a photomultiplier. The liquid samples transfer their decay energy to the cocktail. The cocktail emits photons that can be detected by the scintillation counter (L'Annunziata, 2012). It is possible to detect α- and β-particles simultaneously by α/β-separation. Therefore, the regions of interest (ROI) have to be defined and the pulse length index (PLI) has to be determined. For the simultaneous measurement of ^{226}Ra (α) and ^{228}Ra (β), the ROI were set to 500-900 and 10-800, respectively. The PLI, which separates α- and β- particles according to the deactivation of the excited state of the particle, was set to 5. The ROI for ^{222}Rn measurement was 700-950 for α, 200-900 for β and the PLI 10.

2.3.3 γ-spectrometry

Some of the soil and peat samples from Mont Vully were measured directly by γ-spectrometry without radiochemical treatment. Therefore, the dried and grounded powder was filled into 50 ml plastic bottles and measured with a high purity Ge detector. Some isotopes could be measured directly by their decay energies if the transition probability of the γ-line is high enough and if there is no interference with the decay energy of another isotope. For example, ^{235}U can be directly measured by its decay energy of 186 keV. The transition probability is high enough with 53%, but the decay energy of ^{226}Ra is almost the same. So there is an overlapping of the signals of the two isotopes and a correction has to be made. If secular equilibrium can be assumed, then 43% of all impulses from the 186 keV line can be attributed to ^{235}U and 57% of the impulses can be attributed to ^{226}Ra (Giles, 1998). However, this assumption cannot be applied to all environmental samples and has to be reviewed for each single case. Furthermore, ^{226}Ra can be measured via its progenies ^{214}Pb and ^{214}Bi. However, this is only possible if they are in secular equilibrium with ^{226}Ra. The problem is that the noble gas ^{222}Rn is in between that constantly emanates out of the sample. To prevent this, the soil or peat sample can be packed gas-tightly into a 50 ml glass vial and rested for 3 weeks until secular equilibrium was established. After this waiting time, the activity concentrations of ^{214}Pb and ^{214}Bi can be measured vie its decay energies that now represent the concentration of ^{226}Ra in the sample (Tab. 2). However, the results of the gamma measurements for ^{235}U and ^{226}Ra were not given in this thesis for two reasons: (i) it was not possible to verify the gas-tight packing of the samples and (ii) there was no adequate calibration available for the glass vials.

The two U isotopes from the ^{238}U decay series can also only hardly be determined by γ-spectrometry since they don't have well detectable γ-lines. ^{238}U can be determined by measuring its decay product ^{234}Th via its 63 keV line (Tab. 2). But due to this low energy and the possible occurring self-adsorption of ^{234}Th, this method is as well not suitable for all samples. ^{234}U was not measured via γ-spectrometry. In the case of the soil and peat samples analyzed during this study, the activity concentrations for the U isotopes were all used from the α-analysis since these results were more reliable than the results from the γ-spectrometry where some more uncertainties and assumptions were included.

Tab. 2: Isotopes that were determined by means of γ-spectrometry indicating the isotope of interest and the isotope that can be measured as substitute. The values of half-lives are from Magill et al. (2006), values of decay energies and transition probabilities are from L'Annunziata (2012).

Isotope of interest	*Isotope measured*	*Half-life*	*Decay energy [keV]*	*Transition probability [%]*
^{235}U	**^{235}U**	$7.038 \cdot 10^8$ years	186	53
^{238}U		$4.468 \cdot 10^9$ years	50	0.07
	^{234}Th	24.1 days	63	4
^{226}Ra	**^{226}Ra**	1600 years	186	4
	^{214}Pb	26.8 minutes	351	37
	^{214}Bi	19.9 minutes	609	46

Chapter 3 Uranium in the Swiss Plateau

The following chapter mostly consists of the in 2019 published paper in the Journal of Environmental Radioactivity. Therefore, section 3.1. to 3.7. was integrated literally from the paper into this thesis. Merely section 3.8. was not published since it describes supplementary information in connection with the work of the paper.

Increased Uranium concentrations in ground and surface waters of the Swiss Plateau: A result of Uranium accumulation and leaching in the Molasse Basin and (ancient) wetlands?

Anja Pregler[1,4], Heinz Surbeck[2], Jost Eikenberg[1,†], Simon Werthmüller[3], Sönke Szidat[4,5], Andreas Türler[4]

[1]Paul Scherrer Institute, Department for Radiation Safety and Security, 5232 Villigen PSI, Switzerland
[2]Nucfilm GmbH, Fineta 46, 1792 Cordast, Switzerland
[3]Schenker Korner Richter AG, Büttenenhalde 42, 6006 Luzern, Switzerland
[4]University of Bern, Department of Chemistry and Biochemistry, Freiestrasse 3, 3012 Bern, Switzerland
[5]University of Bern, Oeschger Centre for Climate Change, 3012 Bern, Switzerland
[†]deceased

Manuscript published in Environmental Radioactivity 208-209 (2019) 106026.

3.1 Abstract

Increased Uranium (U) concentrations are found in certain ground and surface waters of the Swiss Plateau. Analysis of more than 100 public fountains revealed that increased ^{238}U concentrations frequently occur close to the interface between the Lower Freshwater Molasse and the Upper Marine Molasse, cropping out in the western part of the Swiss Molasse Basin. Out of these locations, Mont Vully, situated ca. 20 km west of Berne, was studied in detail. As this hill consists of the two aforementioned stratigraphic Molasse units, it represents an ideal case study. Two springs at the northern slopes of Mont Vully exhibit the highest ^{238}U concentrations with more than 300 mBq/L and were thus monitored for almost two years in order to screen possible seasonal variations. Further water samples were collected from spring captures, creeks and drainage pipes. The pipes drain the farmland north of Mont Vully showing ^{238}U concentrations with more than 600 mBq/L. In order to discover the reason for the duplication in concentration, gamma dose rate measurements were accomplished on the farmland, revealing elevated dose rates of up to 160 nSv/h. These are located above ancient pathways of creeks that originated from Mont Vully. At these locations with elevated dose rates, three shallow sediment drill cores were taken and analyzed for their U content. The sediment cores can essentially be divided into three parts: (i) an upper soil with common U concentrations of about 30 Bq/kg ^{238}U, (ii) an U-rich peat horizon with concentrations of up to 500 Bq/kg ^{238}U, and (iii) an impermeable clay unit that acts as an aquitard with again minor ^{238}U concentrations. Radiocarbon dating of the U-rich peat horizon reveals ages younger than 8.1 kyrs. This study suggests that a wetland was formed on top of the impermeable clay layer after the last glaciation during the Holocene. The stream waters with ^{238}U concentrations of more than 300 mBq/L originating from Mont Vully contributed significantly to the water supply for the development of the wetland. Due to the reducing conditions that are present in wetlands, the dissolved U in the incoming streams was reduced and adsorbed onto organic matter. Accordingly, an entrapment for U was generated, persisting for at least 6 kyrs – a sufficient time to accumulate up to 500 Bq/kg. In the course of the last century, numerous wetlands in Switzerland were drained by capturing streams and installing drainage pipes to make the land suitable for agriculture. This kind of melioration was also done at the wetlands north of Mont Vully resulting in a subsequent change in redox conditions within the soil. The solubility of U depends on its oxidation state and U can be oxidized by oxygen-rich rainwater. The rainwater leached the U adsorbed on the peat yielding ^{238}U concentrations of more than 600 mBq/L. Consequently, the duplication of ^{238}U concentrations in the drainage water as compared to the original concentration that creeks brought into the ancient wetlands has been clarified during this study. Twenty of the analyzed public fountains in the Swiss Plateau exhibited a ^{238}U concentration of more than 50 mBq/L. All of them could have contributed to the formation of a wetland after the last glaciation,

which leads to the assumption that the situation at Mont Vully is not a singularity in the Swiss Plateau.

3.2 Introduction

Uranium (U) is a toxic heavy metal that is present in most of the Earth's crust with an average abundance of 1.8 ppm (Mason & Moore, 1982). It occurs in the form of three natural radioisotopes: ^{238}U, ^{235}U and ^{234}U with isotopic ratios of 99.27%, 0.72% and 0.0054%, respectively (Chabaux et al., 2008). U has four different oxidation states, U(III), U(IV), U(V) and U(VI). U(IV) and U(VI), with their corresponding oxides UO_2 and UO_3, are the most common ones. UO_2, which is barely soluble and occurs in hydroxides, phosphates and fluorites (Keith et al., 2015), is the predominant species in reducing environments. Under oxidizing conditions, as encountered in surface and shallow groundwater, U(IV) is oxidized to U(VI), forming the easily soluble uranyl cation UO_2^{2+}, which forms different complexes with carbonates, sulphate ions and organic ligands (Chabaux et al., 2008). Due to the long half-life of ^{238}U ($T_{1/2} = 4.45*10^9$ years) and its heavy atomic mass of 238.05 g/mol, the specific activity of ^{238}U is rather low with 12 kBq/g (L'Annunziata, 2012). The radio-toxicity of U only plays a minor role compared to its more serious chemical toxicity (ESFA, 2009). Since U exposure to the general public predominantly occurs by ingestion via food and drinking water, it can cause critical damage to the human body, especially the kidneys (ATSDR, 2013). Consequently, the World Health Organization (WHO) recommends a limit of 30 µg/L U in drinking water (WHO, 2001). In 2017, the Swiss Federal Department of Home Affairs introduced its limit for U in drinking water to 30 µg/L as well (EDI, 2017). This critical value equals 372 mBq/L ^{238}U in terms of activity concentration. The dimension of ingesting U by liquid food depends strongly on diverse factors, e.g. environment of the catchment area or even personal consumption behavior. Already in 1930, Sale (1930) conducted a first survey on salts and radioactive nuclides in mineral water. Since then, studies were regularly performed all over the world in order to quantify concentrations of naturally occurring radioactivity in drinking and groundwater (Cothern and Lappenbusch, 1983, Vesterbacka, 2007, Walsh et al., 2014, Bajwa et al., 2017, Godoy and Godoy, 2006, Shin et al., 2016, Wu et al., 2014, Baradács et al., 2001, Birke et al., 2010, Baertschi and Keil, 1992). All of these studies demonstrate increased radionuclide concentrations in drinking water, but the reason for it is usually not specified in detail. A comprehensive survey for Switzerland was presented by Stalder et al., (2012), who analyzed more than 5500 water samples from most cantons of Switzerland to illustrate the geographical distribution of U concentrations in drinking water. The published map shows increased U levels along the alpine arc where crystalline bedrock with naturally enhanced U concentration in minerals is common. The map interestingly highlights another area in the western part of the Swiss Plateau, where elevated U contents cannot simply be explained by an underlying crystalline basement. Some cantons of particular interest, e.g. the Canton of Berne, were not covered in the study of Stalder et al., (2012). These data gaps and the fact that the U source in the Swiss Plateau remains rather unclear, represent the main motivation for the present study. U in groundwater, together with Radon (Rn), usually occurs as major fraction within the group of natural radionuclides. But other elements like Radium (Ra) or Polonium (Po), even in lower concentrations, contribute as well to the dose rate. Therefore, certain daughter isotopes of the ^{238}U decay chain such as ^{226}Ra, ^{222}Rn, ^{210}Pb and ^{210}Po are also determined. Since naturally occurring radioactive isotopes rarely display an equilibrium state in water (J. I. Osmond et al., 1983), the relations between the individual isotopes were examined during the study. However, groundwater is not the only hydrological unit susceptible to elevated U concentrations. Werthmüller et al., (2015) found extraordinarily high U concentrations in drainage pipes under an agriculturally used area ending up in the Lyssbach creek (10 km northwest of Berne, Switzerland). The reason for these elevated concentrations in the surface water is an U accumulation in peat ca. 0.5 m below the soil surface that is constantly leached by rainwater. One reason that was considered as U source has been the occurrence of Allalin gabbro in the area around the Lyssbach. This material which commonly contains U ores can be found in the Swiss Plateau due to glacial transportation from the Alps. Another possible explanation are coal beds with enhanced gamma dose rates that can also be found close the Lyssbach area. However, the actual origin of the U accumulation at the Lyssbach area remains unclear. Several authors assumed phosphate fertilizers containing natural U to be responsible for similar accumulations but could not definitely prove this theory (Barisic et al., 1992; Bigalke et al., 2018; Liesch et al., 2015). Another general explanation is the uptake of diverse metals and trace elements that can occur in wetlands as described, amongst others, by Gonzalez et al., (2006), Schumann et al. (2017) , Krachler et al. (2004), Li et al. (2015), Li et al. (2014) and Banning et al. (2013). This would indeed explain the process of accumulation but again does not clarify the origin of U in peat found in the Swiss Plateau. Consequently, the overall goal of this study was to explain the correlation between increased U concentrations in groundwater appearing at the slopes of Mont Vully and the U accumulation that occur underground of the farmland in the north of it. Another objective was to verify the origin of the increased U concentrations in groundwaters that can be found in wide parts of the Swiss Plateau.

3.3 Study area: Swiss Plateau

3.3.1 Geological outline

The Swiss Plateau geologically belongs to the tertiary Molasse basin, which traverses Switzerland on approximately 300 km between Lake Geneva in the SW and Lake Constance in the NE (Fig. 8). The basin is bordered to the SE by the Alps and to the NW by the folded Jura Mountains and has mostly a hillocked morphology. The development of the Swiss Plateau started in the Oligocene when the Alpine orogeny caused the formation of a foreland basin that was successively filled with sediments (Pfiffner, 2014). Although the sedimentary infill is heterogeneous, Studer (1853) classified the Oligocene and Miocene sediments of the Swiss Molasse into four groups: (i) Lower Marine Molasse (UMM); (ii) Lower Freshwater Molasse (USM); (iii) Upper Marine Molasse (OMM) and (iv) Upper Freshwater Molasse (OSM), for which the conventional German abbreviations (brackets) are used in this paper. The four groups themselves are classified into two lithostratigraphic megasequences, UMM/USM and OMM/OSM. Both megasequences display the change from a marine to a continental environment, each one coarsening, thickening and shallowing upward (Sinclair, 1991). Of particular interest for the present study is the transition between the two megasequences, i.e. the interface between USM and OMM. In the middle of the Oligocene, freshwater lakes started to become shallower ending up in a dry area that are now the sediments of the USM. During this process, dying organic material accumulated on large conglomerate and sandy alluvial fans (Matter, 1980) leading to reducing conditions in shallow water. Consequently, dissolved U species in water originating from granitic and metamorphic clasts precipitated as UO2 (uraninite) owing to the anoxic environment at the latest stage of the USM in mainly clayey to marly sediments (Cumberland et al., 2016; Schott & Wiegand, 2003). The transgression of the Burdigalian Sea in Miocene buried the deposited UO2 under glauconitic marine sandstones, leaving behind an interface between USM and OMM partially loaded with U-rich fossils (Schott & Wiegand, 2003). According to Keller (1922), the UMM, USM and OSM act as aquitards with some sporadic water-bearing layers, whereas the OMM represents the only aquifer in the Molasse sequence. In the Pleistocene, the ice of the Würm glaciation locally eroded the OSM, leading to an exhumation of the OMM aquifer that now crops out as the uppermost unit in certain areas (Ramseyer, 1952).

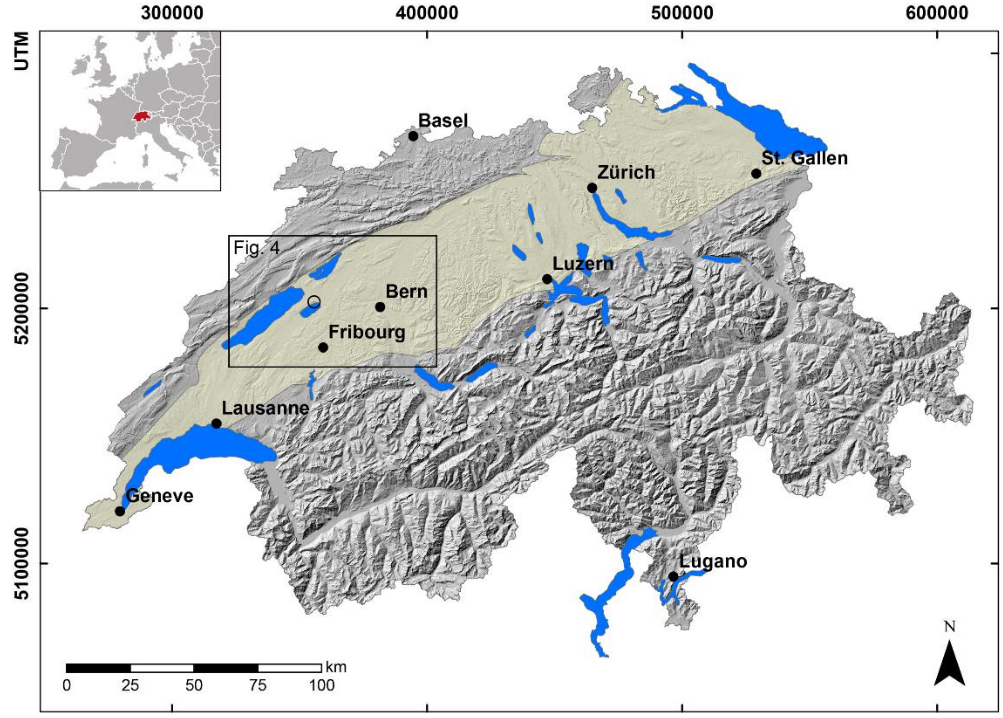

Fig. 8: Shaded relief map of Switzerland indicating the dimension of the Swiss Plateau (yellow), the area of the broader sampling campaign (rectangle) and the location of the intensively studied site Mont Vully (circle).

3.3.2 Case study Mont Vully

Mont Vully, located ca. 25 km west of Berne, was chosen as our main study site to investigate the relationship between increased U concentration in groundwater and accumulated U in soils of the Swiss Plateau (Fig. 8). The site comprises the hill of Mont Vully itself and the adjacent farmlands to the north (Fig. 9). Mont Vully has a height of 653 m a.s.l (the elevation of the surrounding plateau is 430 m a.s.l) and is composed of an USM-OMM sequence (Fig. 10a). Its detailed geology has been extensively studied earlier (Antenen, 1936; Becker, 1973; Ramseyer, 1952; Schott & Wiegand, 2003). Of particular importance for this study is that rainwater infiltrates the OMM aquifer until it is dammed by the impermeable USM. The convex interface between the USM and OMM at Mont Vully acts as a reservoir for the incoming rainwater and consequently leads to the occurrence of several springs at the slopes of the hill (Ramseyer, 1952). The discharged water accumulates to small creeks that have been existing since the last glaciation (Becker, 1973). The continuous supply of water in combination with an underground impermeable layer led to the formation of wetlands north of Mont Vully. At the beginning of the 19th century, numerous wetlands in Switzerland were drained in order to create arable land for agriculture (Klaus, 2007). Commonly, this was accomplished by perforation of the impermeable layers and installation of drainage pipes that allowed runoff of the excess water to leave a dried peat layer underground behind. In the case of

Mont Vully, there are two drainage pipes that feed the Broye Canal north of the hill (Fig. 9). Most of the springs that formerly fed the wetlands are nowadays captured for water supply and only some little creeks are left. Changes in the flow paths of the creeks can be traced in the "Journey through time – maps" provided by the Swiss Federal Office of Topography (2019).

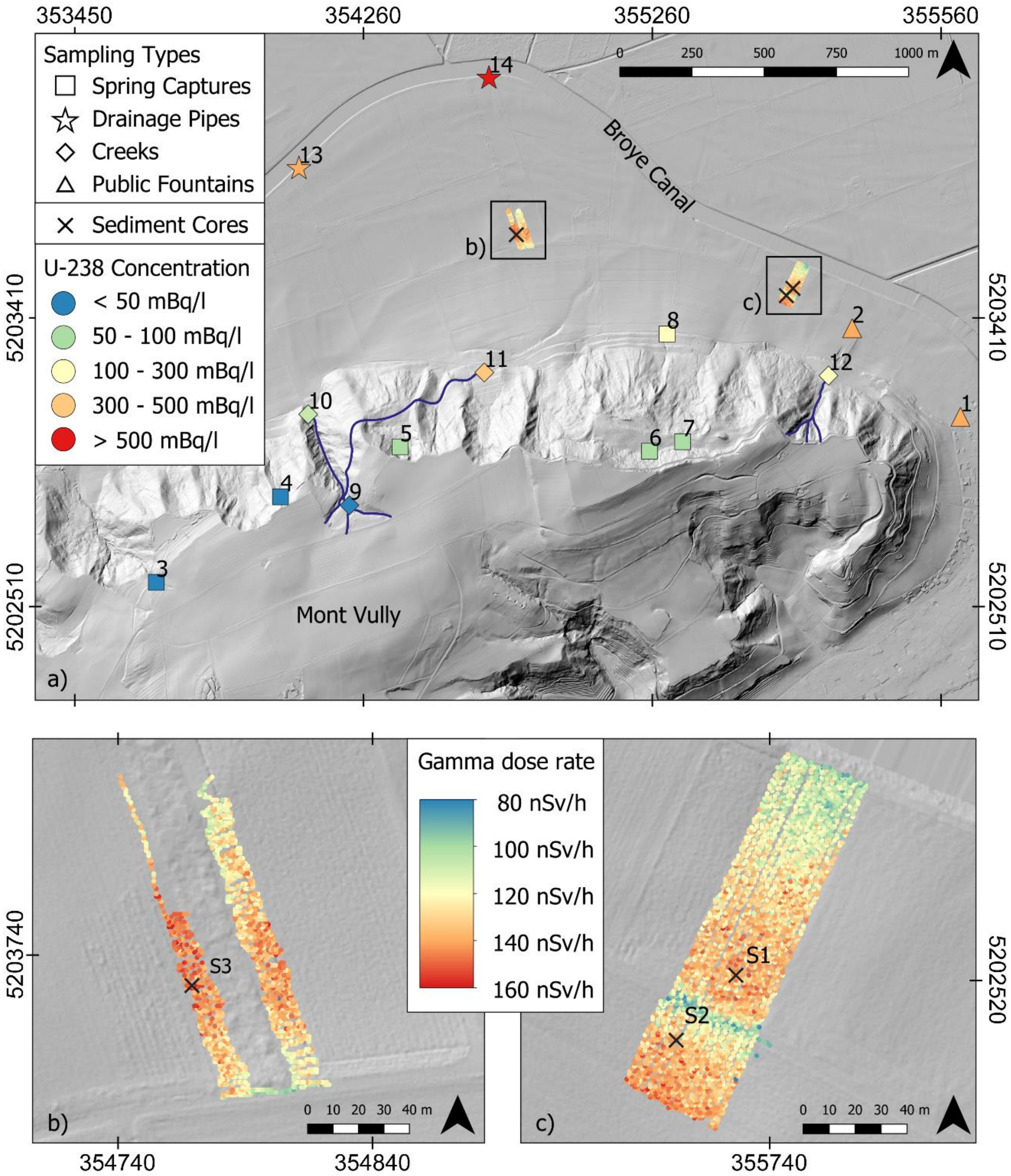

Fig. 9: Shaded relief map of the study site Mont Vully (Source of lidar data: GIS Competence Centre, Department of Land-Registry and Geomatics, Canton Fribourg). a) Four different water sampling types at Mont Vully indicating the 238U concentration of each water sample. Numbers 1-14 correspond to the numbers listed in table 1. Crosses show the location of the 3 sediment cores. b + c) Detailed map of the gamma dose rate measurements north of Mont Vully showing the exact location of the sediment cores in related to the dose rate.

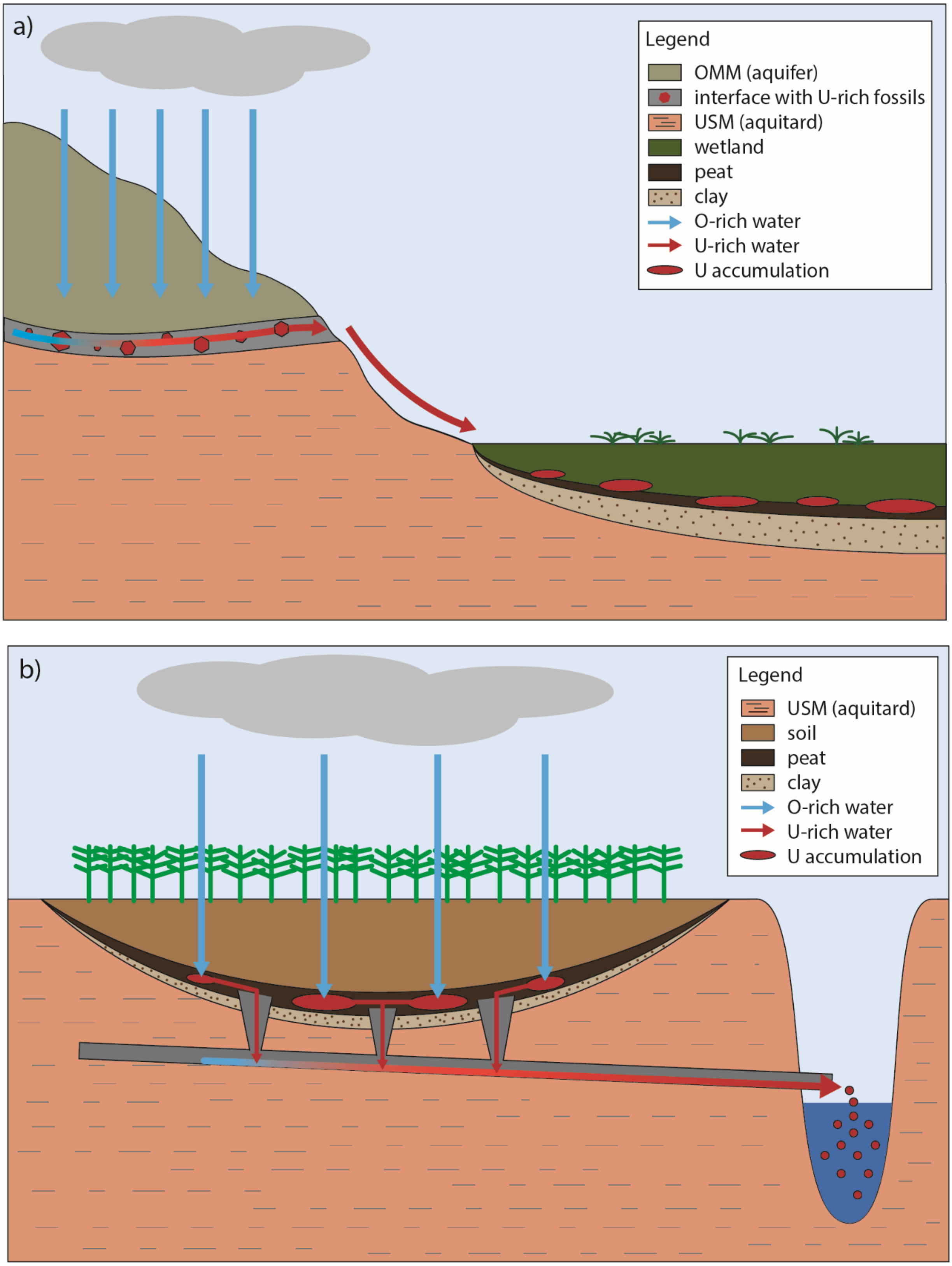

Fig. 10: Schematically drawn cross-section illustrating different stratigraphic units at Mont Vully and the farmland north of it. Not drawn to scale. a) Oxygen-rich rainwater infiltrates OMM, leaches U adsorbed onto fossils and becomes U-rich groundwater that accumulates in the reducing environment of the developing wetland. b) Oxygen-rich rainwater infiltrates drained wetland and leaches accumulated U in a peat horizon before ending up in surface waters.

3.4 Material and Methods

3.4.1 Collection of water samples

In the course of this study, 103 water samples were taken from a broad area in the Swiss Plateau, concentrated along the USM/OMM interface (Fig. 11) in order to map increased U concentrations. Most of the sampling points are public fountains. Formerly used as drinking troughs for farm animals, they can be found in the majority of old parts of towns and villages in Switzerland. The fountains are usually fed by sources from the close vicinity and are not treated by the local water supply facilities. The sampling campaign was accomplished in October 2017 as well as in July, October and December 2018. For each sampling site, one 250 mL polyethylene bottle was completely filled with water and subsequently acidified with a few drops of concentrated nitric acid (HNO_3) to prevent adsorption of radionuclides onto the bottle walls. Filtration was not necessary since there was no suspended matter visible. However, it was tested for several samples and the results in the filtered and unfiltered aliquots were identical within uncertainties. Only U isotopes were analyzed in these water samples.

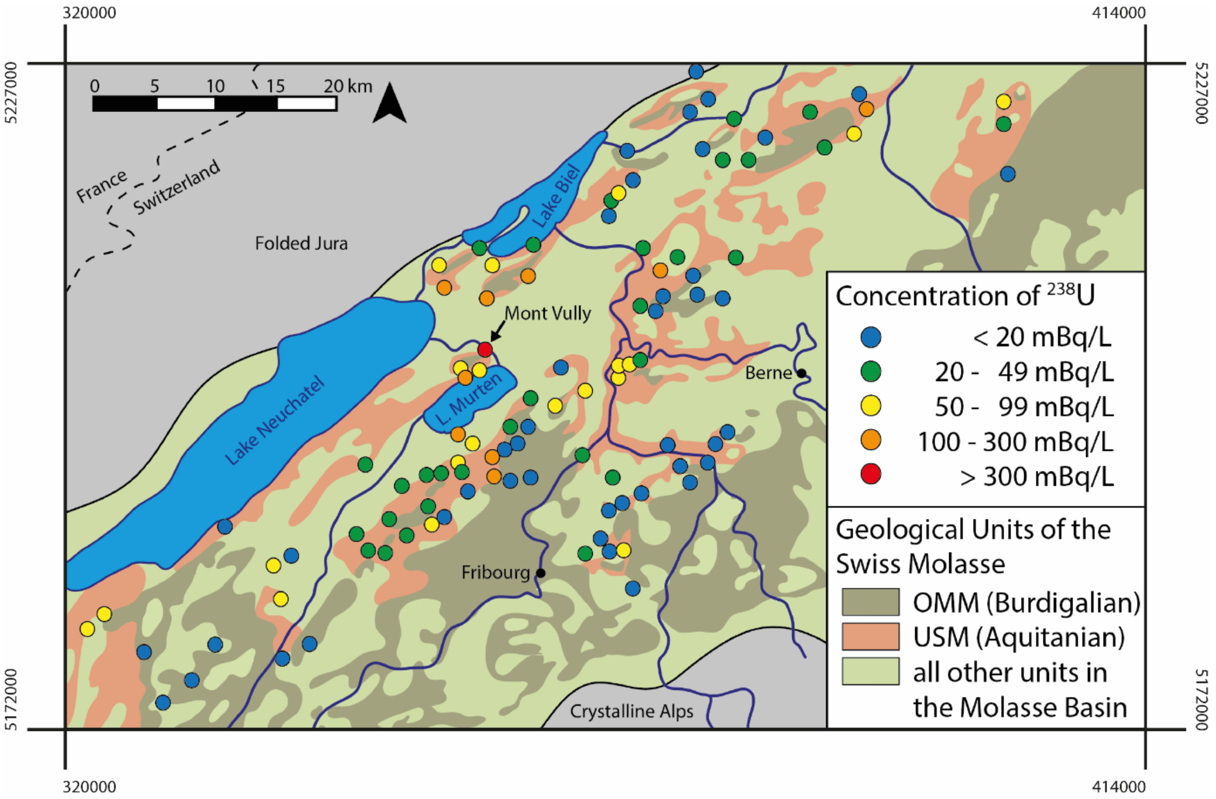

Fig. 11: Geological map of the Molasse basin indicating the areas where USM (pink) and OMM (brownish) are outcropping. Colour-coded dots show the water sampling locations with their according U activity concentrations.

At Mont Vully, the following sites were sampled for radionuclide analysis (Fig. 9): (i) 3 creeks, of which one was sampled at two locations: at the top and at the foot of Mont Vully, (ii) 6 sealed spring captures that are only accessible with the permission of authorities, (iii) 2 drainage pipes that are installed under the farmland north of Mont Vully and (iv) 2 public fountains. The two public fountains (No. 1: Fontaine Marylène in the west and No. 2: Fontaine du Stand in the north of Mont Vully) were continuously sampled in a monthly interval for two consecutive years in order to screen possible seasonal variations. A complete radionuclide analysis of ^{238}U, ^{234}U, ^{226}Ra, ^{222}Rn, ^{210}Pb and ^{210}Po was accomplished for these samples. Two 1L polyethylene bottles were completely filled and acidified with a few drops of concentrated HNO_3. For the ^{222}Rn measurements, special 20 mL glass vials with a gas tight septum in the cap were used in order to preclude the gaseous Rn to degas out of the water. The vials were overfilled and carefully closed in such a way that no air bubbles remained inside the vial. For the public fountains, electrical conductivity, pH and temperature of the outflowing water were immediately determined in the field using a handheld meter (HI98129 COMBO Tester from HANNA Instruments Switzerland AG). Furthermore, the flow rates of the two springs were measured in order to evaluate the radionuclide concentration after subsequent laboratory analyses. Only 250 mL were needed for the remaining 12 sampling locations at Mont Vully (No. 3-14) since they were simply analyzed for their U content.

3.4.2 Laboratory water sample analysis

Determination of ^{238}U and ^{234}U

For the analysis of two of the three naturally occurring U isotopes, 250 mL of the water sample were acidified with 5 mL concentrated HNO_3 and evaporated to complete dryness. Chemical yield was checked by adding ^{232}U as radiotracer. The residue was re-dissolved, filtrated through a 0.45 µm cellulose nalgene filter and passed through a Triskem U/TEVA column to separate U from Ra, Po and Th. The procedure of the chromatographic extraction was adapted from the procedure of Howrwitz et al. (1992). The resulting concentrated U solution was used for electrodeposition onto a stainless steel disk. The detailed electrodeposition procedure is described in Bajo and Eikenberg (1999). The disk was measured using an Octête PC α-spectrometer from ORTEC.

Determination of ^{210}Po

The activity concentration of ^{210}Po was determined by spontaneous adsorption of Po onto a silver disk. The chemical yield of the adsorption process was controlled by adding a defined amount of

^{209}Po tracer. The water sample was acidified with concentrated HCl. Ascorbic acid was added to reduce potential Fe(III) to Fe(II). A silver disk with 28 mm in diameter was mounted into a teflon holder in that way, that only one side of the silver disk was in contact with the solution. The holder was completely placed into the solution for approximately 24 hours under continuous stirring. After adsorption, the disk was directly measured by α-spectrometry for one week. The procedure was adapted from Lee et al. (2014).

Determination of ^{226}Ra and ^{210}Pb

^{226}Ra was analyzed together with ^{210}Pb by means of a 3M Empore Rad Disk filter. The procedure was adapted from Wallner et al. (2008). Since activity concentrations were expected to be extremely low, 1.5 L of sample volume was needed to reach an appropriate detection limit of 50 mBq/L. Pb was extracted from the Rad Disk filter with 5 mL di-Ammonium hydrogen citrate (DHC) and mixed with 15 mL Optiphase Hisafe 3 scintillation cocktail from Perkin Elmer. Ra was eluted with 5 mL alkaline EDTA solution and mixed with 15 mL Goldstar scintillation cocktail from Meridian. Liquid scintillation counting was performed using an HIDEX 300 SL scintillation counter with simultaneous α/β-counting and pulse shape analysis. A detailed explanation of this counting method is given in Eikenberg et al. (2014).

Determination of ^{222}Rn

Radon was also analyzed by means of liquid scintillation counting. With the help of a syringe, 5 mL of the immiscible liquid scintillation cocktail MaxiLight from HIDEX were carefully sublayered with 10 mL of sample water in a 20 mL scintillation vial. After vigorously shaking the vial, ^{222}Rn and its short-lived daughters are equilibrated during 3 hours and measured with a HIDEX 300 SL for 1 hour with α/β-separation.

3.4.3 Gamma dose rate measurements

In order to discover potential U accumulations below the recent farmland at Mont Vully, gamma dose rate measurements were conducted either with a handheld 2”x2” NaI(Tl) detector (a modified Gate Frisker from Ludlum) or with a large plastic scintillator (BDKG-32 from Atomex). These measurements were accomplished by walking grid-wise along the farmland, carrying the detector together with a GPS 1 m above ground. The count rate for the energy region from about 100 to

1000 keV was converted to approximate dose rates by calibration with an Automess 6150 AD-6/H connected to a large plastic scintillator 6150 AD-b/H. The detector records the total gamma radiation, which mainly originates from the decay products of ^{226}Ra such as ^{214}Pb or ^{214}Bi and quantifies the measurements with a sensitivity of 1 cps per nSv/h. Since these dose rate measurements a not precise enough, the results cannot be used for absolute quantification of U concentration in the underground, but they give an indication where U accumulations occur in the soil. Due to the fact that the area north of Mont Vully is intensively used for agriculture, the dose rate measurements were restricted to two small fields where it was possible to walk without destroying any crops (Fig. 9). On the basis of these measurements, locations with elevated dose rates were selected for soil sampling.

3.4.4 Soil sampling and analysis

In March 2018, three sediment cores (S1 – S3) were drilled into 1 m depth at the previously identified locations north of Mont Vully by means of vibrocoring with the portable drilling unit “Cobra” of Atlas Copco (Fig. 9). The cores with an inner diameter of 6 cm were cut into 5-10 cm pieces and packed into plastic bags for protection. In the laboratory, the samples were unpacked, dried in the oven at 105°C for 15 hours and ground to a homogeneous powder. An aliquot of each sample was wet and dry ashed and leached by boiling the residue in 8 M HNO_3 and 30% H_2O_2 for 1 hour. The suspension is filtrated to separate the leached fraction from insoluble compounds. Afterwards, U was analyzed identically to the procedure already used for the water samples (section 3.4.2).

3.4.5 ^{14}C dating

Dating of the peat horizons from the sediment cores was accomplished by the ^{14}C method. Potential fractions of carbonate and humic acids were removed from an aliquot of the samples using an acid-base-acid treatment. Subsequently, the residue was completely combusted and then transformed into graphite targets. Measurements were conducted with the accelerator mass spectrometer (AMS) MICADAS at the LARA laboratory at the University of Bern. The detailed procedure is given in Szidat et al. (2014). The measured ^{14}C ages were calibrated using IntCal13 to provide the calendar ages of the samples (Reimer et al., 2013). The lower and the upper part of the peat horizons from the drilling cores of the former wetland were used for dating in order to estimate the beginning and the end of the peat deposition period and to verify if the sediment cores still show an undisturbed sequence at least below the tillage depth. For the first sediment core (S1), two peat horizons extend from 45-60 cm depth and from 80-90 cm depth, while one peat horizon is located each in sediment core 2 (S2) and sediment core 3 (S3) in 75-100 cm and 65-100 cm depth, respectively.

3.5 Results

3.5.1 Extended sampling campaign in the Swiss Plateau

The U concentrations in water samples of the extended sampling campaign range from 4 ± 2 mBq/L for ^{238}U and 5 ± 3 mBq/L for ^{234}U to 239 ± 35 mBq/L for ^{238}U and 298 ± 43 mBq/L for ^{234}U (Fig. 12). Twenty of the 103 samples display a ^{238}U activity concentration of more than 50 mBq/L and 10 of more than 100 mBq/L. Due to the protection of data privacy, the exact values and locations of the extended sampling campaign are not specified. The highest value in the here studied part of the Swiss Plateau was found for one sampling date at Mont Vully with 395 mBq/L ^{238}U. This was the only sampling location that exceeded the Swiss EDI limit for U of 30 µg/L, which corresponds to 375 mBq/L ^{238}U.

3.5.2 U-series disequilibrium in water at Mont Vully

The two public fountains at Mont Vully were continuously monitored once per month over a two-year period from 2016 to 2018, allowing for a detection of seasonal effects. The sampling campaign for Fontaine Marylène (No. 1) started in June 2016 with a total of 20 water samples; sampling of Fontaine du Stand (No. 2) was initiated in November 2016 with a total of 17 water samples. For these two sampling points at Mont Vully, the flow rate depended upon the amount of precipitation in the catchment area. The monthly and annual precipitation can be tracked at the corresponding maps of MeteoSwiss, which show that a dry period leads to a lower flow rate approximately 6 months afterwards (Swiss Federal Office of Meteorology and Climatology Meteo Swiss, 2019). For both springs, the water temperature was directly coupled with the seasonal outside air temperatures: highest water temperatures were found in September 2017 with 20 °C; lowest in January 2017 with 5°C. The pH of 7.4 ± 0.1 as well as the electric conductivity of 610 ± 15 µS/cm were constant throughout the whole sampling campaign. The activity concentrations exhibit a complete disequilibrium within the ^{238}U decay series, but the concentrations within one particular isotope in the decay chain are fairly constant (Fig. 12). The highest values were found for ^{222}Rn with a mean of 32000 ± 4000 mBq/L and 31000 ± 3000 mBq/L for Fontaine Marylène and Fontaine du Stand, respectively. Lowest concentrations were found for ^{210}Po with 3 ± 2 mBq/L for Fontaine Marylène and 2 ± 1 mBq/L for Fontaine du Stand. ^{210}Pb activity concentration for all samples were below the detection limit of 50 mBq/L. But due to the rather short half-life of ^{210}Po ($T_{1/2}$ = 138 days), ^{210}Pb and ^{210}Po should be in secular equilibrium and the activity concentration of ^{210}Pb can be expected to be in the same range as ^{210}Po. A mean of 62 ± 8 mBq/L for both springs was detected for ^{226}Ra. The activity concentrations of the two U isotopes lie within the same range for both fountains: Fontaine Marylène exhibited mean values of 319 ± 26 mBq/L and 346 ± 25 mBq/L for ^{238}U and ^{234}U, respectively, and Fontaine du Stand displayed mean values of 308 ± 22 mBq/L and 333 ± 18 mBq/L for ^{238}U and ^{234}U. The activity ratio (AR) of ^{234}U/^{238}U was equal with 1.08 ± 0.04 for both fountains. All activity concentrations were constant within uncertainties over the whole sampling period, regardless of seasonal variations like temperature or precipitation. The results of the U analysis for all sampling locations at Mont Vully are listed in Tab. 3.

Tab. 3: ^{234}U and ^{238}U concentrations and AR in different water samples at Mont Vully (uncertainties 2σ). The numbers in the first column correspond to the numbers in figure 2.

No. in fig. 2	*Type*	*^{238}U [mBq/L]*	*±*	*^{234}U [mBq/L]*	*±*	*AR*
1	public fountain (mean value)	319	26	346	25	1.1
2	public fountain (mean value)	308	22	333	18	1.1
3	spring capture	36	7	31	7	0.8
4	spring capture	32	7	28	7	0.9
5	spring capture	82	18	88	18	1.1
6	spring capture	86	15	75	14	0.9
7	spring capture	100	17	88	16	0.9
8	spring capture	290	30	301	30	1.0
9	creek	37	8	39	8	1.0
10	creek	60	11	65	12	1.1
11	creek	361	56	327	51	0.9
12	creek	204	23	193	22	0.9
13	drainage pipe	402	58	361	53	1.1
14	drainage pipe	626	88	648	90	1.0

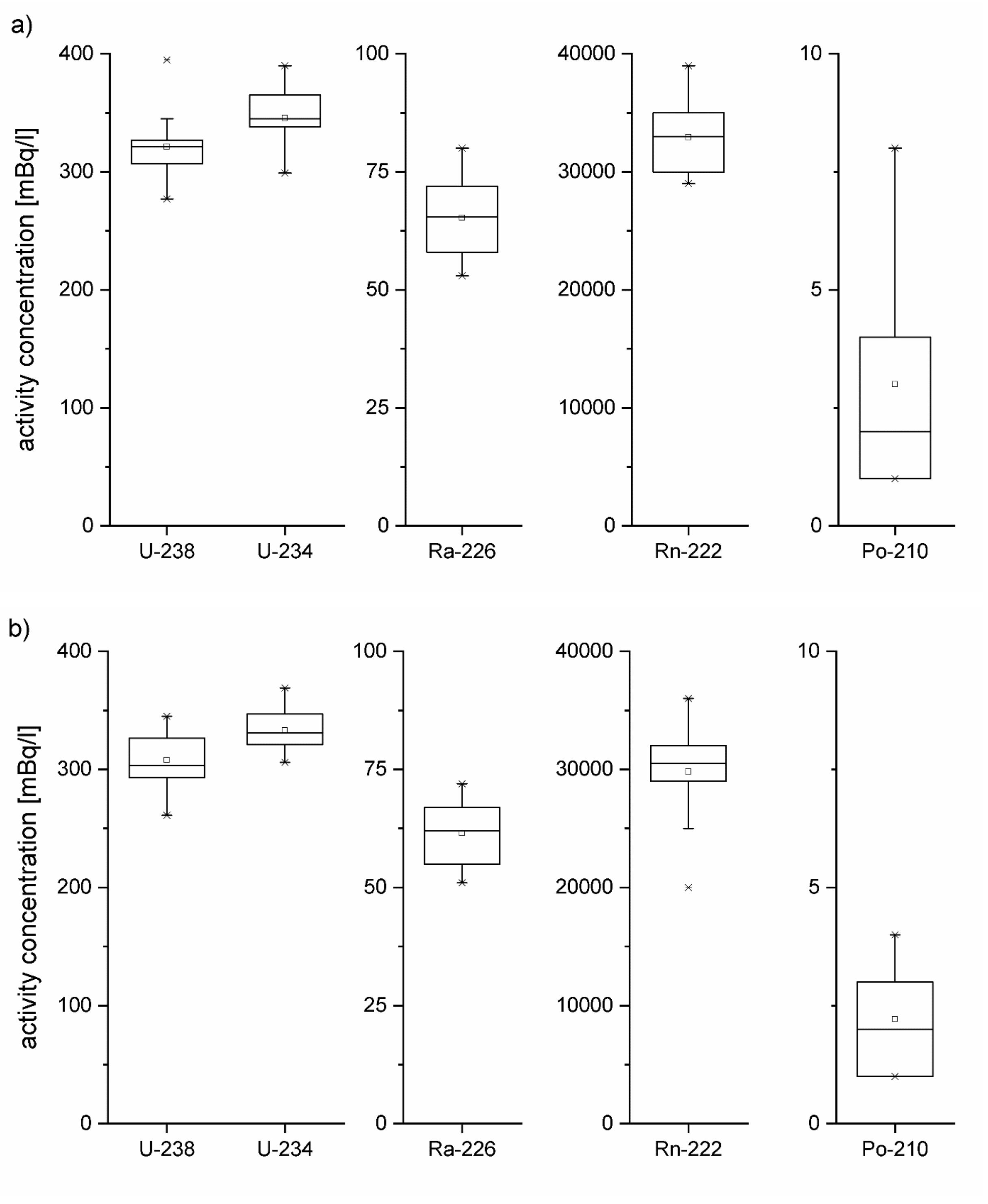

Fig. 12: Boxplot diagrams of a) Fontaine Marylène and b) Fontaine du Stand indicating the activity concentrations for the different radioisotopes of the ^{238}U decay series throughout the whole sampling campaign. Note the different scales of axes.

3.5.3 Gamma dose rates at Mont Vully

Gamma dose rate measurements on the farmland north of Mont Vully revealed increased gamma dose rates of up to 160 nSv/h including background radiation. In other parts of the area north of Mont Vully, only 80 nSv/h was detected (Fig. 9). The locations with elevated dose rates were selected as sites for percussion drilling, since they offer the highest probability of finding an U accumulation.

3.5.4 Uranium content of soil samples

All three sediment cores can essentially be divided into three parts: (i) an upper part that consists of soil and loam with common U concentrations of about 30 Bq/kg ^{238}U, (ii) an U-rich peat horizon with concentrations of more than 500 Bq/kg ^{238}U, and (iii) an impermeable clay unit that acts as an aquitard with again minor ^{238}U concentrations (Fig. 13). However, the sediment cores differed from each other in their total U content as well as in the depth where the U-rich peat horizons were located. S1 exhibited the highest ^{238}U concentrations of all sediment cores at a depth of 55-60 cm with 543 ± 75 Bq/kg. S2, which was taken only 45 m away from S1, showed values of 313 ± 36 Bq/kg ^{238}U at 95-100 cm depth. The highest concentrations in S3 were found at 90-100 cm depth with an activity concentration of 437 ± 49 Bq/kg ^{238}U. The ^{234}U/^{238}U AR in all peat samples was 1.06 ± 0.03.

3.5.5 ^{14}C ages of peat at Mont Vully

Radiocarbon dating of the peat yielded slightly different ages for all three sediment cores. The lower part of the first peat horizon of S1 in 55-60 cm depth was dated to 3765 ± 20 years, the upper part at 40-45 cm depth to 1875 ± 20 years. The second peat horizon of S1, that extends from 80-90 cm depth, was dated to 7180 ± 25 years at the lower end. S2 revealed similar ages of 3415 ± 20 years and 1815 ± 20 years for the lower (95-100 cm) and upper (75-80cm) part of the peat horizon, respectively. S3 showed higher ages of 5230 ± 20 years at 90-100 cm depth and 2765 ± 20 years at 60-70 cm depth. From these ^{14}C ages, the following calibrated age ranges of the peat horizons were deduced (Fig. 13): S1: 1.8-1.9 to 7.9-8.0 kyrs, S2: 1.8-1.9 to 3.6-3.8 kyrs, S3: 2.8-3.0 to 6.0-6.1 kyrs. As these calibrated age ranges only allow an estimation of the duration of the peat formation (see below in the Chapter Discussion), they are given in centennial resolution.

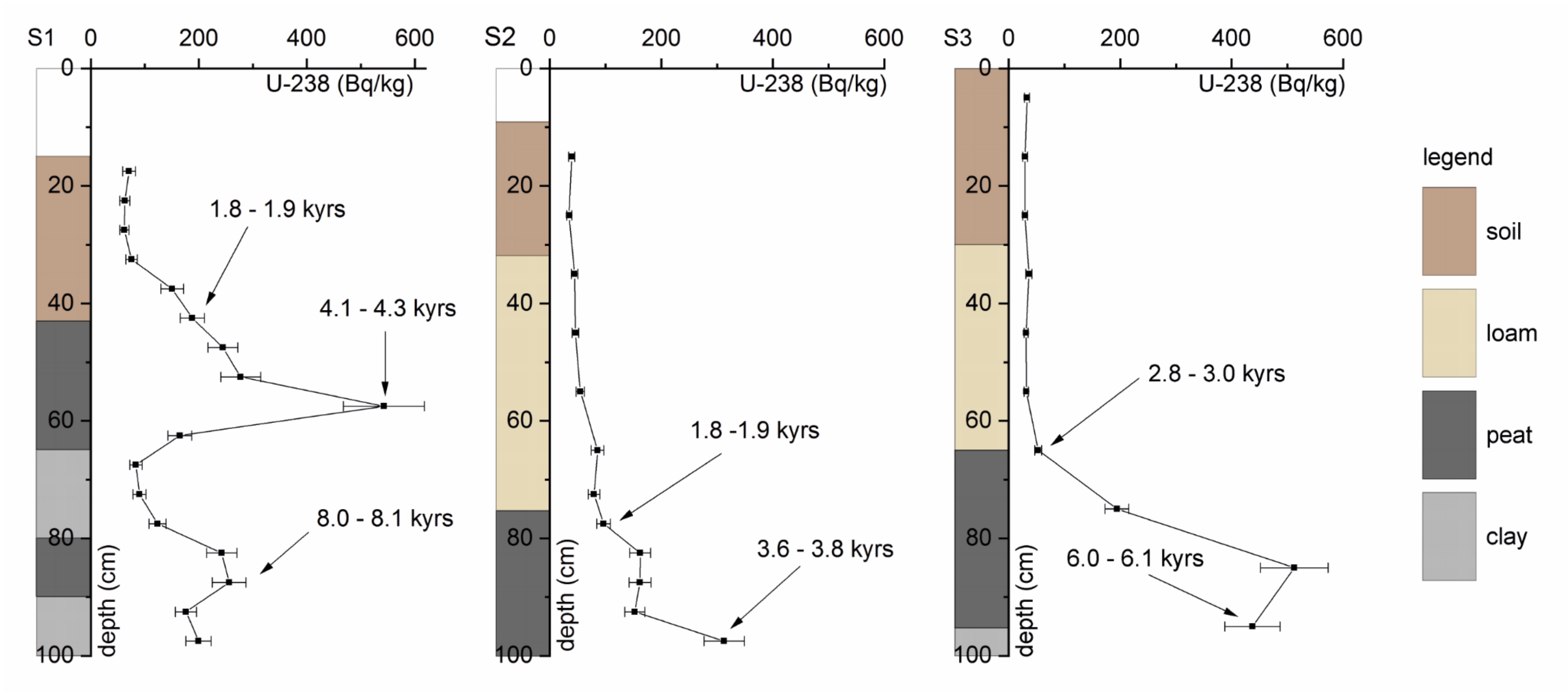

Fig. 13: ^{238}U concentration of 238U concentration of the 3 sediment cores plotted against depth. Colour-coding at the left side of the Y-axis illustrates the different soil components of each sediment core. Additionally, the 14C ages are labelled at the corresponding depth.the 3 sediment cores plotted against depth. Colour-coding at the left side of the Y-axis illustrates the different soil components of each sediment core. Additionally, the ^{14}C ages are labelled at the corresponding depth.

3.6 Discussion

In the following, we present our model for the increased U concentrations in soil, ground and drinking water in the Swiss Plateau as a four-stage process of U accumulation and leaching. The first two steps – originally suggested by Schott and Wiegand (2003) – comprise the accumulation of U at the USM/OMM interface in Oligocene and the ongoing leaching of U-rich fossils by infiltrating rainwater at this interface (Fig. 10a). The third and fourth step are findings of the present study and include the accumulation of U in bogs and wetlands and anew leaching processes that started in the 19th century, when wetlands were drained (Fig. 10b).

As already explained in section 2, fossils encrusted with U can be found at the interface between USM and OMM along the western part of the Swiss Plateau (Ramseyer, 1952). Since the USM represents an aquitard, rainwater with high oxygen content infiltrates the OMM and is retained at the interface between the two Molasse units where U-rich fossils occur (Fig. 10a). The study of Schott and Wiegand (2003) identified the following process: At the USM/OMM interface, the rainwater oxidizes the precipitated insoluble U(IV) to soluble U(VI) resulting in a constant leaching process of the fossils. The rainwater with dissolved U migrates along the impermeable USM until the interface reaches the surface. At these points, springs of groundwater with increased U activity concentrations are welling out of the hills. Extended sampling on the basis of geological maps accomplished by the present study highlights the frequency of enhanced U concentrations along the USM/OMM interface (Fig. 11). The characterization of the water samples that are in connection with the interface is based on the stratigraphy of the two Molasse units, i.e. the OMM (brownish in Fig. 11) lies above the USM (pink in Fig. 11). For water samples that are located only in the OMM it is impossible to pass the interface and therefore cannot leach potential U accumulations. None of these samples in the OMM show increased U concentrations. Water samples that derive from an area where the interface could have been passed show moderate to increased U concentration. Certainly, there are water samples that are located at the interface and do not show increased concentrations. These samples either pass the interface at an area where there is no U accumulation or the interface is not passed at all in spite of its vicinity. This correlation can be seen more in detail at Mont Vully. The sample locations which derive only from the OMM on top of the hill (No. 3, 4 and 9 in Fig. 9) exhibit nearly no U content in comparison with the water samples that are located below the USM/OMM interface (No. 1, 2, 8, 11, 12 in Fig. 9). Waters sampled on the slopes between the top and bottom of Mont Vully show intermediate concentrations (No. 5, 6, 7, 10 in Fig. 9). The creek that was sampled at two locations is the best example in that regard: The ^{238}U concentration doubles in value from the very top (No. 9 in Fig. 9) of Mont Vully until the foot (No.10 in Fig. 9). This implies that there is a groundwater flow with increased U concentration into the creek before it reaches the second sampling location. The two springs with water originating from the USM/OMM interface that were selected for a detailed investigation of U concentrations are Fontaine Marylène (No. 1 in Fig. 9) and Fontaine du Stand (No. 2 in Fig. 9). It is known from the municipal water supply responsible Mr. Biolley (personal communication, January 2017) that they originate from one source deriving from the U-rich interface but cover different distances until they reach the surface. For this reason, the two sources are considered as one in the following explanations. The fairly constant values throughout the whole sampling campaign (Fig. 12) demonstrate that the water of the fountains is rather groundwater that, in comparison with surface water, is not quickly prone to changes in geochemical conditions. As well as Shchott and Wiegand (2003) we assume steady oxidizing conditions at the USM/OMM interface that allow U to be leached (Ivanovich & Harmon, 1992). Therefore, U occurs in increased activity concentrations in the water, whereas its decay products remain unleached. ^{226}Ra is rarely soluble under oxidizing conditions (Faure & Mensing, 2005) and is measured only in small amounts of maximum 80 mBq/L. The same is true for ^{210}Po, which is poorly soluble (Ivanovich & Harmon, 1992) and therefore does not even allow the detection limit to be reached in some of the water samples. However, speciation taking into account that radionuclides may not only be transported as dissolved ions or complexes but also attached to colloids (inorganic and organic matter, e.g. extracellular bacterial material (Larock et al., 1996; Ram et al., 2019) was not covered in this work. Transport by colloids might explain the ^{210}Po values found in some of the water samples but further investigation needs to be done. The radionuclide that exhibits highest activity concentrations is ^{222}Rn with almost 40000 mBq/L. This is obvious since Rn is the only gaseous element in the ^{238}U decay chain and can be transferred into water much easier than solids. The mean AR of ^{234}U/^{238}U was 1.08 ± 0.04. The reason for these increased values of ^{234}U in comparison to ^{238}U in water is preferential leaching from the solid phase, enabled by radiation damage of the crystal lattice. This damage is the result of recoil that breaks the bond which retains the nuclide inside the crystal lattice resulting in a better leachability of the following isotopes in the decay chain (J. K. Osmond & Cowart, 1976). Consequently, the leached solid phase should exhibit depletion in ^{234}U.

The next part in this four-stage process is directly connected to the U-rich groundwater found in certain parts of the Swiss Plateau. After the end of the last glaciation and later during the Holocene, bogs and wetlands had developed on top of an impermeable clay layer north of Mont Vully due to the constant supply of water from the USM/OMM interface on the one hand, and a lack of possibilities to runoff on the other hand (Fig. 10a). Dying organic material and microbial degradation led to a reducing environment in the wetlands and cumulated organic matter was deposited in the peat horizon on top of the clay layer. The solubility of U is very sensitive to redox conditions. When dissolved U species in groundwater deriving from the USM/OMM interface enter the anoxic environment in the wetland, the soluble U(VI) is reduced to insoluble U(IV) and adsorbs onto organic material (Wang et al., 2014). Accumulation over thousands of years led to a considerable amount of U in the wetland peat, although the concentration of the input water was comparably small. Measurements of gamma dose rates on the farmland north of Mont Vully already indicate an accumulation of U in a peat horizon underground, as evidenced by gamma radiation that is highly increased with respect to normal background values. Rybach et al. (1997) reported an average total dose rate of 147 nSv/h in Switzerland combining artificial, cosmic and natural terrestrial dose rates. However, this value considers all parts of Switzerland including highly enhanced dose rates originating from the Alpine region with natural terrestrial dose rates that reach a maximum of 368 nSv/h (Rybach et al., 1997). Considering the average total dose rate in the area of Mont Vully, values above 80 nSv/h are clearly enhanced in comparison to the normal background (Rybach et al., 2002). As these values are no absolute values and vary with depth of the U-rich peat horizon, verification had to be done by analyzing the soil itself. The results of the cores confirm that the peat horizon has accumulated a considerable amount of up to 543 ± 75 Bq/kg ^{238}U (this value equals 43.8 ppm ^{238}U) in spite of the rather low U concentration of the incoming water with only approximately 350 mBq/L ^{238}U (this values equals 0.03 ppm ^{238}U) – assuming these concentrations were constant over the Holocene. Radiocarbon dating of the organic material at the lower end of the peat horizons revealed an onset of the peat formation of around 4-8 kyrs ago (Fig. 13). This verifies the assumption that the wetlands began to form after the Würm glaciation, when an excess of water was available. Sediment core S1 revealed, however, that there is more than one peat horizon, separated from each other by a 15 cm thick clay layer. This indicates that there have been several peat accumulation cycles, which were not covered by the soil cores into 1 m depth. It is very likely that there are more peat horizons below 1 m and that the real onset of peat formation started earlier. We therefore assume that the onset started at the earliest 16 kyrs ago when the Würm glaciation terminated (Ndiaye et al., 2014). The development of the uranium-accumulating peat in sediment core S1 started during the onset of the mid-Holocene summer maximum ~8 ky ago. The maximum U concentrations in all 3 sediment cores are in 4 kyrs old peat layers. This coincides almost with the highest level of the mid-Holocene summer maximum in Central Europe which was ~6 ky ago (Davis et al., 2003). According to the dating results, the end of peat accumulation seems to have occurred 2-3 kyrs ago. We assume, however, that peat formation discontinued only a few centuries ago after a land-use change from near-natural wetland to an intensively managed grassland. This change typically involves a decrease of the water table, which promotes aerobic decomposition of sub-surface peat so that the ^{14}C age of the top peat layer appears to be older than the date of the land-use change (Krüger et al., 2015). Since then, the former wetland was covered with a soil layer of up to 70 cm thickness. The upper soil was not infiltrated with U-rich groundwater and therefore does not show increased U values. The concentrations lie in the normal range for a common soil of around 30 Bq/kg ^{238}U due to its original mineral components. Dating the upper and lower part of the cores also confirms an undisturbed sequence of the sediments.

In the beginning of the 19th century, plenty of wetlands were drained in the Swiss Plateau in order to create arable land (Klaus, 2007). This comprehensive melioration was accomplished on the one hand by capturing incoming streams to reduce water supply (Swiss Federal Office of Topography, 2019b) and on the other hand by perforating the impermeable clay layers to install drainage pipes beneath. These measures effected runoff of the retained water in the bog (Fig. 10b). Breaking up the soil combined with infiltrating oxygen-rich rainwater caused a change in redox conditions from anoxic to oxic. This led to an oxidation of U(IV) to U(VI), which is adsorbed onto soil particles and organic matter. Since then, continuously seeping rainwater resulted in an ongoing leaching process within the U accumulation in the soil. This process yields even higher U concentrations in the resulting drainage water (650 mBq/L ^{238}U of no. 13 in Fig. 9) than those that have been introduced into the ancient wetlands via the creeks (360 mBq/L ^{238}U of no. 11 in Fig. 9) during the accumulation period ~2-8 kyrs ago. All the activity concentrations in groundwater, surface water and water of the drainage pipes under the farmland north of Mont Vully as well as the results of the peat horizon reveal that the described processes are perfectly applicable to Mont Vully: The sampled water of the pipes is rainwater that percolated through the soil and peat horizons before ending up in the Broye canal. This whole process can be traced by the AR of three different stations: the water originating from (i) the USM/OMM interface, (ii) the peat itself and (iii) the drainage pipes. All of them exhibit an AR of 1.1. The initial AR of 1.1 that can be measured through the whole 2 years sampling period at the public fountains at Mont Vully is due to the preferential leaching of ^{234}U in comparison to ^{238}U. Once released from the mineral, ^{238}U and ^{234}U show the same chemical behavior. This means that the accumulation of U in the peat exhibits the same AR ratio of 1.1 as the incoming water since the adsorption processes onto the organic matter is chemically equal for all U isotopes. The same is true for the leaching processes from the peat into the drainage water where the AR again is 1.1. Although this track of AR is associated with some uncertainties, it nevertheless helps to illustrate the fate of U in the whole accumulation and leaching process.

Other U origins like phosphorous fertilizers can be excluded since the highest U concentrations occur at 50 to 100 cm depth while the upper top soil - where fertilizers are applied - does not show any increased values (Fig. 13). The results of the ^{14}C dating also controverts fertilizer as origin because the age of the horizons with highest U concentrations show ages of several thousand years. It is rather unlikely that the U accumulation took place only recently because decay products of ^{238}U such as ^{234}Th, ^{230}Th or ^{226}Ra were determined qualitatively. Due to inaccurate measurements, it was abandoned to publish the quantitative data. However, by considering the rough ingrowth of these ^{238}U daughters, the U accumulation must have started some thousand years ago. This verifies the assumption that the U accumulation and the peat formation happened simultaneously.

The presented study helps to clarify the situation at the Lyssbach creek where an U accumulation with unknown origin was found in a peat horizon (Werthmüller et al., 2015). Although there is currently no USM/OMM interface in the direct vicinity, it is still likely to be the origin since the OMM was only removed by erosion, leaving the USM behind. The two other possible reasons for the U accumulation that have been proposed by Werthmüller et al., (2015) have been considered to be unlikely. Both, the Allaline gabbro as well as the coal beds, can effectively result in increased U concentrations. However, Jouvet et al. 2017 elaborated a model to estimate the diversion of erratic boulders by the Valais glacier and came to the result that nearly no boulders were transported to the Solothurn lobe. The rareness of Allalin gabbro and coal beds in the Swiss Plateau can also be checked by consulting the corresponding geological maps (Swiss Federal Office of Topography, 2019a). This leads to the assumption that the frequency of Allalin gabbro occurrence is too low than having a high enough impact to lead to these increased concentrations.

As a final risk evaluation it has to be mentioned that most of the indicated U concentrations in ground and surface water are still below the Swiss regulatory guideline relating to drinking water (EDI, 2017). U concentrations in groundwaters of the studied part of the Swiss Plateau exceed the limit of 372 mBq/L ^{238}U only at one location at Mont Vully and this fountain is declared as no drinking water.

3.7 Conclusion

Increased U concentrations in groundwaters deriving from the USM/OMM interface have been confirmed by an extended sampling campaign in the Swiss Plateau. The origin of U accumulated in peat horizons is verified to originate from this interface. The whole process can be explained in the following four steps:

a) Adsorption of U onto fossils during the development of the USM/OMM interface.

b) Leaching of U by infiltration of O-rich rainwater into the OMM aquifer.

c) Accumulation of U in a peat horizon due to reducing conditions in wetlands.

d) Leaching of U after drainage of the wetland.

The situation and history at Mont Vully are applicable to other localities in the Swiss Plateau where (i) wetlands were drained and (ii) increased U concentrations are measured in groundwater near the USM/OMM interface. We therefore suggest further investigation of these sites.

3.8 Supplementary information

All further measurements and results that were made in direct correlation with the studies at Mont Vully as well as with the sediment cores drilled at the agricultural fields north of it and which were not mentioned in the publication above are explained and discussed in the following sections.

3.8.1 Sediment cores 4 and 5

Beside sediment cores 1, 2 and 3, two further sediment cores were drilled at the agricultural fields north of Mont Vully which are 10 m and 20 m, respectively, north of sediment core 3 in the same arable field. They were drilled close to each other in order to figure out possible differences in small distances. In Figs. 14a and 14b, the activity concentration of ^{238}U in Bq/kg is plotted against depth for sediment cores 4 and 5, respectively. The y-axis further represents the classification of the soil that was found at the corresponding depth. In sediment core 4, the ^{238}U concentration was constant in the soil and loam components with approximately 30 Bq/kg until a depth of 80 cm. At this depth started the onset of the peat layer and the ^{238}U concentration increased to a maximum of 172 Bq/kg. The last 5 cm of the drilled sediment core (i.e. in depth of 95 – 100 cm) there was again a clay layer where the ^{238}U concentration decreased to 124 Bq/kg. Although only 10 m from sediment core 3 away and in the same depth, there was a difference of 340 Bq/kg in the maximum ^{238}U concentration. Sediment core 5 also displayed another characteristic. In the first 60 cm the ^{238}U concentration was likewise constant at 30 Bq/kg in soil and loam. The peat horizon at this core started at a depth of 63 cm and the maximum ^{238}U concentration was reached at a depth of 82 cm with 225 Bq/kg. After the peat horizon, a clay layer was found at a depth of 85 – 90 cm with a decreased ^{238}U concentration of 120 Bq/kg. But unlike sediment cores 3 and 4, there was another peat horizon that started at 90 cm depth with increasing ^{238}U concentration up to 255 Bq/kg. However, it is not excluded that underneath the end of the sediment cores 3 and 4 started another peat horizon with again increased ^{238}U concentrations. But to proof this assumption, further sediment cores have to be drilled until a greater depth. Drilling this two further sediment cores close to sediment core 3 was important to illustrate how large the differences can be in a very short distance. This verifies the assumption, that the U accumulation is a very local phenomenon and cannot be extrapolated to other areas without verification.

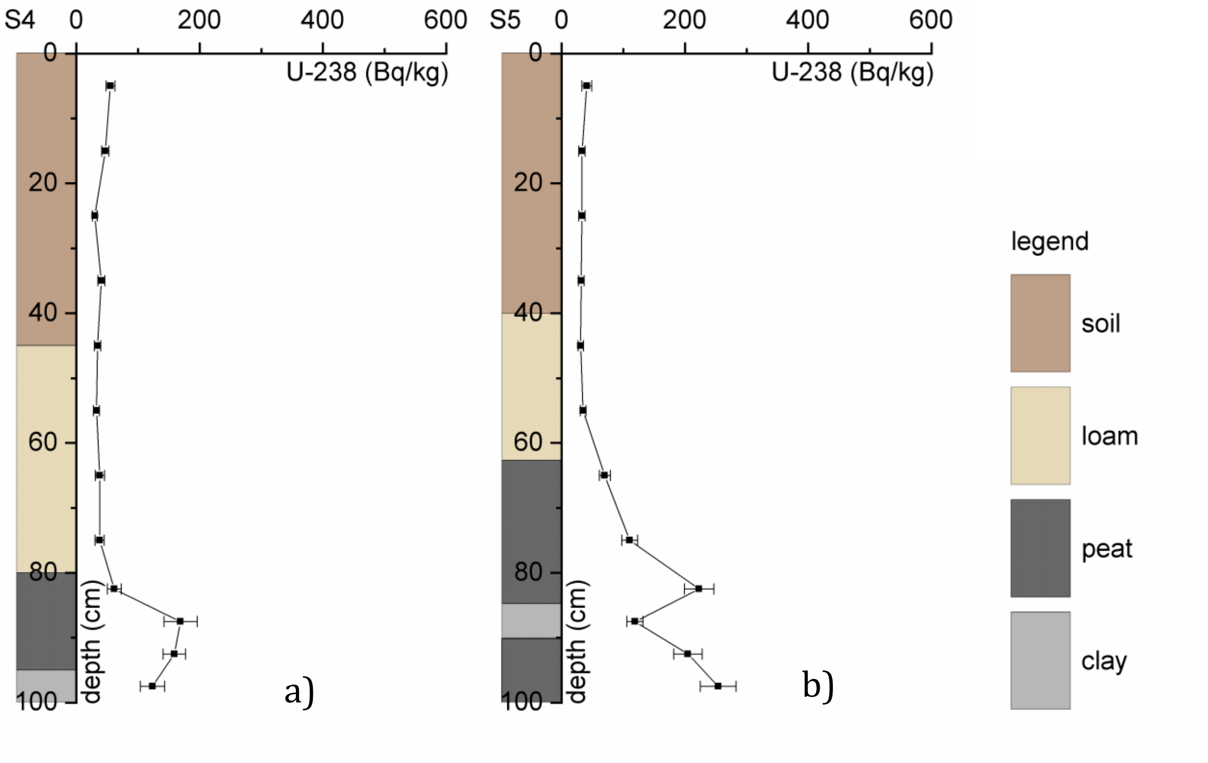

Fig. 14: Two supplementary sediment cores that were drilled close to sediment core 3. The ^{238}U concentration is plotted against depth with illustration of the soil components beside the y-axis. a) Sediment core 4 b) Sediment core 5.

3.8.2 Gamma measurements of the sediment cores

Determination of U concentration in the sediment cores via α-spectrometry is very time consuming since the sample preparation is quite extensive. Therefore, the samples from sediment core 1 were additionally measured by γ-spectrometry to see whether the extensive sample preparation is necessary. The dried and ground soil samples were packed into 50 ml polyethylene bottles and measured for at least 24 hours. The results of the γ-spectrometry in comparison to the α-spectrometry are plotted in Fig. 15. The values from the γ-spectrometry are values that were measured for ^{234}Th that is in secular equilibrium with ^{238}U. The plot interestingly highlights the discrepancy in activity concentrations. The values that were determined via ^{234}Th were consistently too low in comparison to the ^{238}U concentrations that were measured by α-spectrometry. The reason therefore is the high self-attenuation of ^{234}Th. Due to its low decay energy of 63 keV, a certain proportion of the energy was hampered by the soil itself and was not able to reach the detector. It is possible to calculate the percentage that is masked by the self-attenuation. It was not computed for this these samples because the values of ^{234}U were also of importance for this study. And since ^{234}U cannot be measured by γ-spectrometry, the extensive sample preparation for α-spectrometry has to be done anyway.

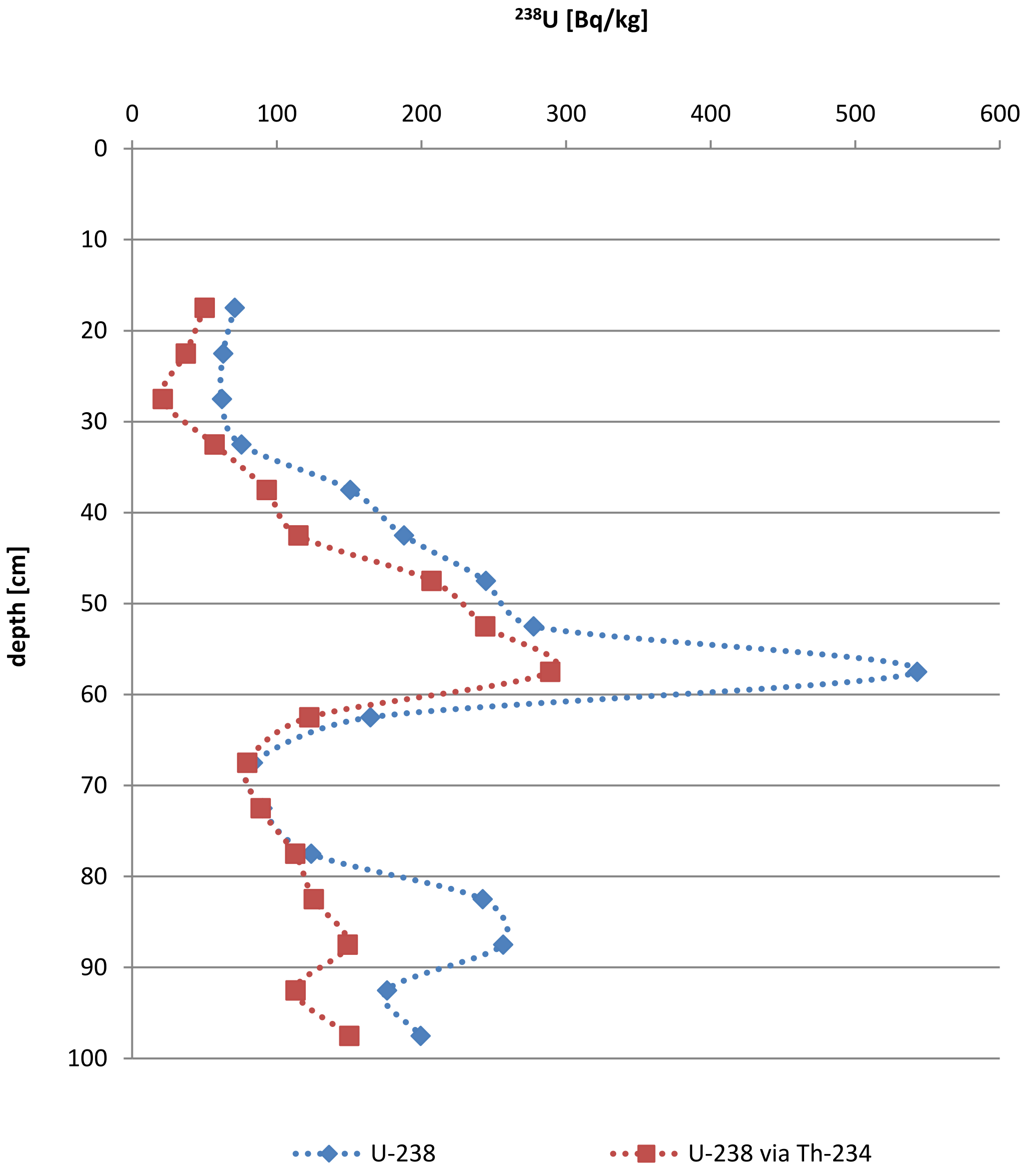

Fig. 15: ^{238}U activity concentration plotted against depth. The concentrations were either determined directly by α-spectrometry or via ^{234}Th by γ-spectrometry.

It was also attempted to measure ^{226}Ra via its short-lived daughters ^{214}Pb and ^{214}Bi. In order to achieve a secular equilibrium between ^{226}Ra and ^{214}Pb and ^{214}Bi, the sample has to be sealed gas tightly because of the intermediate gaseous daughter ^{222}Rn. Unfortunately, it was not possible to achieve a complete secular equilibrium. This is evident as the results of ^{226}Ra scattered enormously. For this reason, the results were considered to be not reliable and it was resigned from publishing the measured values.

3.8.3 Fossils at Mont Vully

During the course of this study, there were several attempts to discover original U-rich fossils that were mentioned numerous times in the literature (Ramseyer, 1952; Schott & Wiegand, 2003). Unfortunately, it was unfeasible to find fossils of vertebrates or invertebrates where U could have been adsorbed onto. Nevertheless, some fossil leaves and wood have been found at the slopes of Mont Vully. The best example can be seen in Fig. 16. Although no U was adsorbed onto these leaves, this fossilization gives evidence that the conditions at the time of deposition were adequate for conservation as can be seen in Fig. 17 where several Molasse layers are outcropping. Since the appropriate fossils could not have been found in nature, a couple of natural or historical museums in Switzerland were contacted and visited in order to find them. Different collections of the Natural History Museum Basel and the fossil collection of the Geological Faculty in Berne were investigated without success.

Fig. 16: Fossil leave that was found at the slopes of Mont Vully.

Fig. 17: Top and Down: Outcropping Molasse layers at Mont Vully.

3.8.4 Measurements of ^{235}U

Although not mentioned in the publication, all water and soil samples with ^{238}U and ^{234}U were simultaneously analyzed for their ^{235}U activity concentration but were not further used for interpretation. Examples for the ^{235}U activity concentration in the water samples are the mean values for Fountaine Marylène and Fountaine du Stand of 12 mBq/L ± 4 mBq/L and 10 mBq/L ± 3 mBq/L, respectively. Examples for soil samples are the results of the sediment core 1 that are listed in Tab. 4.

Tab. 4: ^{235}U activity concentrations in sediment core 1 (2σ uncertainties).

Depth [cm]	*^{235}U [Bq/kg]*	*± [Bq/kg]*
15 – 20	2	1
20 – 25	2	1
25 – 30	2	1
30 – 35	2	1
35 - 40	5	1
40 – 45	7	1
45 – 50	9	2
50 – 55	10	2
55 – 60	22	2
60 – 65	8	1
65 – 70	3	1
70 – 75	3	1
75 – 80	4	1
80 – 85	7	1
85 – 90	8	1
90 – 95	6	1
95 - 100	7	1

Chapter 4 Airborne γ ray spectrometry

The airborne γ ray spectrometry was established in Switzerland for emergency purposes by the Swiss Federal Nuclear Safety Inspectorate (ENSI) together with the National Emergency Operations Centre (NAZ) and the Swiss Army. These purposes can be manifold: for example to localize a radioactive source or to detect radioactive fallout as a consequence of an atomic bomb or a nuclear accident. A flight campaign in a certain area in Switzerland is accomplished every year as exercise for the emergency case. The advantage of the exercise is not only the practice of the method but also the screening of existing (natural) radioactivity in Switzerland under normal conditions. In the course of one of these exercises, it was possible to organize an airborne γ ray spectrometry flight above the study area at Mont Vully. The goal of this flight was to find out, whether the airborne γ ray spectrometry is a possible alternative to the detection of the dose rate by foot which is very time consuming and restricted to accessible areas. With the airborne γ ray spectrometry it is not only possible to detect the dose rate above ground, but also to compute the activity concentration of certain isotopes such as ^{238}U and ^{232}Th.

4.1 Flight above Mont Vully and adjacent wetlands

The flight above Mont Vully took place on the 30th of May 2018 from 9:12 till 10:43 o'clock. The helicopter "SuperPuma" was equipped with 4 Sodium Iodine (NaI) detectors which continuously recorded the γ ray spectra (Fig. 18). The helicopter covered 76 km^2 gridwise in 25 lines with a line spacing of 250 m. The pilot maintained a constant height of 90 m and a velocity of 100 km/h (Fig. 19). The results were evaluated online by the operators and graphically illustrated afterwards by the ground staff.

Fig. 18: Helicopter equipped with 4 detectors for airborne gamma ray spectrometry.

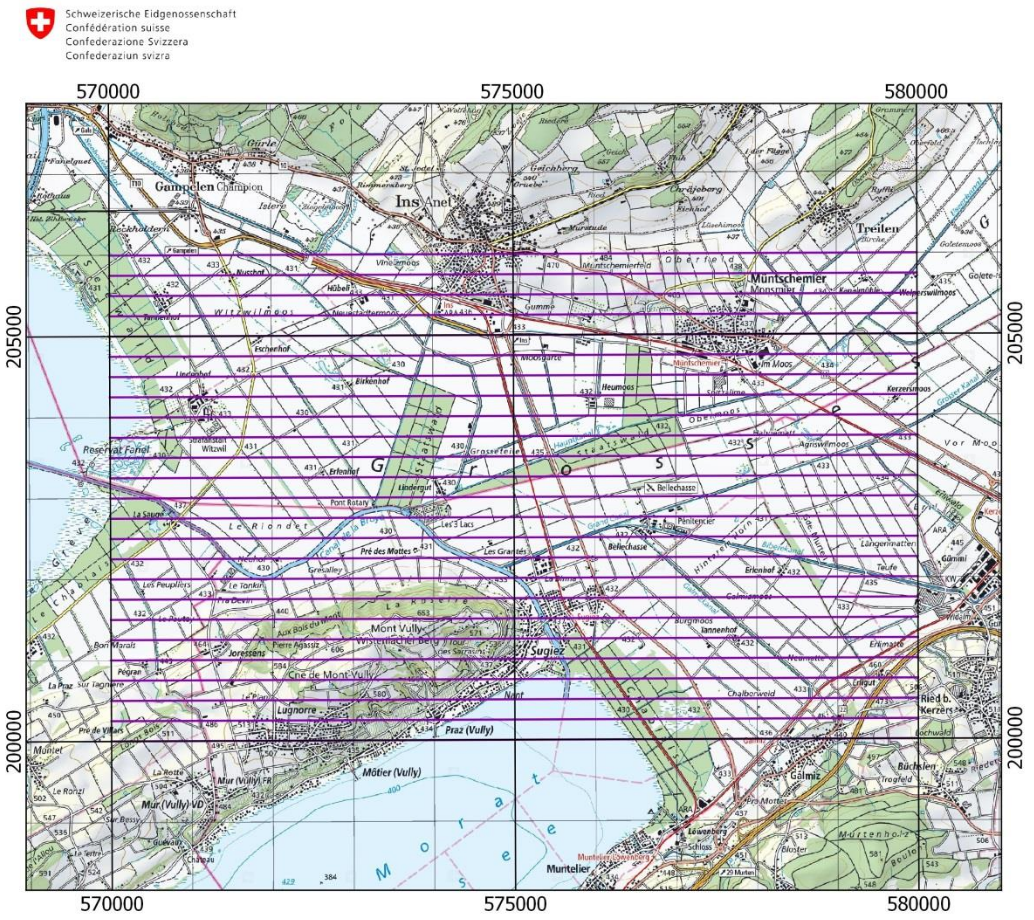

Fig. 19: Planned flight above Mont Vully and adjacent wetlands. In purple: lines 25 lines with a line spacing of 250 m.

4.2 Results and discussion

The results of the flight are shown in Figs. 20 – 23 (note the different units). Fig. 20 illustrates the dose rate at the region around Mont Vully that ranges from 50 – 150 nSv/h. There are three areas that stand out in the figure (see circles in Fig. 20). Circle 1 displays the dose rates that are present at Mont Vully itself (Fig. 21, top). The high rates of up to 150 nSv/h are an effect from the sedimentary rocks Mont Vully consists of (Upper Marine Molasse and Lower Freshwater Molasse; see section 3.3.1). Although not clearly separated from circle 1, circle 2 represents the dose rates that originate from the U-rich peat horizon under the agricultural fields (Fig. 21, down, left side). There are also increased dose rates with values of up to 150 nSv/h in the small band that lies between Mont Vully and the Broye Canal. These values are in accordance with those rates that were measured by foot with the NaI-detector. Therefore, the rough localization of areas with increased dose rates is also possible by airborne γ ray spectrometry. The only disadvantage is the low resolution. Due to the line spacing of 250 m, it is not possible to clearly define the boarders of the increased dose rate values. This can be seen at circle 3 (Fig. 21, down. Right side): there is an indication of an area with increased dose rates, but the extension is not that exactly defined as with the detection by foot. The probability that there is a similar accumulation with a U-rich peat horizon under the agricultural field is high but cannot definitively be proofed by airborne γ ray spectrometry.

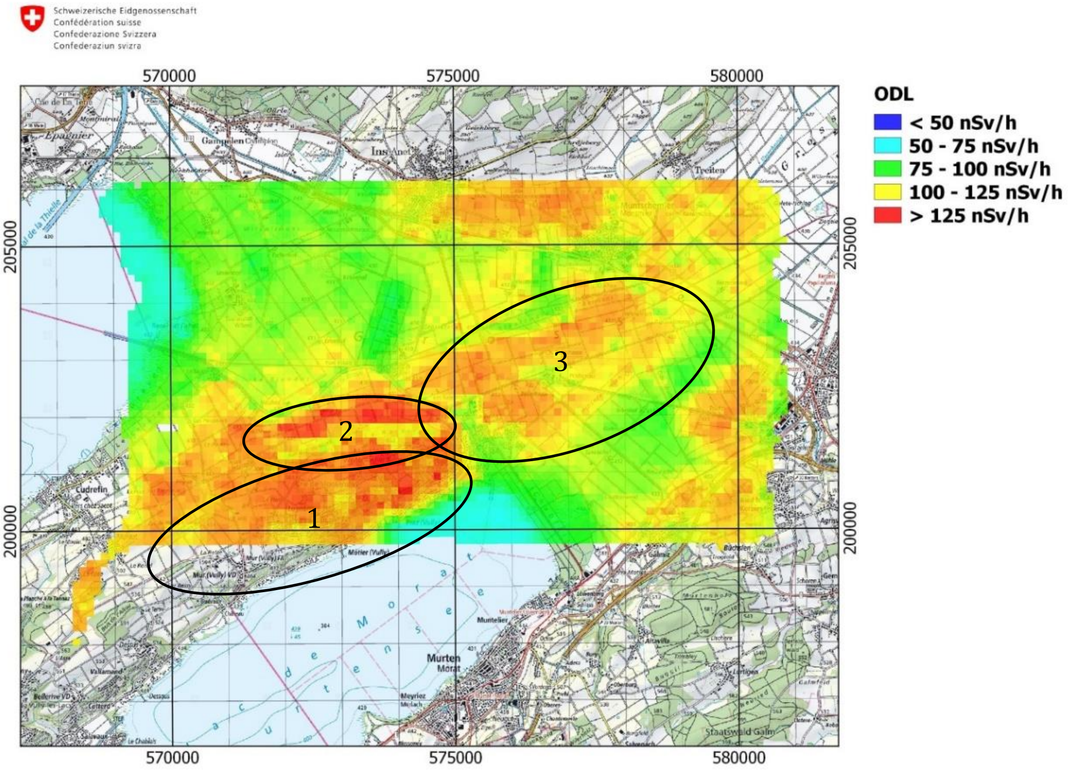

Fig. 20: Dose rates above the area around Mont Vully recorded by airborne γ ray spectrometry.

Fig. 21: Photographs of Mont Vully and the adjacent agricultural fields taken during the flight with the helicopter. Top: Mont Vully. Down, left side: Agricultural fields north of Mont Vully. Down, right side: Agricultural fields northwest of Mont Vully indicating dark brown peat on top of the fields.

The results for the different activity concentrations are more difficult to interpret than the results of the dose rates. The activity concentrations of ^{238}U that were detected by airborne γ ray spectrometry around Mont Vully rage from 0 Bq/kg to 90 Bq/kg (Fig. 22). This is a normal range for U on the Earth's surface but there is a serious discrepancy to the determined values in the sediment cores which reach an activity concentration of more than 500 Bq/kg ^{238}U. The reason therefore is the overburden top soil of up to 1 m thickness that acts as a shielding. The activity concentrations in the peat horizon measured by airborne γ ray spectrometry are underestimated depending on the depth in which they occur because the software estimates a homogeneous U distribution in the soil. Consequently, the pattern is barely evaluable due to an almost random distribution. The same problem appears by considering the ^{232}Th activity concentrations (Fig. 23). The values range from 0 Bq/kg to 56 Bq/kg which is no abnormality for nature. Since there are no measured values in the sediment cores available, it is impossible to make a statement concerning the accuracy of these results.

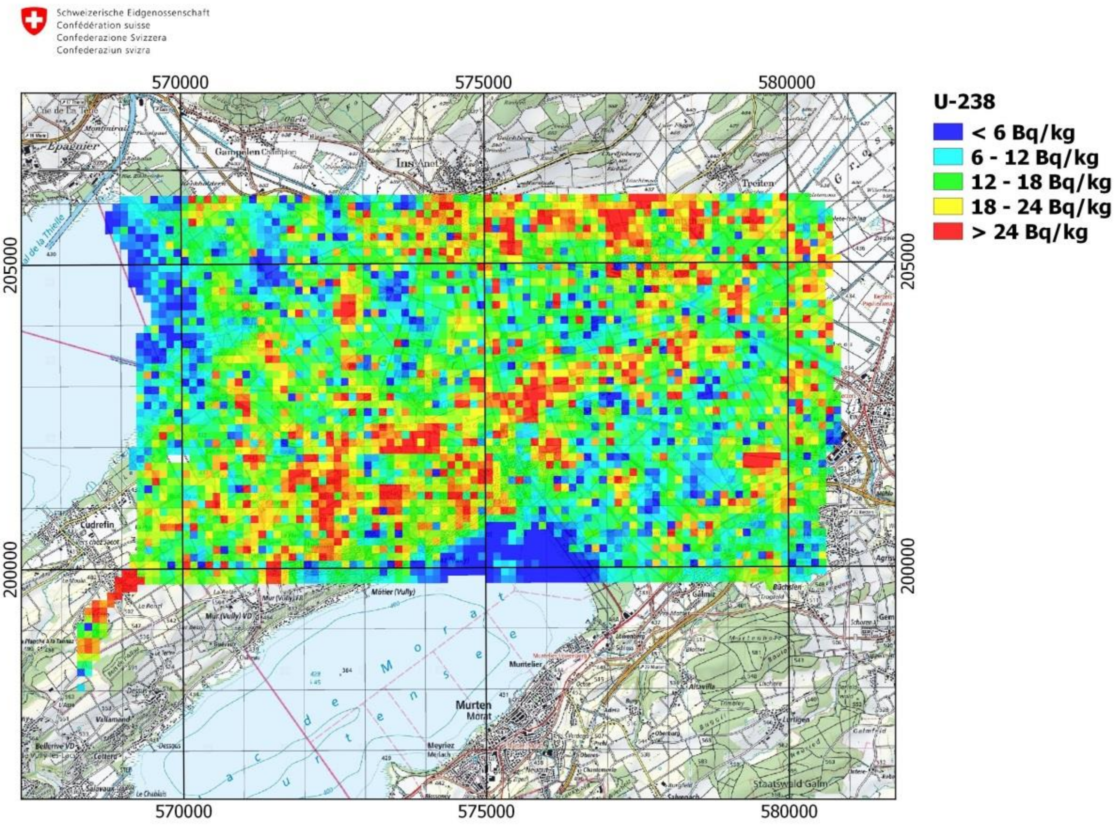

Fig. 22: Activity concentrations of ^{238}U at the area around Mont Vully recorded by airborne γ ray spectrometry.

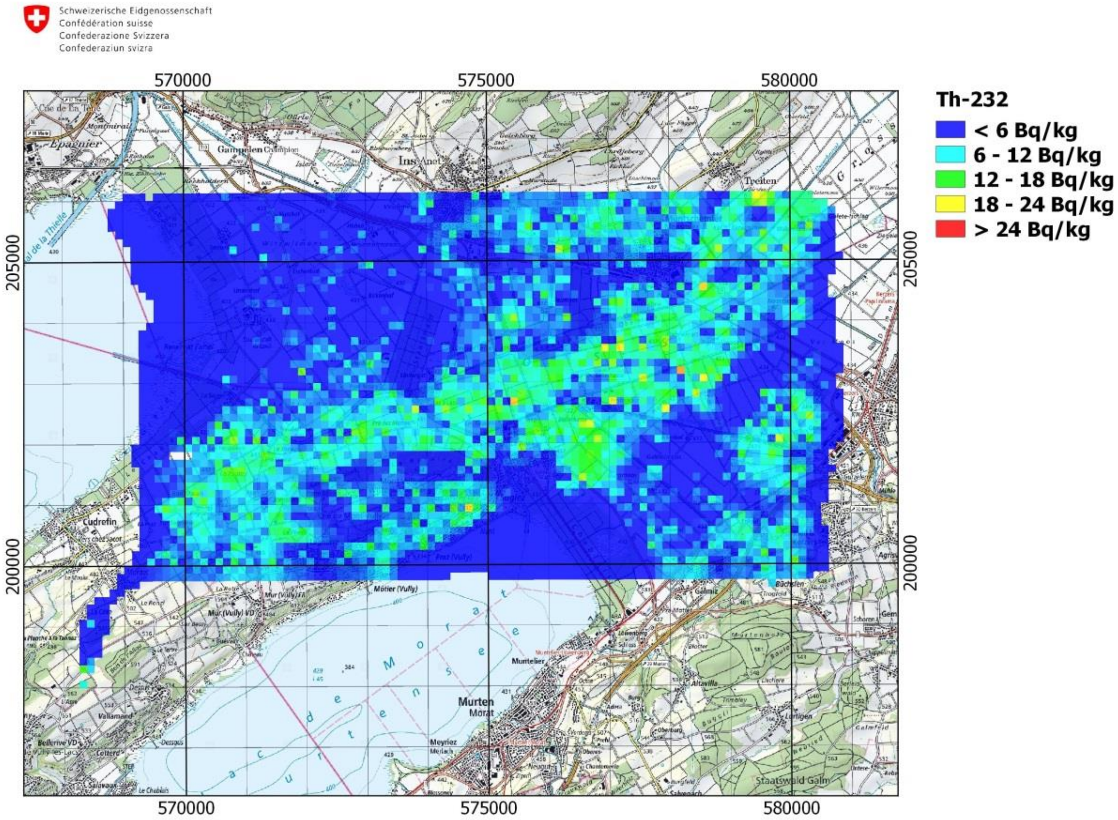

Fig. 23: Activity concentrations of ^{232}Th at the area around Mont Vully recorded by airborne γ ray spectrometry.

4.3 Conclusion

As a conclusion it can be said, that the airborne γ ray spectrometry is a good tool to localize increased γ ray dose rates in a broad area during a very short time. In geological and geomorphological similar situations, increased rates can be a hint for an U accumulation underground, but it is no evidence. To proof whether there are increased U concentrations, the soil itself has to be analyzed.

A possible alternative to the γ ray spectrometry by helicopter would be a drone equipped with a detector. This alternative would diminish the problem of accessibility in comparison to recording the dose rate by foot. Defining the boarders of a potential U accumulation by flying narrower lines in less velocity would be an improvement in comparison to the helicopter. However, carrying a heavy detector is not possible for every simple drone and the weight of the detector reduces the life time of the battery. Another problem of recording the dose rate by drones is the safety during the flight. Drones are prone to crashes which inflates the price for such a tool.

Chapter 5 Leaching experiments

This chapter concerns the chemical mobility of accumulated Uranium from an ancient wetland peat horizon into the environment covering field studies and laboratory experiments.

5.1 Introduction

Uranium-contaminated areas in the environment are commonly associated with man-made origins like radioactive waste disposal or U and ore processing sites (Bister et al., 2015; Corcho-Alvarado et al., 2014; Felipe-Sotelo et al., 2017; Letman et al., 2018). What is often neglected is the fact, that U is a naturally occurring radioisotope that can occur under certain circumstances in large amounts in diverse materials. A good example is the U accumulation in an ancient wetland at Mont Vully (see Chapter 3: Pregler at al., 2019). Increased concentrations in soil or groundwater can lead to long-term problems in the environment if there is the probability that humans are exposed to it. There are similar situations like Mont Vully where organic matter accumulated in the last few thousand years (Campbell et al., 2012; Cumberland et al., 2016; Regenspurg et al., 2010; Schumann et al., 2017; Zielinski & Meier, 1988). However, these studies focussed not on the origin of U but on the nature and strength of U bonding and U speciation. The authors also characterized the redox state and mineralogical and microbiological aspects with respect to the processes that occur while adsorption of U to organic matter. The aim of the study in this chapter was to accomplish leaching experiments of U from peat in the laboratory that can be applied to nature in order to understand the behaviour of U in a special environment. This time the Lyssbach area was chosen as case study because the U concentration in the ancient wetland there was even higher than the U concentration at Mont Vully. The leaching behaviour of U at the Lyssbach area was compared with results that were achieved by leaching experiments of U in the lab. The focus of these experiments was on the identification of environmental implications. Therefore, it was reverted to already existing knowledge of separation methods such as sequential extraction procedures (Pérez-Moreno et al., 2018; Schultz et al., 1998; Suresh et al., 2014; Vandenhove et al., 2014). The sequential extraction was performed for the identification of the U speciation that was present in the peat horizon (section 5.2.6). In order to achieve the most reliable results in the laboratory that can be extrapolated to nature, some further leaching experiments were accomplished to determine the most adequate leaching conditions (section 5.2.7). Finally, a risk assessment for U in the environment was conducted with the connection of laboratory experiments with field studies at the Lyssbach area.

5.2 Material and methods

5.2.1 Study site Lyssbach

The area around the Lyssbach, a small stream approximately 10 km north of Berne in the Swiss Plateau (Fig. 24), is the site for the field studies. It is an agriculturally used valley located between two hills of the Swiss Molasse unit and filled with Quaternary sediments (Gruner 2012). The Lyssbach stream drains the area in the middle of the valley towards NW direction. A significant supply to the stream consists of several drainage pipes that drain the agricultural fields on both sides of the creek. A first study of this site was conducted by Minkowski and Ryser (2015), Surbeck et al., (2015) and Werthmüller et al., (2015) by means of aeroradiometry. A drone was equipped with a 2"x2" sodium iodide (NaI) detector that overflew the agricultural fields in order to localize U accumulations underground detecting γ-dose rates with up to 160 nSv/h. This survey was initiated because a routine control of water quality conducted by the Laboratory for Water and Soil Protection of the Canton of Berne revealed U concentrations of more than 400 µg/L in drainage pipes that end up in the Lyssbach stream (Schmidt, 2013). These investigations provided the basis of the water sampling that focused on the drainage pipe with highest U concentrations.

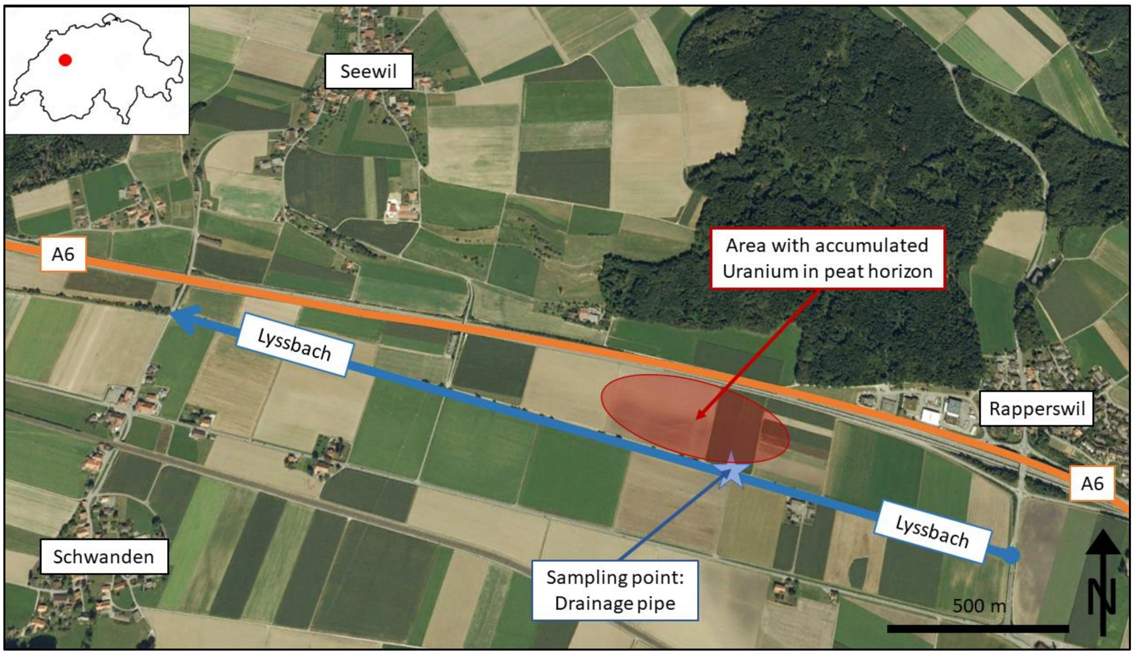

Fig. 24: Area around the Lyssbach indicating the sampling point of the drainage pipe that ends up in the Lyssbach and the area where increased U concentrations have been found in a peat horizon.

5.2.2 Sampling

Water sampling of the drainage pipe (see Fig. 24) that ends up in the Lyssbach stream started in June 2016 and lasted 14 months with a total of 14 water samples in order to screen possible seasonal fluctuations. Two 1L polyethylene bottles were completely filled and acidified with a few drops of concentrated HNO_3 in order to prevent the radionuclides to adsorb onto the bottle walls. Filtration was tested for several samples and the results in the filtered and unfiltered aliquots were identical within uncertainties. On that account, filtration was not performed anymore. Electric conductivity, temperature and pH of each water sample was determined immediately during sampling using a handheld meter (HI98129 COMBO Tester from HANNA Instruments Switzerland AG). Peat sampling was accomplished during canalization works under a field path on the agricultural land in June 2014. It was possible to collect several samples of a peat horizon that is located ca. 0.5 m below the earth's surface (Fig. 25). An aliquot of this sample was used for all following analyses, i.e. the U analysis in peat, ^{14}C dating of peat, sequential extraction and leaching experiments.

Fig. 25: Collection of peat samples during canalization works in June 2014 (Photo: Heinz Surbeck). Above the peat horizon there is approximately 0.5 m soil and below there is a clay layer.

5.2.3 Radionuclide and element analysis in water samples

Each water sample was analysed for six isotopes of the ^{238}U decay series: ^{238}U, ^{234}U, ^{226}Ra, ^{222}Rn, ^{210}Pb and ^{210}Po. The exact procedures for the analysis of each isotope was already explained in detail in chapter 2.

Additionally to the radionuclide analysis, one sample of the drainage water (from June 2016) has been measured by means of ICP-OES (inductively coupled plasma optical emission spectrometry) at the Laboratory of Environmental Chemistry and by means of ion chromatography at the Laboratory for Waste Management, both at PSI, in order to get an insight of the overall element concentration of the drainage water.

5.2.4 Uranium analysis in peat

Peat samples from the Lyssbach area (Fig. 26) were only analysed for its U content. The procedure is identically to the analysis described in chapter 2.

5.2.5 ^{14}C dating of peat

In order to determine the time of peat formation, the sample from the peat horizon at the Lyssbach area was dated by the ^{14}C method. After grinding the peat to a homogeneous powder, potential fractions of carbonate and humic acids were removed from an aliquot using an acid-base-acid treatment. After the complete combustion of the residue, it was transformed into graphite targets. Measurements were conducted with the accelerator mass spectrometer (AMS) MICADAS at the LARA laboratory at the University of Bern. The detailed procedure is given in Szidat et al. (2014). The measured ^{14}C ages were calibrated using IntCal13 to provide the calendar ages of the samples (Reimer et al., 2013).

5.2.6 Sequential extraction of peat samples

In order to determine the mobility of U from the peat horizon into the surface water, a validated BCR (in French "Bureau Communautaire de Référence; in English "Community Bureau of Reference") sequential extraction procedure for natural radionuclides from Pérez-Moreno et al. (2018) was applied. The procedure was designed to identify the different speciation of radionuclides that can be present in the environment. The present study focused on four different fractions but only in regard to U isotopes (Tab. 5). The first step is aimed to extract water and slightly acid soluble as well as exchangeable species. This fraction is the most easily leachable fraction and can therefore be seen as most hazardous for the environment. The second step extracts the reducible fraction that is bound to Fe and Mn oxyhydroxides. This fraction can be mobilized under anoxic conditions. The third step was designed for the oxidizable fraction with organic compounds and sulphides as nominal target phases. The release of this fraction is enabled if the conditions in the environment change from anoxic to oxic. The fourth and last step identifies the non-mobile fraction that is considered as residue. It is very unlikely to be released into the environment under natural conditions since the radionuclides are enclosed in mineral structures. For the analytical procedure, 1 g of dry peat sample (see section 5.2.4) was mixed with a defined amount of extractant and shaken for a certain time. The specifications are listed in table 5. After shaking, the mixture was centrifuged for 15 minutes at 4000 rpm and the extractant was decanted. The residue was washed with 20 mL deionized water, shaken for 5 minutes and again centrifuged for 15 minutes at 4000 rpm. The washing water was decanted and added to the extractant. This solution was then evaporated to complete dryness and further processed identically to the U analyses of water (see section 5.2.3). The solid residue was continued with the next extraction step. The last residue after extraction step 4 was prepared in the same way as the peat was analysed (see section 5.2.4) but with aqua regia instead on concentrated HNO_3. The whole procedure was accomplished four times.

Tab. 5: Sequential extraction procedure adapted from Pérez-Moreno et al. (2018)

Step	*Fraction*	*Nominal target phases*	*Extractant (1 g of dry solid)*	*Conditions*
1	Water/acid soluble exchangeable	Soluble species, carbonates and cation exchange sites	40 ml 0.11 M CH_3COOH	16 h shaking at RT[a]
2	Reducible	Iron and Manganese oxyhydroxides	40 ml 0.5 M $NH_2OH{\cdot}HCl$ (pH 2)	16 h shaking at RT
3	Oxidizable	Organic matter and sulphides	10 ml H_2O_2 50 ml 1 M NH_4Oac (pH 2)	1 h at RT, 1 h at 85°C and 16 h shaking at RT
4	Residual	Non-mobile fraction	20 ml aqua regia 3:1 ($HCl:HNO_3$)	16 h at RT, 2 h boiling under reflux, 15 h at 500°C in oven

[a] RT = room temperature

5.2.7 Leaching experiments

Modelling the concentration of species that were present in the drainage water that end up in the Lyssbach creek using PHREEQC reveals that most U is present as carbonate species (cf. section 5.3.1). In order to identify the leaching behaviour of U in the peat horizon that was shown in Fig. 25, several leaching experiments were accomplished with varying carbonate content (varied with sodium carbonate (Na_2CO_3), Fig. 27), pH (accomplished by adding HNO_3 (Fig. 28)) and leaching time (Fig. 29) all listed in Tab. 6. Exactly 1 g of dry peat that was homogenized as described in section 5.2.4 and 40 mL of extractant was used for each leaching experiment. Shaking was performed in centrifuge tubes with a laboratory shaker.

Tab. 6: Leaching experiments of Lyssbach peat with varying parameters.

Na_2CO_3 concentration (at unmodified pH 11; leaching time 16 h)	*pH (leaching time 8 h; Na_2CO_3 concentration 0.005 M)*	*Leaching time (at unmodified pH 11; Na_2CO_3 concentration 0.005 M)*
0	7	10 minutes
0.1 M	8	1 h
0.05 M	9	8 h
0.01 M	10	24 h
0.005 M		
0.001 M		

5.3 Results

5.3.1 Radionuclide and element concentrations in drainage water

The activity concentrations for all measured radionuclides (^{228}U, ^{234}U, ^{226}Ra, ^{222}Rn, ^{210}Po), their measurement uncertainties as well as the sampling date, flow rate while sampling, temperature, pH and electric conductivity are listed in Tab. 7. Since the drainage pipes are installed only about 1 m below the surface, the flow rate of the pipe is very sensible to fluctuations in precipitations and thus varies from 0.1 l/min to 30 l/min as maximum. The same holds true for the temperature that ranges from 17°C in summer to 5°C in winter. Electric conductivity and pH, however, exhibit similar values for all seasons with a mean electric conductivity of 819 ± 23 µs/cm and a mean pH of 7 ± 0.3. Since the determined isotopes show differences in concentration within three orders of magnitude, the sampled drainage displays a complete disequilibrium within the ^{238}U decay series.

Highest values are measured for ^{222}Rn with 37’000 ± 1’000 mBq/L in summer and lowest values with 16’000 ± 1’000 mBq/L in winter. Concentrations of ^{238}U range between 827 ± 99 mBq/L and 3’226 ± 199 mBq/L. ^{234}U concentrations were measured in the same order of magnitude and range between 1’033 ± 122 and up to 4’000 mBq/L. The activity concentrations of both isotopes strongly correlate with the flow rate, i.e. if the flow rate is high, activity concentration in the water is high as well and vice versa. ^{226}Ra displays lower activity concentrations ranging from 20 ± 5 mBq/L up to 37 ± 12 mBq/L. In each water sample, ^{210}Pb did not reach the detection limit of 40 mBq/L. ^{210}Po reached the detection limit of 1 mBq/L with a maximum of 8 mBq/L ± 1 mBq/L.

The results of the ICP-OES and ion chromatography measurements of the drainage water from June 2016 are listed in Table 8. These concentrations were used for modelling the different U species in the drainage water using the computation programme PHREEQC. The computation yielded that most of the U(VI) species are present as carbonate species (e.g. $(UO_2)_2CO_3(OH)_3^-$ and $CaUO_2(CO_3)_3^{2-}$). For this reason, Na_2CO_3 was used as carbonate species for the leaching experiments.

Tab. 7: Radionuclide concentration in the water of the drainage pipe at Lyssbach (2σ uncertainties).

date	*flow rate*	*T*	*pH*	*el. cond.*	^{238}U	±	^{234}U	±	^{226}Ra	±	^{222}Rn	±	^{210}Po	±
	l/min	°C		µS/cm	mBq/L	mBq/L	mBq/L	mBq/L	mBq/L	mBq/L	mBq/L	mBq/L	mBq/L	mBq/L
09.06.2016	30.0	14.2	6.7	863	3067	149	3711	176	33	11	37000	1000	6	3
14.07.2016	16.0	15.8	7.0	828	3226	199	3936	241	23	8	20000	1000	8	1
16.08.2016	6.0	16.0	7.2	777	2326	120	2884	144	37	12	15000	1000	5	2
30.08.2016	3.0	16.1	7.2	785	1744	107	2134	130	24	7	18000	1000	5	2
17.10.2016	1.0	13.3	7.8	840	1223	74	1466	87	25	8	16000	1000	2	1
29.11.2016	4.0	8.8	7.5	832	1803	161	2213	196	20	5	18000	1000	3	1
19.12.2016	1.5	7.2	7.7	833	1221	112	1446	132	36	15	17000	1000	3	1
10.01.2017	1.0	5.0	-	-	1147	107	1373	127	24	6	16000	1000	1	1
23.02.2017	1.3	6.4	7.3	805	1336	183	1528	208	23	6	23000	1000	2	1
31.03.2017	2.0	9.1	6.9	810	1413	190	1716	228	25	5	28000	1000	3	1
27.04.2017	1.4	9.4	7.3	821	1344	169	1602	199	26	5	7500	1000	1	1
24.05.2017	0.4	12.5	7.1	830	846	110	1053	134	28	5	-	-	2	1
08.06.2017	0.7	13.0	6.7	799	827	99	1033	122	29	5	26000	1000	2	1
11.08.2017	0.1	16.9	-	833	1037	126	1329	159	36	10	-	-	3	1

Tab. 8: Results of the ICP-OES and ion chromatography measurements of the drainage water from June 2016.

element/anion	*concentration [ppm]*
Al	0.013
B	0.039
Ba	0.196
Ca	167
Cr	0.0006
Cu	0.0044
Fe	0.008
K	1.13
Li	0.0049
Mg	14.8
Mn	0.00438
Mo	0.0016
Na	11.2
Ni	0.0108
P	0.009
S	14.5
Si	3.68
Sr	0.000725
U	0.186
SO_4^{2-}	43.52
F^-	0.18
ClO^{2-}	38.29

5.3.2 Analysis of peat

The analysis of ^{238}U was accomplished for 8 aliquots of the sieved a homogenized peat in order to achieve reliable results of the total activity concentration. The values range from 1’821 ± 206 Bq/kg to 2’296 ± 287 Bq/kg with a mean value of 2’023 ± 173 Bq/kg. Dating of the peat reveals an age of 6’631 ± 47 years before present (LARA Lab Code: BE-7448.1.1.). From these ^{14}C ages, a calibrated age of 7.5 – 7.7 kyrs was deduced for the peat horizon.

5.3.3 Results of the sequential extraction

The sequential extraction procedure according to Pérez-Moreno et al. (2018) was performed with 8 aliquots of the sample described in section5.2.2. The following percentages are mean values of the 8 aliquots and the individual results for each of the 8 aliquots are illustrated in Fig. 30. The first extraction step for the exchangeable fraction reveals that 1% of the total U in the peat are soluble species, carbonates or at cation exchange sites. The second extraction step designed for the reducible fraction accounts for 2% of the total U and is bound to Fe and Mn oxyhydroxides. The major part is bound to organic matter and sulphides since the third extraction step identifies that 85% of U in the peat is oxidizable. The fourth and last step comprises the non-mobile fraction in the residue that makes up 12% of the total U inventory.

5.3.4 Results of the leaching experiments

The leaching experiments with varying Na_2CO_3 content reveal that the carbonate concentration in the extractant is a major factor. Carbonate-free water does not leach any U fraction at all from the peat. Gradually adding Na_2CO_3 leads to a continuously improved leachability of U from the peat resulting in leaching of 93% with 0.1 M Na_2CO_3 (Fig. 31). Leaching experiments that were accomplished with varying pH demonstrate that the original high pH 11 of the 0.005 M Na_2CO_3 solution is the best pH to leach U from the peat. Decreasing pH leads to decreasing leachability (Fig. 32). Leaching experiments that consider time as a factor illustrate that the longer the duration of leaching is, the more U is leached from the peat into the extractant (Fig. 33).

Fig. 26: U-rich peat from the agricultural fields around Lyssbach.

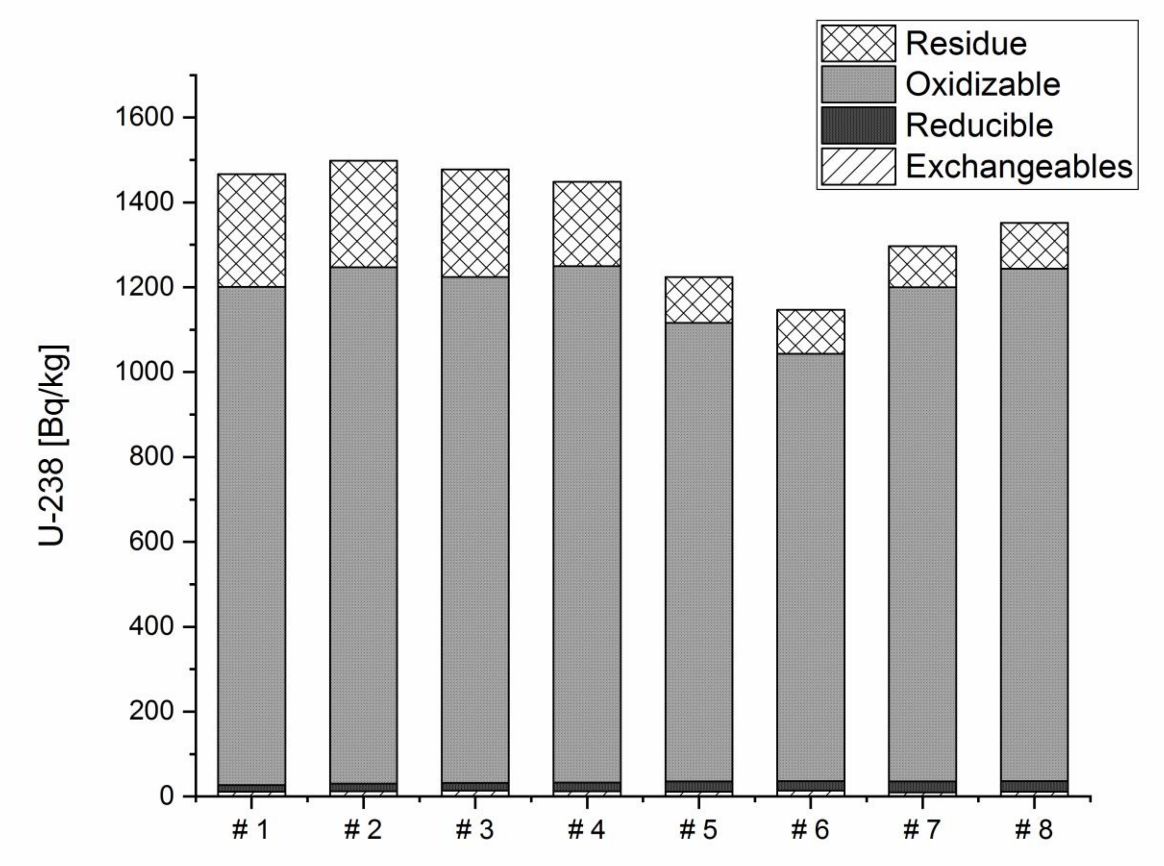

Fig. 30: Results of the sequential extraction according to Pérez-Moreno et al., 2018.

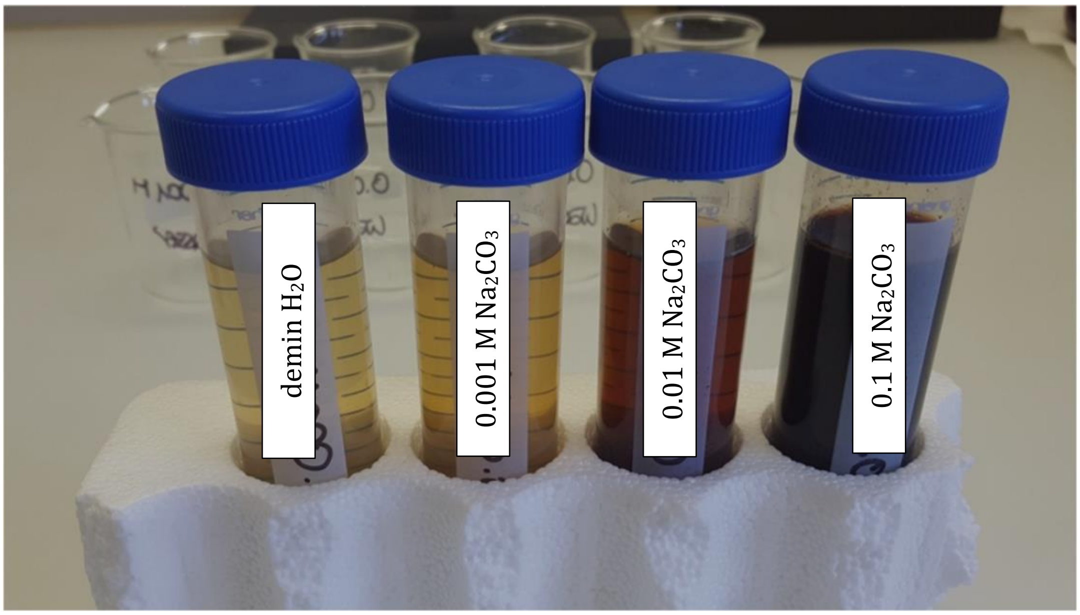

Fig 27: Centrifuge tubes for leaching experiments with varying carbonate (Na_2CO_3) concentration, a pH of 11 and 16 h leaching time.

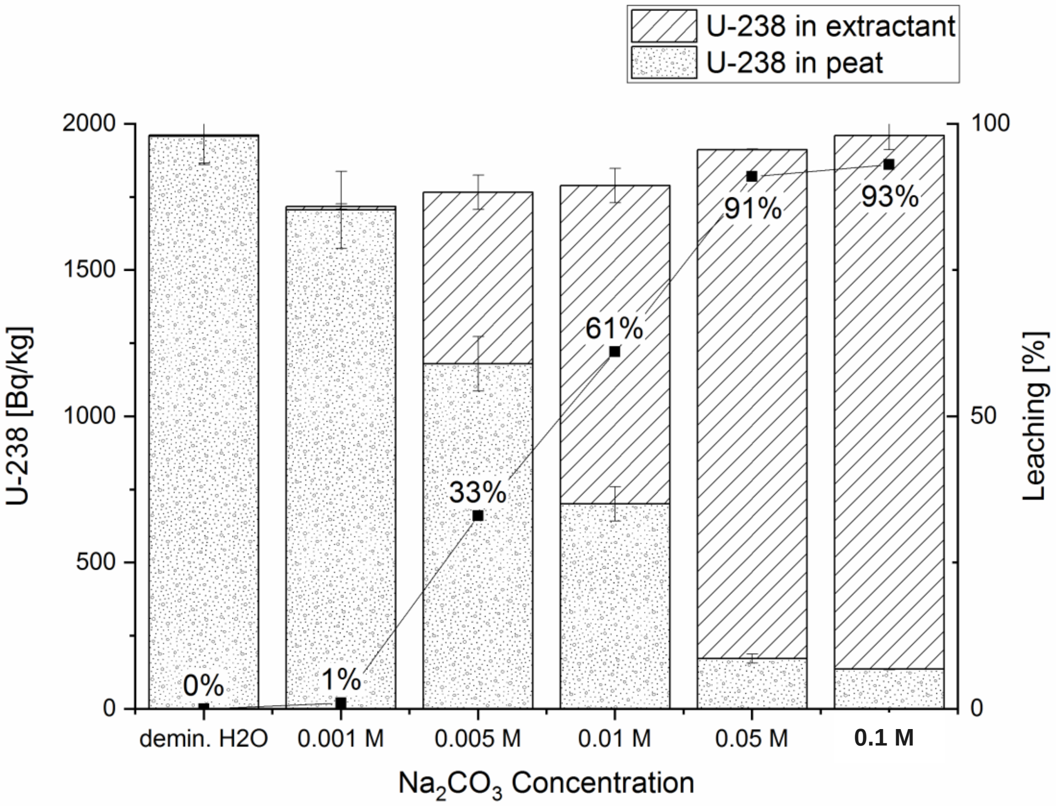

Fig. 31: Results of leaching experiments with varying carbonate (Na_2CO_3) concentration, a pH of 11 and 16 h leaching time.

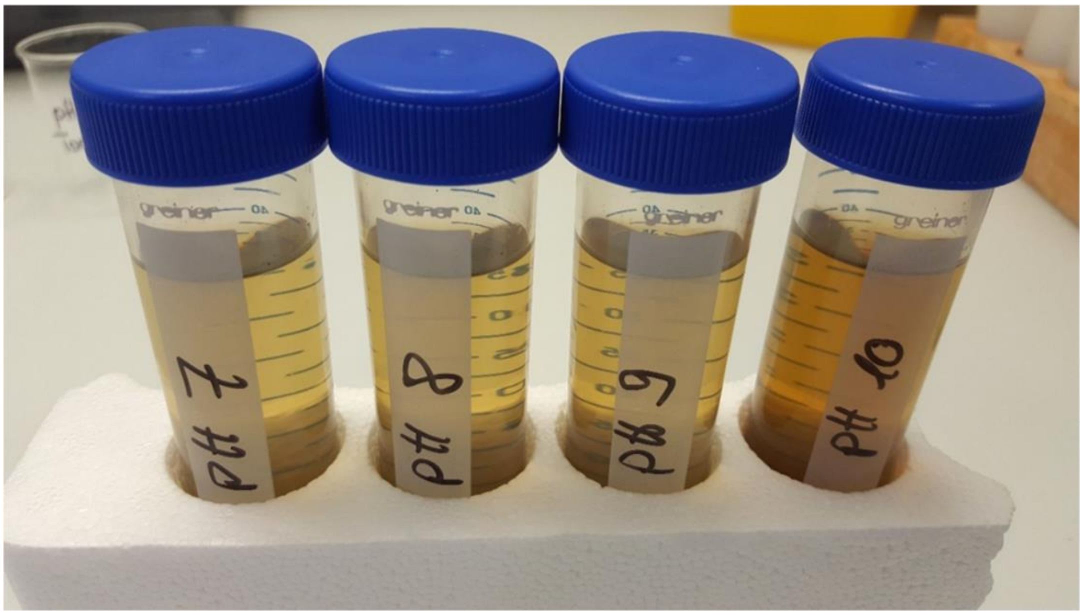

Fig. 28: Centrifuge tubes for leaching experiments with varying pH, a Na_2CO_3 concentration of 0.005 M and 8 h leaching time.

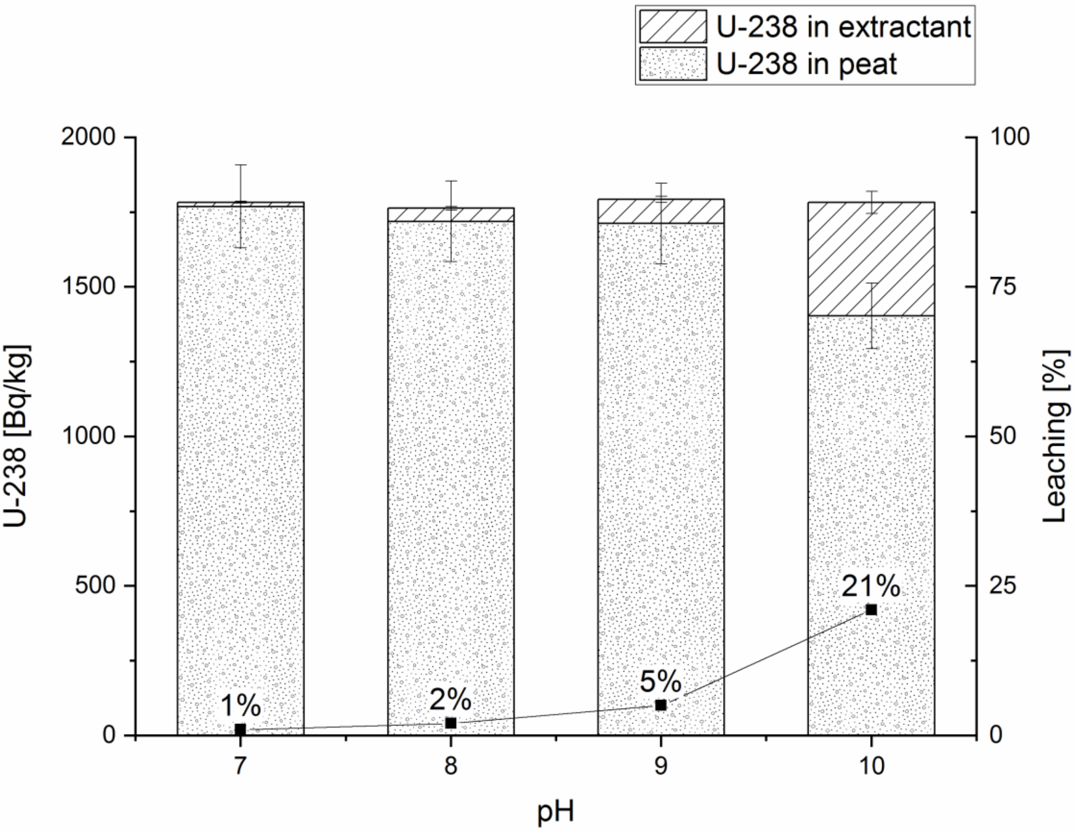

Fig. 32: Results of leaching experiments with varying pH, a Na_2CO_3 concentration of 0.005 M and 8 h leaching time.

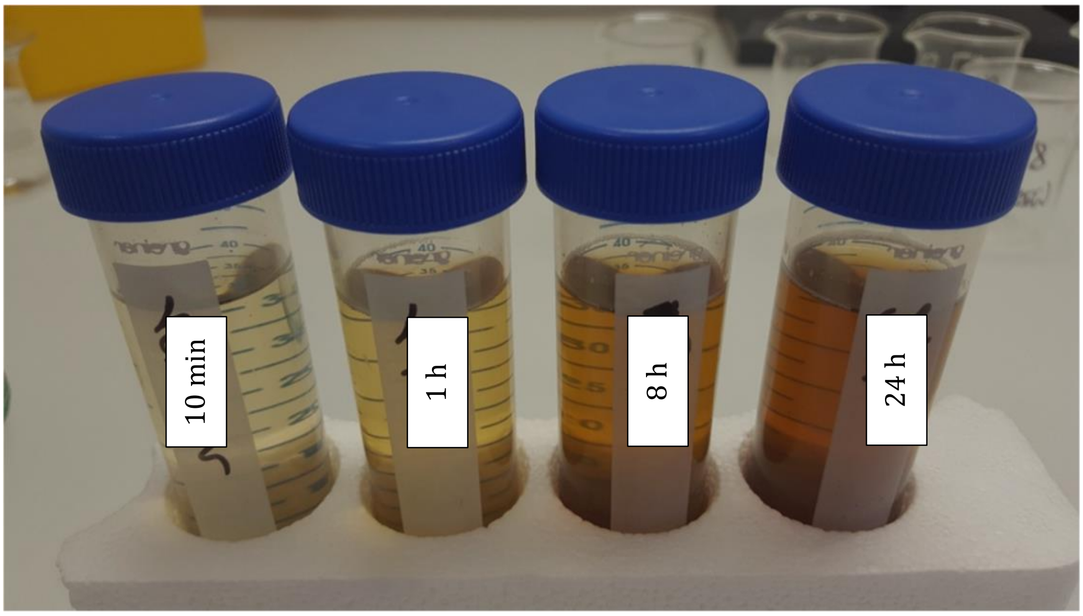

Fig 29: Centrifuge tubes for leaching experiments with varying leaching time, a pH of 11 and a Na_2CO_3 concentration of 0.005 M.

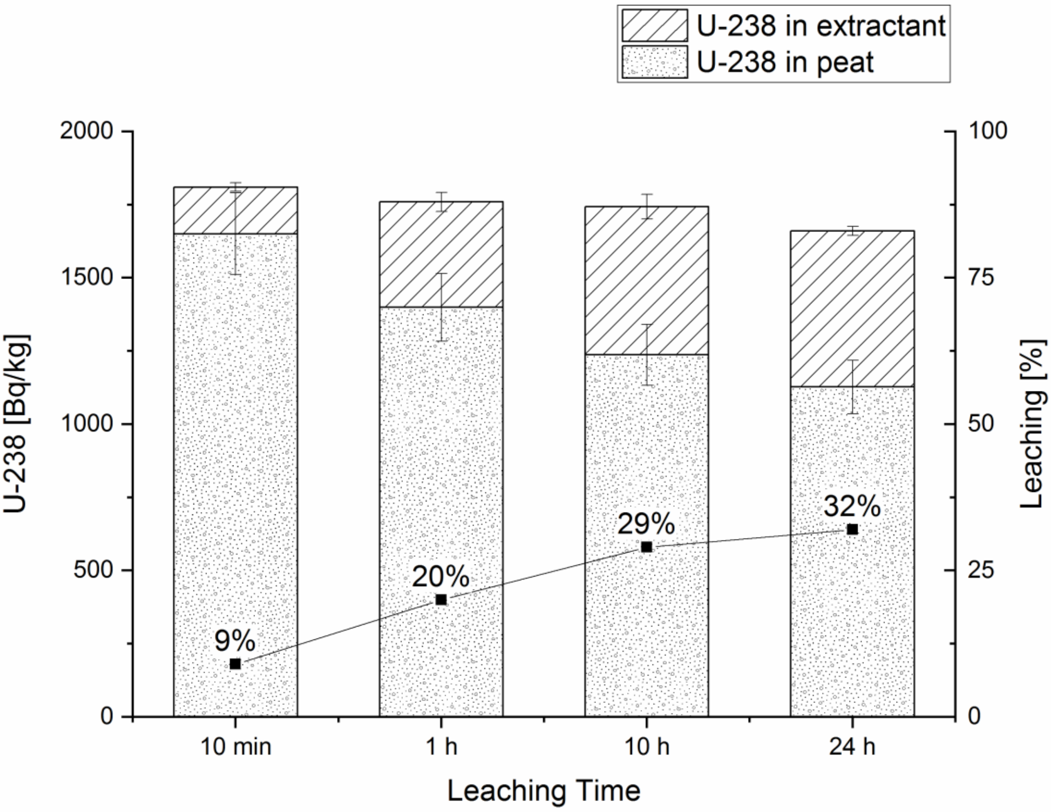

Fig. 33: Results of leaching experiments with varying leaching time, a pH of 11 and a Na_2CO_3 concentration of 0.005 M.

5.4 Discussion

The presented results illustrate that the leaching of U from the peat strongly depends on various factors taking into consideration the natural leaching and the leaching experiments in the laboratory. The results from the drainage pipe show no correlation between the temperature, which is higher in summer than in winter, and the U concentration in the drainage water, i.e. the leaching of U is independent of the temperature. The pH remained more or less the same through the sampling year which makes it impossible to define a relationship from the field study for the factor pH. The electric conductivity as well did not significantly change its value. Hence, for this factor it is again not possible to deviate a relationship from the nature observations. The only factor during the field study that varied and seems to influence the U concentration is the flow rate. The flow rate is the result of rainfall: after a heavy rainfall, the amount of water flowing out of the drainage pipe is high. On the contrary: there is a small flow rate if there was no or only little rainfall. This implies that the U concentration does not depend on the flow rate but rather on the amount of water circulating through the soil with its peat horizon. As can be seen in Fig. 34, the U concentration apparently reacts upon the amount of water available. When the amount of precipitation is high, the activity concentration of U in the drainage water is high. For dry periods it is the other way round and activity concentrations are rather low. The reason for this correlation cannot concludingly be identified. There are two possible explanations: (i) the low U concentration that appears at low flow rate is the effect of a base flow. This means that the water originating from low rainfall does not reach the peat horizon with its extraordinarily high U content. The rainwater in this case either evaporates or incorporates into the plants of the agricultural field. If the rainwater would be connected to the peat horizon, the reaction time for leaching would be much longer at low flow rate than at high flow rate and the consequence would be a higher concentration at low rate. In turn, the high U concentrations at high flow rate only occur after having an intense rainfall. In this case, the peat horizon is flushed with rainwater and U can be leached resulting in an increased U concentration in the drainage water. This means, that the water coming out of the drainage pipe has different origins depending on the intensity of the rainfall: if there is no or only low rainfall, the drainage water consists of a kind of groundwater that did not percolate through the top soil. If there is a more intense rainfall, the water percolates through the top soil including the peat horizon and reaches together with the base flow water the drainage pipe (Fig. 35a). The second, but more implausible explanation for the correlation could be the following: (ii) having an intense rainfall, all soil particles are coated with water and the available U-complexes fixed onto the particles can be oxidatively leached. If the rainfall event is rather small, only a fractional amount of the complexes is moistened and thus not the total disposable amount of U can be transferred into water (Fig. 35b). However, both assumptions are only true until a certain threshold. At some point, of heavy precipitation, the whole soil is saturated with water and all available U complexes are in contact with it. At approximately 3’000 mBq/L ^{238}U there is no further leaching possible (Fig. 36).

The most important factor for leaching of U from the peat horizon is the amount of water that percolates through the soil, independent which scenario is the truth. This means that a humid climate with wet seasons promotes the leaching of U in nature. This was the case in the beginning of the study that started in June 2016. The following months it was still possible to collect water samples from the drainage pipes and thus to proceed the study. However, one year later in the middle of 2017, the drainage pipe fell dry and no further sampling was possible. The pipe was monitored frequently in order to collect a water sample in case the drainage water returned. But the following months were that dry that the sampling was abandoned. This impressively highlights that an arid climate restricts the leaching of U. In the case of the Lyssbach area, no U leached from the peat horizon reached the Lyssbach though the drainage pipe during this very dry periods. But even in dry climates there will be rain events although they can be fewer and shorter but with a more intense rainfall. This means, that the fate of U in this special kind of environment is difficult to predict. These heavy rainfall events have to be studied more in detail in order to gain a better understanding of the leaching processes during such events.

Other elements were not considered for the U leaching studies. For example, the concentration of ^{226}Ra in the drainage water is constant through the year of sampling and the mean activity concentration of 28 mBq/L ± 5 mBq/L is only a fractional amount of the U concentration. One explanation therefore could be that the ^{226}Ra accumulated at the coatings or sedimentations of the drainage pipes because Ra likely adsorbs onto Fe-oxyhydroxides (Schott and Wiegand, 2003). One thing that can be deduced is that the mechanisms of Ra leaching are completely different from the conditions that are suitable for U leaching. But from the results of this study it is impossible to evaluate the influence of Ra on the leaching behaviour of U.

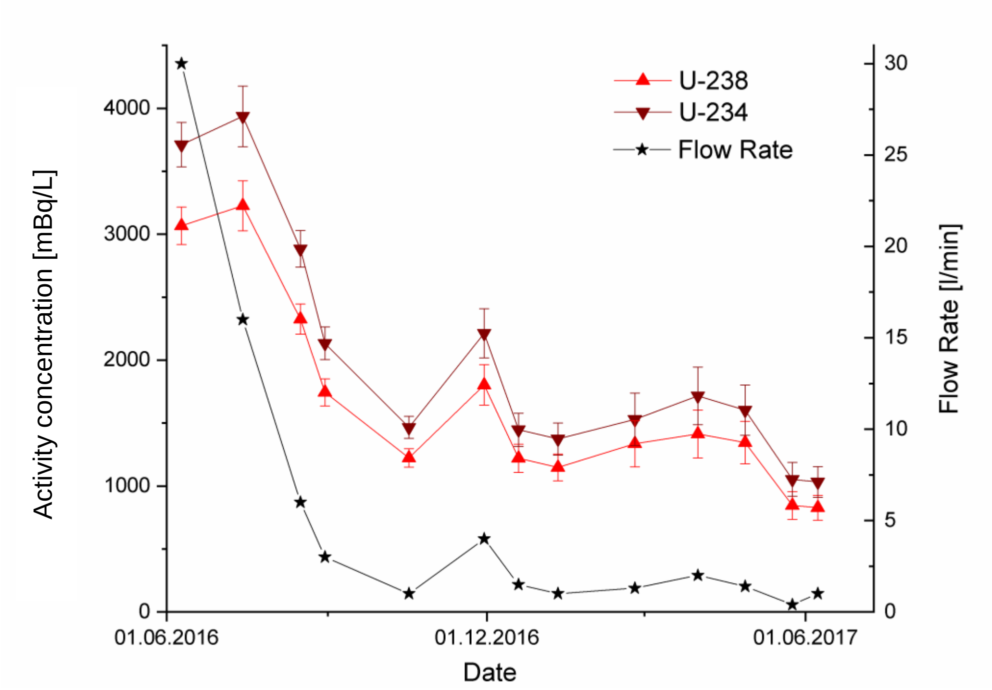

Fig. 34: Correlation of the ^{234}U and ^{238}U concentration with the flow rate, i.e. with the amount of water percolation through the soil with its U rich peat horizon.

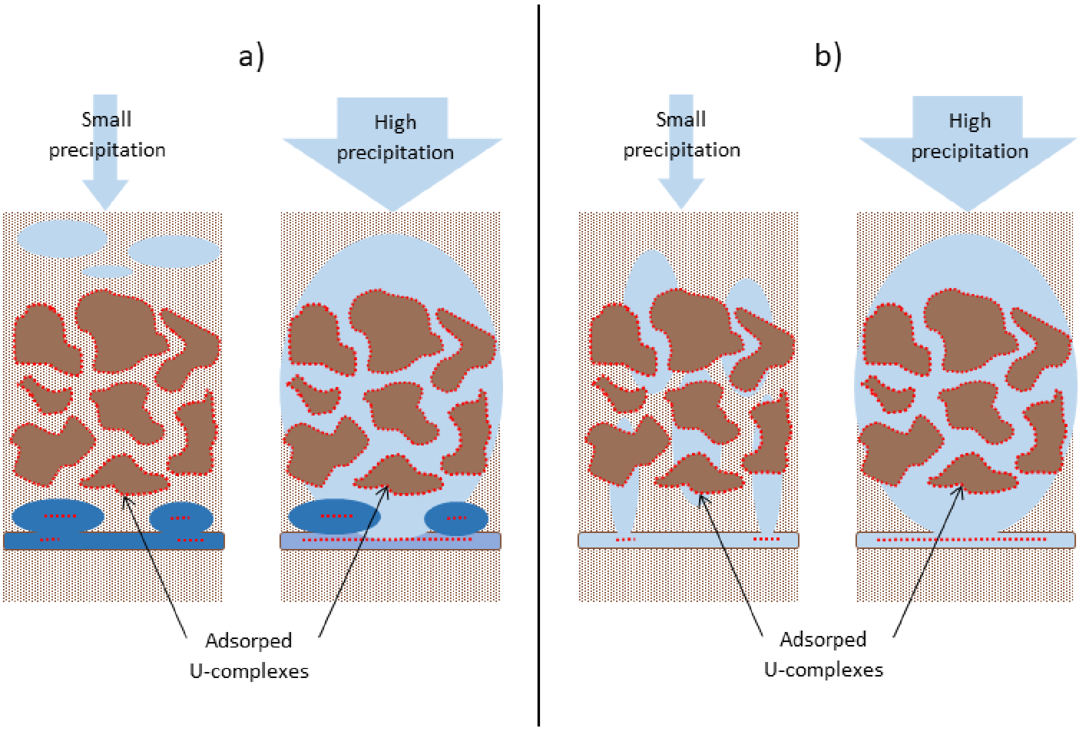

Fig. 35: U-complexes (red dots) that are adsorped onto organic matter (brown). a) Left side: small precipitation does not reach the peat horizon and only the base flow reaches the drainage pipe. Right side: high precipitation leads to a flush of the peat horizon where the U can be leached. b) Left side: small precipitation leads to a small amount of water that circulates througth the soil, i.e. not all particles are covered with water and not all of them can be leached. Right side: high precipitation leads to a huge amount of water that circulates through the soil, i.e. all particles are in contact with water and can be leached.

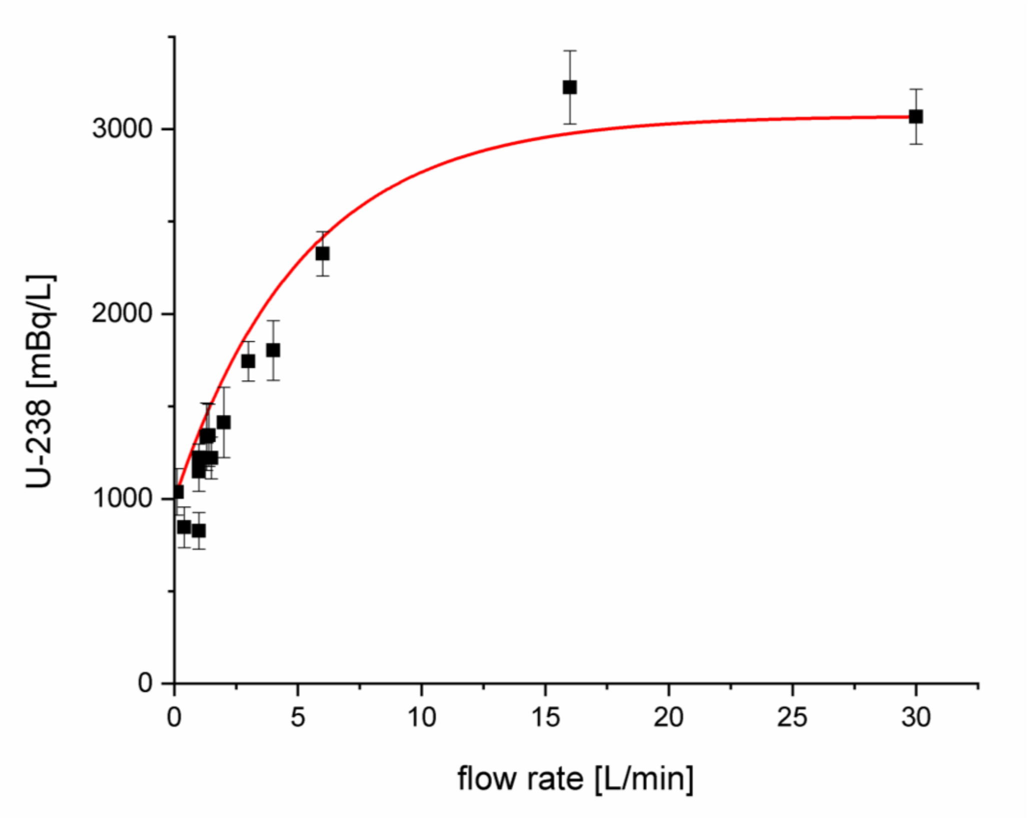

Fig. 36: ^{238}U concentration plotted against the flow rate indicating a threshold at approximately 3000 mBq/L where no further leaching is possible.

The leaching experiments in the laboratory were designed in order to expand the evaluation of the leaching behaviour of U at the Lyssbach area. The sequential leaching experiments verified the assumption that most of the U consists of the oxidizable fraction and is bound to organic matter (85%). Together with the exchangeable fraction (1%) it is easily leachable from the peat and therefore most available for the environment. The reducible fraction of U is bound to Mn and Fe oxi-hydroxides and can only be released into the environment if the conditions change from an oxic to an anoxic state (Pérez-Moreno et al., 2018). However, oxi-hydroxides could not have been formed under the reducing conditions that have been present during the formation of the peat layer. Consequently, the reducible fraction is only 1% due to this absence and this fraction is neglected for the calculation. The percentage of the residue with 12% is in fact not small, but the U in fraction is bound to crystalline structures in minerals and therefore not mobile in the natural conditions of the Lyssbach environment. The analysis of the peat horizon revealed a mean value of rounded 2’000 Bq/kg ^{238}U in the peat. Taking into account that the reducible fraction is in principle not existing and that the residual fraction of U in the peat cannot be leached in a natural environment, 86% of the total inventory from the peat horizon of the Lyssbach area can be leached. This yields 1’720 Bq/kg U that is potentially leachable.

The following laboratory leaching experiments were designed in a natural way, i.e. no extreme conditions such as boiling the peat in concentrated acid. The only chemical reactant that was added to the leaching liquid was Na_2CO_3 since the PHREEQC model revealed that U in the drainage water is present as carbonate complex. As can be seen in Fig. 31, the higher the carbonate concentration, the better the leachability of U from the peat into the drainage water. Since the leaching experiment with demineralised water yields 0% and 0.001 M Na_2CO_3 yields only 1 %, there has to be a sufficient CO_3^{2-} concentration in order to form stable complexes with U. Another criterion that favours the leaching of U is the pH. Fig. 32 shows that U stays adsorbed onto organic matter unless the pH reaches a higher value. Further, the leaching is time dependent (Fig. 33): the longer the peat is in contact with water, the more U is transferred from the peat into the extractant. Taking all these experiments into account, the most favourable condition for leaching U is a liquid with at least 0.05 M Na_2CO_3 content, a pH of 9-10 and a leaching time of 10 hours. However, the environmental conditions at the agricultural fields around Lyssbach cannot be designed according to the laboratory results and we assume that the conditions in nature are not too close to the most promoting scenario for best leaching: (i) the carbonate content in the drainage water derives from the rain water that dissolves some carbonate species from the upper soil until it reaches the peat horizon and does not reach too high concentrations; (ii) the measured pH in the drainage water is constantly around 7; (iii) there is sufficient residence time of the rainwater in the soil but without the other two parameters longer leaching time cannot increase the leaching rate.

Finally, an estimation of the lifetime of U in the environment of peat horizon at the Lyssbach area was accomplished by calculating the total U inventory and an overall leaching rate. Parameters used for the calculation are mean values from the year of sampling. The calculation is explained in the following:

- The mean flow rate of the drainage pipe (5 L/min ≙ 2’628’000 L/year) is combined with the mean annual precipitation of the area (1’000 L/m^2) in order to evaluate the extension of the catchment area of the drainage pipe:

$$Catchment\ area\ of\ the\ drainage\ pipe = \frac{2'628'000\,\frac{L}{year}}{1'000\,\frac{L}{m^2}/year} = 2628\,m^2 \ \approx 50\,x\,50\,m$$

- The thickness of the peat horizon (0.2 m) and the density of dry peat (1.5 g/cm^3) yield the total peat inventory at the catchment area:

$$Total\ peat\ inventory: 0.2\ m\ \cdot 1'500 \frac{kg}{m^3} = 300 \frac{kg}{m^2}$$

- Combing this inventory with the U concentration in the peat (2’000 Bq/kg) yields the total U inventory at this area:

$$Total\ U\ inventory = 300 \frac{kg}{m^2}\ \cdot 2'000 \frac{Bq}{kg} = 600 \frac{kBq}{m^2}$$

- The leachable fraction according to the sequential extraction experiments is 86%:

$$Total\ leachable\ U\ at\ Lyssbach = 600 \frac{kBq}{m^2} \cdot 86\% = 516 \frac{kBq}{m^2}$$

- Combining the annual precipitation with the mean U concentration in the drainage pipe (1.6 Bq/L) reveals the leaching rate:

$$Leaching\ rate = \frac{1'000 \frac{L}{m^2}}{year} \cdot 1.6 \frac{Bq}{L} = 1.6 \frac{kBq}{m^2\ \cdot y}$$

- Taking into account the total leachable U inventory the annual leaching rate can be calculated:

$$Annual\ leaching\ rate = \frac{1.6 \frac{kBq}{m^2\ \cdot y}}{516 \frac{kBq}{m^2}} \cdot 100\% = 0.3 \frac{\%}{year}$$

- The remaining time until all U from the Lyssbach area is leached is computed as follows (assuming a linear decrease):

$$Remaining\ time = \frac{516 \frac{kBq}{m^2}}{1.6 \frac{kBq}{m^2\ \cdot y}} = 322\ years$$

- The total annual U content in the drainage water can be calculated with the 0.3 % leaching per year:

$$Total\ annual\ U\ content\ in\ drainage\ water =\ 516 \frac{kBq}{m^2} \cdot 0.003\ \cdot 2628\ m^2 = 4\ \frac{MBq}{year}$$

- This calculation can be checked by combining the mean flow rate of the drainage pipe (5 L/min ≙ 2’628’000 L/year) with the mean U concentration of drainage water (1.6 Bq/L):

$$Total\ annual\ U\ content\ in\ drainage\ water = 2'628'000 \frac{\mathrm{L}}{\mathrm{year}} \cdot 1.6 \frac{Bq}{L} = 4\ \frac{MBq}{year}$$

Unfortunately, these calculations comprise plenty uncertainties and approximations like the assumption of a homogeneous distribution of the U accumulation or the averaging of the flow rate. But it is not only questionable whether the accumulation is homogeneously distributed but also whether the concentration is constant over the whole area. However, it is known from investigations with a drone that the elongation of the U accumulation is even more widespread than the 50x50 m (Surbeck et al., 2015; Werthmüller et al., 2015) but the real concentration remained uncertain. Another large uncertainty concerns the mathematical law of the leaching. The calculation above assumes a linear decrease of U due to the leaching by rainwater. It is not verified if this assumption is correct. A more exponential decrease of U in the peat, comparable to a biological half-life, is also very likely. Nonetheless whether a linear of exponential decrease of U in the peat is correct, these calculations give a first hint that the U accumulation in this huge amount will remain for a long time in the environment at the Lyssbach area until all or at least nearly all U is leached.

The calculated leaching rate of 0.3% of the total U inventory per year is in a good agreement with the leaching experiments in the laboratory: The leaching experiment where the leaching liquid varied in pH revealed that leaching is enhanced by a more alkaline pH and at neutral pH, as it is the case in the drainage water, the leaching percentage is only 1%. This implies that a change in the pH at the agricultural fields would lead to an increased leaching rate. This scenario is rather unlikely. The other variable is the concentration of CO_3^{2-} in the leaching extractant which is also of importance for the leaching behaviour. This parameter is influenced by the soil above the peat horizon where the rainwater first circulates and therefore very unlikely to change in a greater extend. However, there is another big obscurity for the real estimation of the leaching rate: climate change. The calculation considers a mean annual precipitation of 1’000 L/m^2 and year. But the future prospects for the next some hundreds of years predict a more and more extreme climate with dry periods but also heavy rainstorms. This makes the evaluation of the leaching rate for the next 100 years nearly impossible. However, the risk that humans are dangerously exposed to U concentrations in water followed by leaching from the peat is rather small because (i) there is not enough U leached from the peat to the drainage pipe, and (ii) if the U concentration increases over the years, the drainage water is immediately diluted by the Lyssbach itself.

5.5 Conclusions

This chapter has shown that the leaching of U that is associated with organic materials is a complex issue and depends on diverse factors. Leaching at the agricultural fields around Lyssbach is a constant process but with varying intensities. The field studies have shown that the leaching strongly depends on the amount of water available. The more precipitation, the more U complexes can be leached. The laboratory experiments have shown that the leaching is also strongly controlled by the concentration of CO_3^{2-} present in the leaching liquid. Other factors are the pH as well as the leaching time. The field studies and its following calculation of the leaching rate are in good agreement with the leaching experiments that have been accomplished in the laboratory. The overall leaching rate at the peat horizon near the Lyssbach is approximately 1% per year. If the conditions remain the same, it will need more than 300 years until all U is leached. However, there are several uncertainties within this calculation with the climate as the principle unknown. But nevertheless, that the U will be transferred into the Lyssbach where it is diluted and finally transported via the Aare and the Rhine to the North Sea is a fact, it is only a question of time.

Chapter 6 Uranium in rice

In 2018, Agroscope (Swiss centre for agricultural research, nutrition and the environment) launched a project about rice cultivation in Switzerland. The goal of this project was to promote biodiversity in areas which have been wetlands before drainage in the 19th century. A long-term objective was to identify crop growing conditions for rice in Switzerland since climate change forces farmers into a new direction of cultivation. One of the seven study sites for the rice cultivation was an agricultural field north of Mont Vully. As the previous study at Mont Vully has shown, the probability is high that increased U concentrations in soils occur in this area. That's the reason why a collaboration between Agroscope and PSI was initiated to identify whether U from the fields migrate into rice plants.

6.1 Radioactivity in food

Previous studies of radioactivity in food are manifold covering natural and anthropogenic nuclides in various kinds of agricultural stuffs and from different parts of the world. For example, Al-Harmaneh et al. (2016) analysed 13 types of vegetables and agricultural crops cultivated in the northwestern part of Saudi Arabia for its radionuclide content. The highest transfer factor for U showed beans with 0.16 (for a definition of the transfer factor see chapter 6.3 below). And Chen et al. (2005) determined the soil to plant transfer of ^{238}U, ^{226}Ra and ^{232}Th for different plants such as lupines, Chinese mustard, white clover or ryegrass. Sasaki et al. (2002) investigated U, Th, Ra and Pb in rice, potato, onion, cabbage, mandarin orange, spinach and apple in Japan. The results of these three studies have shown that the transfer factors of radionuclides were rather small. Almayahi and Aljarrah (2020) investigated the emission of alpha particle rates from rice and several other heavy metals in rice such as Fe and Cd and came to the result, that all values are below a critical limit for food consumption. Alrefae and Nageswaran (2013) studied the annual effective dose from rice consumption correlated to the natural radionuclides ^{238}U, ^{232}Th and ^{40}K as well as the anthropogenic nuclide ^{137}Cs in Kuwait. The annual effective dose was several orders of magnitude less than the world average of 0.29 mSv/year resulting from the ingestion from natural sources (UNSCEAR, 2000). The authors concluded that the rice consumption in Kuwait is radiologically safe. Asaduzzaman et al. (2015) investigated the soil-to-rice grain transfer factors in Malaysia for the radionuclides ^{226}Ra, ^{232}Th and ^{40}K with the conclusion that the estimated transfer factors were lower comparing to the values reported by the IAEA (2010). Pulhani et al. (2005) investigated the uptake of U, Th Ra, and K into wheat in India and found out that most of the radionuclides (54-75%) were concentrated in the roots and only a minor part (16%) were found in the grains. Further, there are several studies about the uptake of ^{137}Cs to rice or other plants (Choi et al., 2011; Uchida et al., 2009) and a lot of studies accomplished especially about the consequences after the accident in Fukushima (Endo et al., 2013; Harada & Nonaka, 2012; Yamada et al., 2017). All of them came to the result that the uptake of radionuclides is rather small (transfer factors of ~ 0.01 from soil to rice), independent of its natural or anthropogenic origin.

Nonetheless, the U concentration in rice produced during the project of rice cultivation in Switzerland was performed to have reliable results even for the special region around Mont Vully where U concentration in soil were increased.

6.2 Sampling locations, procedure and measurements

Agroscope chose different study sites for rice cultivation which have been former wetlands since the chances to successfully create a new wetland is high at areas that have been a wetland before drainage. Six study sites have been selected for the investigation of U in soil: Brugg, Schwadernau, Witzwil, La Sauge, Bavois North and Bavois South (Fig. 37). The analysis of U in plants has been accomplished at four of the six sites: Witzwil, La Sauge, Bavois North and Bavois South.

Soil samples from the six study sites where taken in April 2019 when the fields have been prepared for cultivation (Fig. 38). At the same date, samples were taken from water that was used for watering and filling the reservoirs. In September 2019, rice plants were grown and samples were taken from each cultivated area (Fig. 39). In the PSI laboratory, the plants were separated to stem, leaves and rice panicles (Fig. 40). As soon as the rice has been harvested, samples from each field were sent to the laboratory for further preparation.

Soil and water samples were analysed identically to the water and soil samples from chapter 2. Samples from the rice plants were first dried at approximately 60°C and afterwards cut into small pieces of about 1 cm. Then, the samples were transferred into a muffle oven. Temperature was slowly increased from room temperature to 150°C, then to 300°C and finally the samples rested at 500°C for 15 hours. The residue was transferred to a beaker and poured with concentrated HNO_3 so that all ash was covered with acid. The beaker was covered with a glass and the solution was boiled for 2 hours. Afterwards, the solution was evaporated to complete dryness and again incinerated at 400°C for 2 hours. The following leaching, filtration and separation step was identically to the method explained in chapter 2.

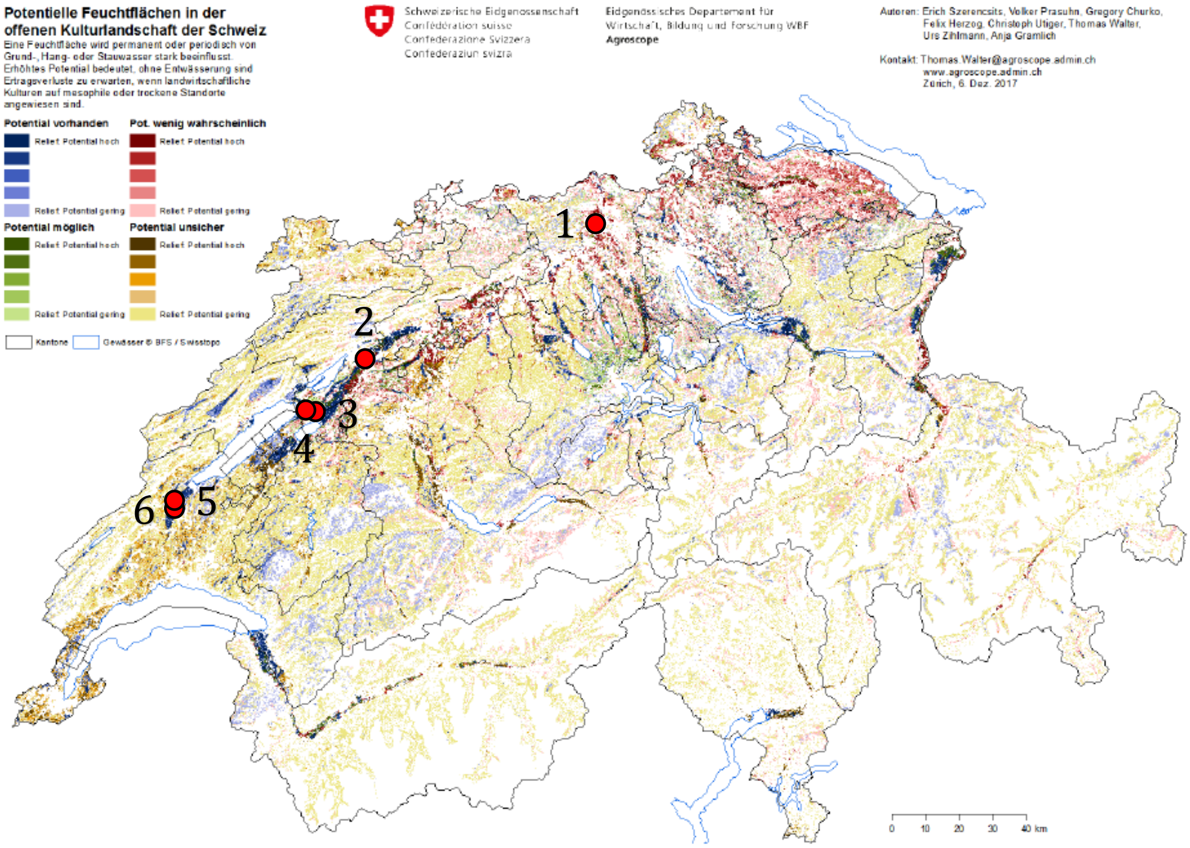

Fig. 37: Areas for potential establishments of wetlands and therefore rice cultivation (www.feuchtaker.ch). Red points indicate the study sites for U investigation. 1 = Brugg; 2 = Schwadernau; 3 = Witzwil; 4 = La Sauge; 5 = Bavois North; 6 = Bavois South.

Fig. 38: Study fields prepared for rice cultivation. Left side: Witzwil; Right side: Bavois North.

Fig. 39: Study fields with cultivated rice. Left side: Bavois South; Right side: La Sauge.

Fig. 40: Final cultivated rice. Left side: Rice plant cluster in the field shortly bevor harvesting; Right side: Single rice plant indicating the stem, the leaves and the panicles.

6.3 Results and discussion

The results of the U concentration in soil and water samples are listed in Tab. 9. The soil of the study sites near Brugg and Schwadernau show very minor U concentrations of <10 Bq/kg for ^{238}U and ^{234}U. The water used for flooding of the fields is taken at both sites from the river Aare and was not sampled for analysis. Therefore, no further investigation was done for these two fields since a whole U determination of rice plants was meaningless if there was no U available in the direct environment. The soil of the field near Witzwil had a normal concentration of 28 ± 3 Bq/kg and 34 ± 4 Bq/kg for ^{238}U and ^{234}U, respectively (mean ^{238}U concentration of soils in Switzerland: 40 Bq/kg (UNSCEAR, 2000)). The field near La Sauge showed again a minor U concentration of <10 Bq/kg for both U isotopes. The water used for flooding at these sites was water from the Broye canal. This water has an U concentration of 26 ± 5 mBq/L and 30 ± 5 mBq/L for ^{238}U and ^{234}U, respectively which is not increased comparing to the values measured elsewhere in the Swiss Plateau (cf. chapter 3). However, since the fields were in direct vicinity to Mont Vully where high U concentration are known, it was decided to do further investigation at these fields, too. The two fields near Bavois showed moderate U concentrations. Bavois North had a U concentration of 23 ± 3 Bq/kg and 25 ± 3 Bq/kg for ^{238}U and ^{234}U, respectively, which again was a normal range for U concentrations in soils. The only field that had slightly increased U values was Bavois South with approximately 65 ± 6 Bq/kg and 73 ± 7 Bq/kg for ^{238}U and ^{234}U, respectively. At these two sites, water from a pumping station of drainage pipes was used for watering and flooding the field. The concentrations in the drainage of Bavois North is slightly increased in comparison to the drainage water from Bavois South: 98 ± 12 mBq/L and 112 ± 13 mBq/L in Bavois North and 40 ± 6 and 48 ± 7 mBq/L in Bavois South each for ^{238}U and ^{234}U, respectively.

Tab. 9: U concentrations in soils and water used for flooding of different study sites for rice cultivation (2σ uncertainties).

Location	*^{238}U soil [Bq/kg]*	*^{234}U soil [Bq/kg]*	*^{238}U water [mBq/L]*	*^{234}U water [mBq/L]*
Brugg	<10	<10	-	-
Schwadernau	<10	<10	-	-
Witzwil	28 ± 3	34 ± 4	26 ± 5	30 ± 5
La Sauge	<10	<10		
Bavois North	23 ± 3	25 ± 3	98 ± 12	112 ± 13
Bavois South	65 ± 6	73 ± 7	40 ± 6	48 ± 7

The results of the rice plants and the rice itself are listed in Tab. 10 for ^{238}U concentrations and in Table 11 for the ^{234}U concentrations. The concentrations scatter fairly for all parts of the rice plant. The sample preparation was not always successful due to the high starch content which complicated the passing of the sample solution through the U/TEVA resin. These problems resulted in a low chemical yield which in turn led to the fact that some uncertainties had the same value or even exceeded the measurement value. Further, it was only possible to accomplish one analysis per sample. However, these values are listed in the table nonetheless since it gives an indication of the activity concentration range. Obvious is, that the leaves and the stems from Bavois North, where the higher U concentrations in drainage water were found, show also higher U concentrations than the rest. The plants from Bavois South, where U concentrations in the soil were slightly increased, did not reflect this fact. Unfortunately, it was possible to organize only a pool sample of the final rice from Bavois North and Bavois South (mixing of the final rice already during harvesting by the farmers). This mix of both sites does not show any increased U concentration. The highest U concentration seems to be from the field near La Sauge. However, if you consider the large measurement uncertainty and the fact, that there were only minor U concentrations in the panicles, this value cannot be regarded as verified.

Tab. 10: ^{238}U concentrations in stems, leaves panicles and rice from Witzwil, La Sauge, Bavois North and Bavois South. Rice samples from Bavois North and South were mixed. All values are single values from an aliquot of a homogenized sample and given in mBq/kg and 2σ uncertainties.

^{238}U [mBq/kg]	*Stems*	*Leaves*	*Panicles*	*Rice*
Witzwil	63 ± 12	22 ± 8	24 ± 29	8 ± 5
La Sauge	16 ± 6	30 ± 16	14 ± 11	91 ± 107
Bavois North	183 ± 23	63 ± 16	9 ± 6	30 ± 16
Bavois South	28 ± 6	28 ± 9	14 ± 5	

Table 11: ^{234}U concentrations in stems, leaves panicles and rice from Witzwil, La Sauge, Bavois North and Bavois South. Rice samples from Bavois North and South were mixed. All values are single values from an aliquot of a homogenized sample and given in mBq/kg and 2σ uncertainties.

^{234}U [mBq/kg]	*Stems*	*Leaves*	*Panicles*	*Rice*
Witzwil	76 ± 13	28 ± 8	24 ± 29	12 ± 6
La Sauge	21 ±7	11 ± 10	6 ± 7	61 ± 87
Bavois North	176 ± 23	77 ± 18	14 ± 8	43 ± 19
Bavois South	183 ± 23	63 ± 16	9 ± 6	

In order to get an evaluation whether U is transferred from soil to the plant, a transfer factor had to be determined. This factor makes it possible to compare different study sites with each other. Transfer factors from the soil to the different plant parts are calculated according to the following equation (Cierjacks & Albers, 2004):

$$Transfer\ Factor\ TF = \frac{dry\ weight\ plant\ [\frac{Bq}{kg}]}{dry\ weight\ soil\ [\frac{Bq}{kg}]}$$

Transfer factors from the flood water to the different plant parts are calculated according to the following equation (Cierjacks & Albers, 2004):

$$Transfer\ Factor\ TF = \frac{dry\ weight\ plant\ [\frac{Bq}{kg}]}{water\ used\ for\ flooding\ [\frac{Bq}{kg}]}$$

These calculations were done for each study site and in term for each part of the rice plant. The transfer factors are listed in Tab. 12 for the soil-plant transfer and in Tab. 13 for the water-plant transfer. It is obvious that the transfer factors from soil to plant are three orders of magnitude lower than the water to plant factors. The fact that the transfer factors from soil to plant start at the third decimal place (excluding the factor for rice in La Sauge) confirm, that the U concentration that is present in soil cannot or only to a very small percentage be transferred to the plant. However, the U concentrations in the flooding water lies in the same order of magnitude as the U in plants. This implies that the U that is dissolved in the water can much more easily be incorporated into the plants. This leads to the assumption that nearly all of the U available in the flooding water is disposable for the plant. The reason therefore could be, that the U in soil is normally bound in crystalline structures as explained in section 3.6. Even higher U concentrations than what is present in normal soil can be found especially at the area around Mont Vully. In this case, the U is adsorbed onto organic matter and supposedly buried under half a meter of soil. The probability that this U is available for the rice plants is rather small because i) the roots of rice plants only reach a depth of a few centimetres (Barison & Uphoff, 2001) and ii) the U is not leachable under reducing conditions that are present under the flooded area. Comparing to the sparce results from the literature, the transfer factors from soil/water to rice grains are rather small.

Tab. 12: Transfer factors from the soil to the different plant parts.

	Witzwil	*La Sauge*	*Bavois North*	*Bavois South*
Stems	0.0023	0.0017	0.0081	0.0004
Leaves	0.0008	0.0033	0.0028	0.0004
Panicles	0.0009	0.0015	0.0004	0.0002
Rice	0.0003	0.0100	0.0013	0.0005

Tab. 13: Transfer factors from the flooding water to the different plant parts.

	Witzwil	*La Sauge*	*Bavois North*	*Bavois South*
Stems	2.4	0.6	1.9	0.7
Leaves	0.8	1.1	0.6	0.7
Panicles	0.9	0.5	0.1	0.4
Rice	0.3	3.4	0.3	0.8

6.4 Conclusions

In conclusion it can be said that the risk of increased U concentrations in rice are rather small. The literature review has already shown, that the uptake of radionuclides, whether natural or anthropogenic, were marginal. This has been verified by the first studies of U in rice shown in this chapter although the stated results give only a first hint. In order to proof the results of this pilot study, further investigations have to be done including analyses of soil, water and plants. Especially the transfer factor should be determined more precisely. Another interesting question for the cultivation of rice in an area with increased U concentrations would be the concentration and distribution of several U daughters such as Ra, Pb or Po. These nuclides have not been analysed during this study. In the literature, these nuclides were partially covered with the result, that the uptake and thus the transfer factors were also small.

Considering legal requirements of U in rice in Switzerland, further studies are not necessarily required since there are no concentration limits of natural radionuclides in food anymore (Eidgenössisches Departements des Innern, 2016).

Chapter 7 Conclusion & Outlook

7.1 Conclusion

In the course of the presented work, the fate of geogenic U in the environment has been intensively investigated with regard to the special situation in the Swiss Plateau. The origin of U in groundwater of the Swiss Plateau has been verified to derive from two Molasse Units that were constantly leached. A double stage processes of leaching and accumulation in a peat horizon of former wetlands was identified and illustrated in this thesis. This process was investigated in detail at Mont Vully where extensive field studies have been accomplished. The study sites seem to be a special case, but if we take into account that the whole Swiss Plateau consists of Molasse Units and that until the 19th century there have been plenty of wetlands in this area, the probability is high that similar situations also occur in other locations. A first attempt has been made by recording the γ dose rate with a helicopter. However, the results were not definite but give a first hint where similar accumulations occur and following studies can resort to these findings.

Another study area with a comparable situation as it was found at Mont Vully was the Lyssbach area. At this site, the focus of the study has not been the origin of U but the future of it. The U accumulation in a peat horizon has been investigated with regard to the leaching behavior of U under natural conditions. The results of sampling water from a drainage pipe revealed that the release of U that is adsorbed onto organic material strongly depends on diverse factors such as amount of water available and the carbonate content of the leaching water. A calculation of a total leaching rate was elaborated from the observed conditions at Lyssbach. Additionally, laboratory experiments were performed in order confirm the results from the study site. The fate of U in this environment was to rest for the next several hundreds of years (or even longer) until it is completely leached and transported to surface water.

Owing to the analysis of the distribution of U in rice plants, the health risks due to the consumption of rice from an U rich soil can probably be excluded. The transfer factors from soil and water to plants are small enough to prevent concerns about this issue. However, the launch of the project about rice cultivation in Switzerland has shown the importance of knowledge where U can occur in nature so that potential problems can be avoided in the beginning.

7.2 Outlook

Within the knowledge of the fate of U in the environment there will always be situations that have to be investigated. The study site at Mont Vully has now been intensively studied that no further question to this site remains unexplained. However, the broader sampling campaign in the Swiss Plateau revealed, that there are more springs with increased U concentrations. These springs could have also fed ancient wetlands that have been drained in the 19th century in order to create arable land. Such former wetlands with a high organic matter content are potential sites for similar U accumulations likewise the arable land north of Mont Vully or the Lyssbach area. A comprehensive study of ancient wetlands in the Swiss Plateau regarding its U content would be essential for the knowledge of U occurrences in nature.

The results from the airborne γ ray spectrometry revealed that the helicopter was not the appropriate tool for the discovery of small scaled U accumulations with low dose rates. A possible alternative could be the survey by means of a drone. A drone that is equipped with a detector could fly more closely to the fields and with a smaller line spacing than a helicopter. The advantage over recording the dose rate by foot is the speed and the intactness of potential crops on arable land. The disadvantage would be short flight times due to the heavy weight of the detector that has to be carried by the drone and the risk of an accidental crash destroying the expensive detector. Balancing the pros and cons, a drone would be a suitable way to easily detect U accumulations.

Further investigations about the leaching behaviour of U at the Lyssbach area would be helpful to precise the leaching rate. The calculation of the rate in this thesis is based on 1 year screening the drainage pipe once month. A more frequent sampling in combination with a detailed recording of the precipitation in exactly this region can improve the background for the evaluation. However, this is only possible if the drainage pipe can be reinstalled in case of a blockage within the pipe. In combination with an enhanced field study, continuative laboratory experiments could be elaborated to support the findings in nature.

The last continuative study following this doctoral thesis would be a more detailed investigation of the U uptake of plants. A first direction has been set by analysing U in rice plants but were not accurate enough. More samples from rice and especially different local plants should be analysed not only for their U concentration but also for certain decay products such as Ra or Po. Most important would be analysing plants from agricultural areas that have been constructed onto ancient wetlands. First example: the Lyssbach area.

References

Al-Hamarneh, I. F., Alkhomashi, N., & Almasoud, F. I. (2016). Study on the radioactivity and soil-to-plant transfer factor of ^{226}Ra, ^{234}U and ^{238}U radionuclides in irrigated farms from the northwestern Saudi Arabia. Journal of Environmental Radioactivity, 160, 1–7.

Almayahi, B. A., & Aljarrah, N. (2020). Relationship between heavy metals and alpha particles as a marker of environmental pollution in rice consumed in Najaf, Iraq. Heliyon, 6(1).

Alrefae, T., & Nageswaran, T. N. (2013). Radioactivity of long-lived gamma emitters in rice consumed in Kuwait. Journal of the Association of Arab Universities for Basic and Applied Sciences, 13(1), 24–27.

Antenen, F. (1936). Geologie des Seelandes. Verlag der Heimatkundekommission.

Asaduzzaman, K., Khandaker, M. U., Amin, Y. M., & Mahat, R. (2015). Uptake and distribution of natural radioactivity in rice from soil in north and west part of peninsular Malaysia for the estimation of ingestion dose to man. Annals of Nuclear Energy, 76, 85–93.

ATSDR. (2013). Toxicological Profile for Uranium.

Baertschi, P. & Keil, R. (1992). Urangehalte von Oberflächen-, Quell- und Grundwässern der Schweiz. NAGRA Report, Wettingen.

Bajo, S., & Eikenberg, J. (1999). Electrodeposition of actinides for alpha-spectrometry. In Journal of Radioanalyttcal and Nuclear Chemistry, 242(3).

Bajwa, B., Kumar, S., Sahoo, S. & Tripathi, R. (2017). Uranium and other heavy elements distribution in the drinking water samples of SW-Punjab, India. Journal of Radiation Research and Applied Sciences, 10(1), 13-19.

Banning, A., Demmel, T., Rüde, T. R., & Wrobel, M. (2013). Groundwater uranium origin and fate control in a river valley aquifer. Environmental Science and Technology, 47(24), 13941–13948.

Baradács, E., Hunyadi, I., Dezso, Z., Csige, I. & Szerbin, P. (2001). ^{226}Ra in geothermal and bottled mineral water of Hungary. Radiation measurements, 34(1-6), 385-390.

Barisic, D., Lulic, S., & Miletic, P. (1992). Radium and uranium in phosphate fertilizers and their impact on the radioactivity of waters. Wat. Res., 26(5), 607–611.

Barison, J., & Uphoff, N. (2001). Rice yield and its relation to root growth and nutrient-use efficiency under SRI and conventional cultivation: An evaluation in Madagascar. Paddy and Water Environment, 9(1), 65–78.

Becker, F. (1973). LK 1165 Murten Erläuterungen. In: Geologsicher Atlas der Schweiz. Schweizerische Geologische Kommission.

Bigalke, M., Schwab, L., Rehmus, A., Tondo, P., & Flisch, M. (2018). Uranium in agricultural soils and drinking water wells on the Swiss Plateau. Environmental Pollution, 233, 943–951.

Birke, M., Rauch, U., Lorenz, H. & Kringel, R. (2010). Distribution of Uranium in German bottled and tap water. Journal of Geochemical Exploration, 107(3), 272-282.

Bister, S., Birkhan, J., Lüllau, T., Bunka, M., Solle, A., Stieghorst C., Riebe, B., Michel, R., Walther, C. (2015). Impact of former uranium mining activities on the floodplains of the Mulde River, Saxony, Germany. Journal of Environmental Radioactivity, 144, 21-31.

Brugge, D., Bichner, V. (2011). Health effects of Uranium: new research findings. Rev. Environ. Health, 26 (4), 231-249.

Campbell, K. M., Kukkadapu, R. K., Qafoku, N. P., Peacock, A. D., Lesher, E., Williams, K. H., Bargar, J. R., Wilkins, M. J., Figueroa, L., Ranville, J., Davis, J. A., & Long, P. E. (2012). Geochemical, mineralogical and microbiological characteristics of sediment from a naturally reduced zone in a uranium-contaminated aquifer. Applied Geochemistry, 27(8), 1499–1511.

Chabaux, F., Bourdon, B., & Riotte, J. (2008). Chapter 3: U-Series Geochemistry in Weathering Profiles, River Waters and Lakes. Radioactivity in the Environment, 13, 49–104.

Chen, S. B., Zhu, Y. G., & Hu, Q. H. (2005). Soil to plant transfer of ^{238}U, ^{226}Ra and ^{232}Th on a uranium mining-impacted soil from southeastern China. Journal of Environmental Radioactivity, 82(2).

Choi, Y.-H., Lim, K.-M., Jun, I., Keum, D.-K., Han, M.-H., & Kim, I.-G. (2011). Transport behavior and rice uptake of radiostrontium and radiocesium in flooded paddy soils contaminated in two contrasting ways. Science of The Total Environment, 412–413, 248–256.

Cierjacks, A., & Albers, B. (2004). Zusammenstellung und Auswertung von radioökologischen Messdaten zum Transfer Boden/Pflanze unter Berücksichtigung der lokalen Variabilität in Deutschland. In: Schriftrenreihe Reaktorsicherheit und Strahlenschutz, BMU-2004-642.

Corcho Alvarado, J.A., Balsiger, B., Röllin, S., Jakob, A., Burger, M. (2014). Radioactive and chemical contamination of the water resources in the former uranium mining and milling sites of Mailuu Suu (Kyrgyzstan). Journal of Environmental Radioactivity, 138, 1-10.

Cothern, R. C. & Lappenbusch, W. L. (1983). Occurrence of Drinking Water in the U.S.. Health Physics, 45, 89-99.

Cumberland, S. A., Douglas, G., Grice, K., & Moreau, J. W. (2016). Uranium mobility in organic matter-rich sediments: A review of geological and geochemical processes. In Earth-Science Reviews, 159, 160–185.

Davis, B. A. S., Brewer, S., Stevenson, A. C., Guiot, J., Allen, J., Almqvist-Jacobson, H., Ammann, B., Andreev, A. A., Argant, J., Atanassova, J., Balwierz, Z., Barnosky, C. D., Bartley, D. D., de Beau-lieu, J. L., Beckett, S. C., Behre, K. E., Bennett, K. D., Berglund, B. E. B., Beug, H. J., Zernitskaya, V. P. (2003).

The temperature of Europe during the Holocene reconstructed from pollen data. Quaternary Science Reviews, 22(15–17), 1701–1716.

DiGregorio, D (2020). Discovery of Radioactivity, Reference Module in Earth Systems and Environmental Sciences.

EDI. (2017). Verordnung des EDI über Trinkwasser sowie Wasser in öffentlich zugänglichen Bädern und Duschanlagen (TBDV). Swiss Federal Department of Home Affairs.

Eidgenössisches Departements des Innern. (2016). Verordnung des EDI über die Höchstgehalte für Kontaminanten.

Eikenberg, J., Beer, H., & Jäggi, M. (2014). Determination of ^{210}Pb and ^{226}Ra/^{228}Ra in continental water using HIDEX 300SL LS-spectrometer with TDCR efficiency tracing and optimized αβ-discrimination. Applied Radiation and Isotopes, 93, 64–69.

Eikenberg, J. (2002). Radium Isotope Systematics in Nature: Applications in Geochronology and Hydrogeochemistry. Habilitation

Endo, S., Kajimoto, T., & Shizuma, K. (2013). Paddy-field contamination with ^{134}Cs and ^{137}Cs due to Fukushima Daiichi Nuclear Power Plant accident and soil-to-rice transfer coefficients. Journal of Environmental Radioactivity, 116, 59–64.

ESFA. (2009). Uranium in foodstuffs, in particular mineral water. EFSA Journal, 1018, 1–59.

Fantel, R. P., Stowasser, W. (1985). Natural Ressources Forum, 9, 5-24.

Faure, G., & Mensing, T. M. (2005). Isotopes - Principles and Applications. John Wiley & Sons.

Felipe-Sotelo, M., Hinchliff, J., Field, L.P., Milodowski, A.E., Preedy, O., Read, D. (2017). Retardation of uranium and thorium by a cementitious backfill developed for radioactive waste disposal. Chemosphere, 179, 127-138.

Giles, J. R. (1998). Radium-226 Concentrations and Corrections. TAN TSF-07 Pond.

Godoy, J., & Godoy, M. (2006). Natural Radioactivity in Brazilian groundwater. Journal of Environmental Radioactivity, 85(1), 71-83.

Gruner, U. (2012). Erläuterungen zum geologischen Atlas der Schweiz, Blatt 1146 Lyss. Swiss Federal Office of Topography – swisstopo.

González A, Z. I., Krachler, M., Cheburkin, A. K., & Shotyk, W. (2006). Spatial distribution of natural enrichments of arsenic, selenium, and uranium in a minerotrophic peatland, Gola di Lago, Canton Ticino, Switzerland. Environmental Science and Technology, 40(21), 6568–6574.

Harada, N., & Nonaka, M. (2012). Soil radiocesium distribution in rice fields disturbed by farming process after the Fukushima Daiichi Nuclear Power Plant accident. Science of The Total Environment, 438, 242–247.

Horwitz, E. P., Dietz, M. L., Chiarizia, R., Diamond, H., Essling, A. M., & Graczyk, D. (1992). Separation and preconcentration of uranium from acidic media by extraction chromatography. Analytica Chimica Acta, 266(1), 25–37.

Hübner, H. (1989). Uran und seine Entdeckungsgeschichte durch Martin Heinrich Klaproth. Isotopenpraxis – Isotops in Environmental and Health Studies, 25(9), 361-367.

IAEA. (2010). Handbook of parameter values for the prediction of radionuclide transfer on terrestrial and freshwater environments. Technical Reports Series, 472, 1–208.

Ivanovich, M., & Harmon, R. S. (1992). Uranium-series Disequilibrium: Application to Earth, Marine and Environmental Sciences. Clarendon Press.

Jouvet, G., Seguinot, J., Ivy-Ochs, S., & Funk, M. (2017). Modelling the diversion of erratic boulders by the Valais Glacier during the last glacial maximum. Journal of Glaciology, 63(239), 487–498.

Keith, L. S., Faroon, O. M., & Fowler, B. A. (2015). Handbook on the Toxicology of Metals: Fourth Edition.

Keller, & Beat. (1922). Hydrogeologie des schweizerischen Molasse-Beckens: aktueller Wissensstand und weiterführende Betrachtungen. Eclogae Geologicae Helvatiae, 85(3), 611–651.

Klaus, G. (2007). Zustand und Entwicklung der Moor in der Schweiz. Ergebnisse der Erfolgskontrolle Moorschutz. Umwelt-Zustand Nr. 0730. Bundesamt für Umwelt.

Krachler, M., & Shotyk, W. (2004). Natural and anthropogenic enrichments of molybdenum, thorium, and uranium in a complete peat bog profile, Jura Mountains, Switzerland. Journal of Environmental Monitoring, 6(5), 418–426.

Krüger, J. P., Leifeld, J., Glatzel, S., Szidat, S., & Alewell, C. (2015). Biogeochemical indicators of peatland degradation - A case study of a temperate bog in northern Germany. Biogeosciences, 12(10), 2861–2871.

L'Annunziata, M. F. (2012). Handbook of Radioactivity Analysis. Academic Press.

Larock, P., Hyun, J.-H., Boutelle, S., Burnett, W. C., & Hull, C. D. (1996). Bacterial mobilization of polonium. Geochimica et Cosmochimica Acta, 60(22), 4321–4328.

Lee, H. M., Hong, G. H., Baskaran, M., Kim, S. H., & Kim, Y. I. L. L. (2014). Evaluation of plating conditions for the recovery of 210Po on a Ag planchet. Applied Radiation and Isotopes, 90, 170–176.

Letman, M.M., Drage, J., Ryan, A.-M., Lake, C., Jamieson, R. (2018). Development of a leaching procedure to assess the risk of uranium leaching due to construction and demolition waste disposal. Waste Management, 78, 144-150.

Li, D., Kaplan, D. I., Chang, H. S., Seaman, J. C., Jaffé, P. R., Koster Van Groos, P., Scheckel, K. G., Segre, C. U., Chen, N., Jiang, D. T., Newville, M., & Lanzirotti, A. (2015). Spectroscopic evidence of uranium immobilization in acidic wetlands by natural organic matter and plant roots. Environmental Science and Technology, 49(5), 2823–2832.

Li, D., Seaman, J. C., Chang, H. S., Jaffe, P. R., Koster van Groos, P., Jiang, D. T., Chen, N., Lin, J., Arthur, Z., Pan, Y., Scheckel, K. G., Newville, M., Lanzirotti, A., & Kaplan, D. I. (2014). Retention and chemical speciation of uranium in an oxidized wetland sediment from the Savannah River Site. Journal of Environmental Radioactivity, 131, 40–46.

Liesch, T., Hinrichsen, S., & Goldscheider, N. (2015). Uranium in groundwater - Fertilizers versus geogenic sources. Science of the Total Environment, 536, 981–995.

Maaz, M., Elzein, T., Barroca-Aubry, N., Simoni, E., Costa, L., Nsouli, B., Roger, P. (2020). Applied Materials Today, 18, 100461.

Magill, J., Pfenning, G., & Galy, J. (2006). Chart of the Nuclides (Vol. 7). Karlsruhe.

Mason, B. H., & Moore, C. B. (1982). Principles of Geochemistry.

Matter, A. (1980). Excursion No. V: Flysch and Molasse of Western and Central Switzerland. In: Geology of Switzerland - A guide book. Geologische Kommission.

Meija, J., Coplen, T. B., Berglund, M., Brand, W. A., de Bièvre, P., Gröning, M., Holden, N. E., Irrgeher, J., Loss, R. D., Walczyk, T., & Prohaska, T. (2016). Isotopic compositions of the elements 2013 (IUPAC Technical Report). Pure and Applied Chemistry, 88(3), 293–306.

Minkowski C. and Ryser R., (2015). Urananomalie im Lyssbach. Abschlussbericht. Bau-, Verkehrs- und Energiedirektion des Kantons Bern, AWA Amt für Wasser und Abfall.

Ndiaye, M., Clerc, N., Gorin, G., Girardclos, S., & Fiore, J. (2014). Lake Neuchâtel (Switzerland) seismic stratigraphic record points to the simultaneous Würmian deglaciation of the Rhône Glacier and Jura Ice Cap. Quaternary Science Reviews, 85, 1–19.

Osmond, J. I., Cowart, J. B., & Ivanovich, M. (1983). Uranium Isotopic Disequilibrium in Ground Water as an Indicator of Anomalies. Int. J. Appl. Radiat. Isotopes, 34.

Osmond, J. K., & Cowart, J. B. (1976). The theory and uses of natural uranium isotopic variations in hydrology. Atomic Energy Review, 14(4), 621–679.

Pérez-Moreno, S. M., Gázquez, M. J., Pérez-López, R., & Bolivar, J. P. (2018). Validation of the BCR sequential extraction procedure for natural radionuclides. Chemosphere, 198, 397–408.

Pfiffner, O. A. (2014). Geology of the Alps. Wiley.

Pregler, A., Surbeck, H., Eikenberg. J., Werthmüller, S., Szidat, S., Türler, A. (2019). Increased Uranium concentrations in ground and surface waters of the Swiss Plateau: A result of Uranium accumulation and leaching in the Molasse Basin and (ancient) wetlands? Journal of Environmental Radioactivity, 208-209, 106026.

Pulhani, V. A., Dafauti, S., Hegde, A. G., Sharma, R. M., & Mishra, U. C. (2005). Uptake and distribution of natural radioactivity in wheat plants from soil. Journal of Environmental Radioactivity, 79(3), 331–346.

Ram, R., Vaughan, J., Etschmann, B., & Brugger, J. (2019). The aqueous chemistry of polonium (Po) in environmental and anthropogenic processes. IJournal of Hazardous Materials, 380.

Ramseyer, R. (1952). Geologie des Wistenlacherberges (Mont Vully) und der Umgebung von von Murten (Kt. Freiburg). Eclogae Geologicae Helvetiae.

Regenspurg, S., Margot-Roquier, C., Harfouche, M., Froidevaux, P., Steinmann, P., Junier, P., & Bernier-Latmani, R. (2010). Speciation of naturally-accumulated uranium in an organic-rich soil of an alpine region (Switzerland). Geochimica et Cosmochimica Acta, 74(7), 2082–2098.

Reimer, P. J., Bard, E., Bayliss, A., Warren Beck, J., Blackwell, P. G., Bronk Ramsey, C., Buck, C. E., Cheng, H., Lawrence Edwards, R., Friedrich, M., Grootes, P. M., Guilderson, T. P., Haflidason, H., Hajdas, I., Hatté, C., Heaton, T. J., Hoffmann, D. L., Hogg, A. G., Hughen, K. A., van der Plicht, J. (2013). IntCal13 and MARINE13 radiocarbon age calibration curves 0-50,000 years CAL BP. Radiocarbon, 55.

Rybach, L., Bächler, D., Bucher, B., & Schwarz, G. (2002). Radiation doses of Swiss population from external sources. Journal of Environmental Radioactivity, 62.

Rybach, L., Medici, F., & Schwarz, G. F. (1997). Construction of radioelement and doserate baseline maps by combining ground and airborne radiometric data.

Sale, J. W. (1930). Control of Mineral Waters and Their Salts under the Federal Food and Drugs Act. Industrial and Engineering Chemistry, 22(4), 332–335.

Sasaki, T., Tashiro, Y., Fujinnaga, H., Ishii, T., & Gunji, Y. (2002). Determination of transfer factors or uranium, thorium, radium and lead from soil to agricultural product in Japan for estimating internal radiation dose though ingestion. Japanese Journal of Health Physics, 37(3), 208–221.

Shin, W., Oh, J., Choung, S., Cho, B., Lee, K., Yun, U., Woo, N. & Kim, H. (2016). Distribution and potential health risk of groundwater Uranium in Korea. Chemosphere, 163, 108-115.

Schmidt, F. (2013). Schwermetalle im Lyssbach - Herkunft und Bedeutung. Bachelor Thesis, ETH Zürich.

Schott, B. & Wiegand, J. (2003). Processes of radionuclide enrichment in sediments and ground waters of Mont Vully (Canton Fribourg, Switzerland). Eclogae Geologicae Helvetiae, 93, 99–107.

Schultz, M. K., Burnett, W. C., & Inn, K. G. W. (1998). Evaluation of a Sequential Extraction Method for Determining Actinide Fractionation in Soils and Sediments. In Journal of Environmental Radioactivity, 40(2).

Schumann, R. R., Zielinski, R. A., Otton, J. K., Pantea, M. P., & Orem, W. H. (2017). Uranium delivery and uptake in a montane wetland, north-central Colorado, USA. Applied Geochemistry, 78, 363–379.

Sinclair, H. D. (1991). Simulation of Foreland Basin Stratigraphy using a diffusion model of mountain belt uplift and erosion: An example from the central Alps, Switzerland. Tectonics, 10(3), 599–620.

Stalder, E., Blanc, A., Haldimann, M., & Dudler, V. (2012). Occurrence of uranium in Swiss drinking water. Chemosphere, 86(6), 672–679.

Studer, B. (1853). Geologie der Schweiz. Zweiter Band: Nördliche Nebenzone der Alpen, Jura und Hügelland. Stämpflische Verlagshandlung.

Surbeck, H., Werthmüller, S., Perret, R. (2015). Aeroradiometrie mit einer Drohne zur Suche nach Urananreicherungen. 17. Geoforum Umhausen Tirol, 15.-16.10.2015, Tagungsband, 111-112.

Suresh, P. O., Dosseto, A., Handley, H. K., & Hesse, P. P. (2014). Assessment of a sequential phase extraction procedure for uranium-series isotope analysis of soils and sediments. Applied Radiation and Isotopes, 83, 47–55.

Swiss Federal Office of Meteorology and Climatology Meteo Swiss. (2019). Monthly and annual precipitation maps. https:\\www.meteoswiss.admin.ch.

Swiss Federal Office of Topography. (2019). Swisstopo Journey through time maps. https:\\map.geo.admin.ch.

Szidat, S., Salazar, G. A., Vogel, E., Battaglia, M., Wacker, L., Synal, H.-A., & Türler, A. (2014). ^{14}C Analysis and Sample Preparation at the New Bern Laboratory for the Analysis of Radiocarbon with AMS (LARA). Radiocarbon, 56(2), 561–566.

Takeda, A., Tsukada, H., Takaku, Y., Hisamatsu, S., Nanzyo, M. (2006). Accumulation of uranium derived from long-term fertilizer applications in a cultivated Andisol. Science of the Total Environment, 367(2-3), 924-931.

Tsoulfanidis, N. (2018). Nuclear Energy – A volume in the Encyclopedia of Sustainability Science and Technology Serie. Springer Verlag, New York.

Uchida, S., Tagami, K., Shang, Z. R., & Choi, Y. H. (2009). Uptake of radionuclides and stable elements from paddy soil to rice: a review. Journal of Environmental Radioactivity, 100(9), 739–745.

UNSCEAR (1993). Sources and effects of ionizing radiation. United Nations Scientific Committee on the Effect of Atomic Radiation. New York.

UNSCEAR (2000). Sources and effects of ionizing radiation. United Nations Scientific Committee on the Effects of Atomic Radiation. New York.

Vandenhove, H., Vanhoudt, N., Duquène, L., Antunes, K., & Wannijn, J. (2014). Comparison of two sequential extraction procedures for uranium fractionation in contaminated soils. Journal of Environmental Radioactivity, 137, 1–9.

Vesterbacka, P. (2007). Natural Radioactivity in Drinking Water in Finland. Boreal Environment Research, 12, 11-16.

Wallner, G., Wagner, R., & Katzlberger, C. (2008). Natural radionuclides in Austrian mineral water and their sequential measurement by fast methods. Journal of Environmental Radioactivity, 99(7), 1090–1094.

Walsh, M., Wallner, G. & Jennings, P. (2014). Radioactivity in drinking water supplies in western Austria. Journal of Environmental Radioactivity, 130, 56-62.

Wang, Y., Bagnoud, A., Suvorova, E., McGivney, E., Chesaux, L., Phrommavanh, V., Descostes, M., & Bernier-Latmani, R. (2014). Geochemical control on uranium(IV) mobility in a mining-impacted wetland. Environmental Science and Technology, 48(17), 10062–10070.

Werthmüller, S., Surbeck, H., Ryser, R. (2015). Airborne exploration of anomalous high uranium contents in water and soil in the region of the "Lyssbach" – Canton of Bern. Poster Abstract, Volume 11 Hydrology, Limnology and Hydrogeology. Swiss Geoscience Meeting, Basel, 20.-21.11.2015, P11.14.

WHO. (2001). Guidelines for Drinking-water Quality.

Wu, Y., Wang, Y. & Xie, X. (2014). Occurrence, behavior and distribution of high levels of uranium in shallow groundwater at Datong basin, northern China. Science of the total Environment, 472, 809-8017.

Yamada, T., Kikuchi, M., Yagihashi, D., Yamakawa, S., Ishizu, H., & Shiina, T. (2017). Screening test for radioactivity of self-consumption products in Fukushima after the Fukushima Daiichi NPP accident in Japan. Applied Radiation and Isotopes, 126, 93–99.

Zielinski, R. A., & Meier, A. L. (1988). The association of uranium with organic matter in Holocene peat: an experimental leaching study. Applied Geochemistry, 3.

Erklärung

gemäss Art. 28 Abs. 2 RSL 05

Name/ Vorname:	Pregler Anja
Matrikelnummer:	16-124-141
Studiengang:	Doktorat Phil NAT Chemie und Molekulare Wissenschaften Dissertation
Titel der Arbeit:	The fate of geogenic uranium in the environment: An example from the Swiss Plateau.
LeiterIn der Arbeit:	Prof. Dr. Andreas Türler

Ich erkläre hiermit, dass ich diese Arbeit selbstständig verfasst und keine anderen als die angegebenen Quellen benutzt habe. Alle Stellen, die wörtlich oder sinngemäss aus Quellen entnommen wurden, habe ich als solche gekennzeichnet. Mir ist bekannt, dass andernfalls der Senat gemäss Artikel 36 Absatz 1 Buchstabe r des Gesetzes vom 5. September 1996 über die Universität zum Entzug des auf Grund dieser Arbeit verliehenen Titels berechtigt ist. Ich gewähre hiermit Einsicht in diese Arbeit.

Bern, 21.08.2020

Ort/Datum Unterschrift